Adaptive Explicit Time Delay, Frequency Estimations In Communications Systems

by

Cheng Zheng
(M.E., Huazhong University of Science and Technology)

A DISSERTATION SUBMITTED FOR THE DEGREE OF

PHILOSOPHY OF DOCTORAL IN ENGINEERING

DEPARTMENT OF ELECTRICAL AND COMPUTER

ENGINEERING

NATIONAL UNIVERSITY OF SINGAPORE

2003

ACKNOWLEDGMENTS

First and foremost, my deepest gratitude to my supervisor, Professor Tjeng Thiang Tjhung, who has given me guidance with much patience and kindness, without which the completion of PH.D research would not have been possible.

Special thanks also go to Ms. Serene Oe and Mr. Henry Tan at the Wireless Communications Laboratory for their helps.

Lastly, My deepest gratitude goes to my family.

Contents

SUMMARY

In this dissertation we address the problems of time delay estimation (TDE), frequency estimation (FE) in the presence of additive white noise. These estimation problems arise in the study of many communications systems. For example in the hostile mobile radio communications environment, there will be multi-paths, Doppler frequency drift, and oscillator's inaccuracy that will degrade system performance. Accurate estimations of signal frequency as well as time delay between multipaths are essential to ensure good mobile radio communications. Also since the mobile radio channels are time-varying, adaptive signal processing is necessary.

In this dissertation, the basic adaptive technique that is exploited is gradient-based LMS. The main purpose is to look into the currently available LMS-based TDE, FE, and then to find new algorithms, which can be implemented in real time to explicitly obtain TDE and FE efficiently.

We have developed a new so-called mixed modulated Lagrange explicit time delay estimation (MMLETDE) algorithm using approximation techniques. In the proposed algorithm we incorporated the modulated Lagrange interpolation filter into explicit time delay estimation (ETDE) and replaced the gradients of the Lagrange interpolation filter's

coefficients with that of the 'sinc' function filter's coefficients. Furthermore, we have also proved the convergence of the algorithm and derived the variance of the delay estimate.

For the explicit adaptive frequency estimation, we first defined the cost function of the algorithm, and then designed the explicit modulated Lagrange adaptive frequency estimation algorithm (EMLAFE). We also proved the convergence of EMLAFE.

We have conducted extensive computer simulation to verify our TDE and FE algorithms. From the simulation results we verify that the MMLETDE can give an accurate and fast unbiased time delay estimate over a wide frequency range for single tone signal using a filter with a very low order. The algorithm is also suitable for narrow-band signals. We have also proved that the theoretically obtained variance of MMLETDE for single sinusoid agrees with the simulation result. However we have observed that the MMLETDE is slightly biased when the bandwidth of the signal becomes relatively larger. For FE, we have seen from our simulation results using time-invariant and chirp frequency signals that our new EMLAFE algorithm can give accurate and fast frequency estimation for stationary and non-stationary signals.

Our two new MMLETDE and EMLFE algorithms can also be jointly used to offer an accurate and fast estimation of time delay and frequency of signal.

List of Figures

List of Tables

Chapter 1

Introduction

1.1 Background

In wireless communications systems, the transmission path between the transmitter and the receiver can vary from a simple line-of-sigh to one that is severely obstructed by buildings, mountains, and foliage. The presence of these obstacles in the channel cause reflection, diffraction, and scattering of radio signal. These effects result in multiple versions with different time delays of the transmitted radio signal to arrive at the receiving antenna. This is called multi-path propagation. Each individual path also arrives at its own amplitude and carrier phase, and the superposition of these multi-path components will result in the transmitted signal to be dispersed in time. In direct sequence spread spectrum (DSSS), code division multiple access (CDMA) system adopted in the third generation (3G) cellular mobile radio standards, the Rake receiver requires the knowledge of multi-path parameters, such as time delays among multi-paths in [1].

In radar, sonar, remote speed sensing and locating systems, the time delay between the received signals at two spatially separated sensors or sensor array has to be estimated. Least mean square time delay estimation (TDE) algorithm has been commonly used in such cases [2], the time delay are not known a priori, and might change from time to time due to motion of the signal source or the receiver, or due to the time-varying characteristics of the transmission medium [3].

The relative motion between the base station and the mobile station results in Doppler shift in frequency. A varying speed of mobile station or surrounding objects will introduce a time-varying Doppler shift. In addition to Doppler shift, the frequency of the local oscillator may also drift. These effects will introduce the frequency offset.

With the rapidly increasing market for high-speed data, image and video applications, bit rates in excess of 2Mbps are required for future cellular system. In Europe, wide-band CDMA (WCDMA) concept has been decided by the European Telecommunications Standards Institute (ETSI) to be standardized for Universal Mobile Telecommunications System (UMTS) as air interface for paired band [4] in January 1998. In the standard of ETSI WCDMA [5], bit rates from a few kbps to 2Mbps for packet data operation can be provided with the basic chip rate of 4.096Mcps. The higher the data rates, the harder it is to maintain a lower bit error rate. In WCDMA the modulation adopted is QPSK with coherent demodulation. Signal synchronization is critical to coherent demodulation, and accurate phase and frequency offset compensation is required between the local carrier and the received signal.

Orthogonal frequency division multiplexing (OFDM) is a popular communication

scheme that has been adopted in several standards, e.g. digital audio broadcasting (DAB), digital video broadcasting (DVB) or in broadband local area network (LAN), like e.g. HIPERLAN [6]. Because of its inherent simplicity in equalizing the adverse effect of frequency-selective linear time-invariant channels, OFDM has also become a popular multi-carrier transmission scheme for transmission of data requiring high data rates [7]. It is well known that OFDM systems are highly sensitive to time and/or frequency offsets [8] [9] which cause inter-symbol interference (ISI) and inter-block interference (IBI) [10].

In this dissertation we focus on time delay estimation and frequency estimation and we shall describe them in the following sections.

1.2 Time Delay Estimation

The Time Delay of Arrival (TDOA) estimation problem is encountered in seismology, sonography, Global Position System, radar, sonar, geographical remote sensing, and communications systems [11]. Modern techniques of TDOA estimation which rely on standard covariance methods not only require a large computation time, but also their performance prediction exhibits poor correlation with actual estimated results [11]. For non-stationary signal, adaptive signal processing is required. One method is to use Least Mean Square (LMS) adaptive filter to estimate the time delay (TDE) [12].

The conventional TDE is based on the generalized correlator, which requires a priori knowledge of signal and noise spectra [13]. The time delay is estimated by calculating the location of the peak of the correlation function between two signals that originate

from the same source but travel through different paths. This conventional technique in theory can achieve an arbitrarily accurate time delay estimate. However there are two main disadvantages:

1. The cross-correlation of the two signals must be estimated. This is an averaging and estimation process. The longer is the observation time, the more accurate is the estimation of the cross-correlation. But a very long observation time is impractical, because it will mean a longer computation time, and therefore the technique is not suitable for non-stationary signal. On the other hand, with a limited observation time, this method is in fact biased in the presence of noise.

2. In analog time domain, signal processing is vulnerable to noise. All modern techniques exploit the power of digital signal processing, in which the analog signal is converted to its discrete version. Then the power of post-digital conversion processing can be exploited. However, the resolution of conventional TDE is limited by the sampling interval T.

Notwithstanding the fact that resolution is limited by the sampling interval T for conventional TDE, a more accurate time delay estimation where a resolution smaller than a sampling interval is nevertheless needed in many fields. When a high resolution and possibly time-varying TDE is required, especially for coherent demodulation, an on-line interpolation is necessary. Let the signal of interest be

$$x(k) = s(k) + \theta(k) \tag{1.1a}$$

$$y(k) = s(k - D) + \phi(k) \tag{1.1b}$$

where $-\infty < k < \infty$ is the time index, $s(k) = A(k)e^{j\,\omega_0 k}$ is the original source signal with center frequency ω_0, D is time delay normalized by the sampling interval T. The $\theta(k)$ and $\phi(k)$ are the corrupting stationary zero-mean white complex Gaussian noises. The main task is to track the delay D as fast as possible. This means that the algorithm requires a moderate amount of computation cycles and should be implemented in real time. Reed [12] reported in 1981 the use of an LMS filter to estimate the time delay difference between two waveforms. The time delay estimate is obtained by interpolating on the weights of the filter to select the point in the tapped delay line that corresponds to the peak weight [14]. Also many researchers have done extensive work on finite impulse response (FIR) delay filter in order to approximate the delay to a signal in discrete time domain. If one ideal FIR discrete delay system can be constructed, one signal can be intentionally delayed and compared with another delayed version of the signal whose delay is to be determined. The unknown delay can be determined when the difference between the original signal and its delayed version reaches a minimum.

1.2.1 Explicit Time Delay Estimation (ETDE)

Chan et al. [15] introduced a parameter estimation approach to time delay estimation by modelling the delay as a FIR filter whose coefficients are samples of a sinc function. In 1988, Ching et al. [16] made an improvement on this parameter estimation approach by only updating the maximum coefficient of a sinc function. In 1994, So et al. [17] proposed an explicit time delay estimation (ETDE) algorithm, in which the delay was parameterized in the coefficients of the fractional delay filter (FDF). As we know, this

ETDE, which uses the LMS algorithm, is attractive as the delay estimate $\hat{D}$ is explicitly parameterized in the filter coefficient in the iterative adaptation process. The time delay estimate of this algorithm has been shown to be unbiased in [17] for wide band white-noise-like signals under a relatively longer filter length. In [17], the signal was assumed to be white-noise-like, the noise was also limited to be within the Nyquist bandwidth. However the assumption that the noise is band-limited within the Nyquist bandwidth is unacceptable in practice since the bandwidth of noise is always larger than that of practical communication systems. Another disadvantage of the ETDE is that the filter order is large. Furthermore it has been proved that the ETDE is in fact biased in [18] when the filter order is finite. Despite the fact that single sinusoid and narrow-band signals are encountered frequently in communications systems, the ETDE algorithm has been proved only for dealing with white-noise-like signal.

Nandi showed in 1999 [13] that Lagrange interpolation technique can be incorporated into ETDE to estimate the time delay between two single tone signals. However, the valid center frequency range of this new approach was not reported and needed further investigations. Though the modulated ETDE(METDE) [13] depends less on signal frequency and filter order, the delay estimate is still biased and the required filter order is high. We observe in our simulation results to be presented in Chapter 3 that the mean delay of METDE does not converge to the actual delay. The modulated Lagrange ETDE (MLETDE) algorithm [13] is valid for certain range of single tone signals but biased in its estimates.

In summary, the conventional ETDE is confined to full-band white-noise signal while

the MLETDE is proposed for single tone signal and many technical issues have yet to be tackled, such as the convergence to the true delay. The narrow-band or bandpass signals are often encountered in many areas such as communications, sonar, radar. One of the purposes of this dissertation is to find an algorithm for delay estimation for a bandpass signal that can provide an unbiased estimate with as small a filter order as possible for easy implementation.We shall also consider delay estimation for non-stationary band-pass signal, in which convergence rate is also important.

1.2.2 Frequency Estimation

Many problems in statistical signal processing may be ones that attempt to estimate signals with linear as well as nonlinear parameters in additive white Gaussian noise. A common example is the estimation of frequencies of multiple sinusoids in noise. The popular and accurate modern methods are based on the eigen-structure of the data auto-covariance matrix [19]. However, when the frequency in question is time varying, adaptive realization of such methods poses heavy computation burden because the auto-covariance matrix has to be recalculated at each iteration.

Signals with time-varying frequency are often encountered in a variety of fields. There are many methods to estimate the instantaneous frequencies. The Short Time Fourier Transform (STFT) and Wigner Distribution (WD) are two popular algorithms based on time-frequency representations (TFR) [20]. These algorithms require a large computation time. A fast adaptive algorithm is required which means that the algorithm should be simple and easily implemented in real-time. Etter et al. [21] proposed in

1987 an adaptive frequency estimator (AFE) which is based on an FIR delay filter with fixed coefficients. By delaying the frequency fixed or varying single tone signal and by comparing the filtered signal or delayed signal with the source signal, an algorithm to estimate the instantaneous frequency can be developed. The frequency can be estimated when the error (difference) reaches a maximum value. However a disadvantage of this AFE algorithm is that the frequency estimation is biased unless $\frac{\pi}{\omega_0}$ is an integer and unless ω_0 is small.

In [22] Nandi et al. introduced an adaptive Lagrange interpolation filter (LIF) , and in this AFE technique the author modulates the LIF coefficients by multiplying a complex exponential function [23]. However, they did not give a theoretical analysis on this algorithm. Both the above algorithms adjusted the time delay between the source signal and filtered signal, and compared the difference between them first, then converted this delay to a frequency estimate when the difference reaches a maximum value.

In this thesis we attempt to develop a fast and accurate explicit frequency estimation algorithm for non-stationary, frequency-varying signal. Our goal is in finding an appropriate filter and an updating algorithm for the filter coefficients.

1.3 Contributions

In this dissertation we first investigated in detail explicit time delay estimation algorithms which are based on fractional delay interpolation filter. Then we develop new algorithms for time delay and frequency estimation as described below.

- Develop a new time delay estimator: mixed modulated Lagrange interpolation ex-

plicit time delay estimation (MMLETDE) algorithm. The algorithm is proposed for estimating fractional sample time delays that draws from and combines both explicit time delay estimation and modulated Lagrange interpolation. This algorithm can be used to estimate the delay of narrow band signal. We develop statistical descriptions of its performance and, finally, present simulation results. We show that MMLETDE can give accurate time delay estimate of a narrow-band signal over a large signal center frequency range even under a very low filter order. The benefits of low filter order are simpler and faster estimation and operation in a non-stationary environment where convergence rate is important.

- In this dissertation, we also analyzed and developed a new explicit modulated Lagrange interpolation adaptive frequency estimation (EMLAFE) algorithm. The new proposed algorithm can be used to track the frequency of non-stationary single tone signals rapidly.

- We also combine the MMLETDE and EMLAFE algorithms together to form joint time delay-frequency estimation algorithm (JTDFE) to jointly estimate the carrier frequency and time difference of arrival. In the case of only single carrier signal, JTDFE can give signal frequency and phase directly so that we can simplify carrier synchronization circuitry.

1.4 Summary

In this dissertation we address the problems of time delay and frequency estimation with the goal of ensuring good radio signal reception in the presence of additive white noise and in the hostile mobile communications environment where there exist multi-paths, Doppler frequency drift, in addition to oscillator's inaccuracy. We have developed a new so-called MMLETDE algorithm for time delay estimation, which is suitable for band pass signal, and a so-called EMLAFE algorithm for frequency estimation which can be used to track a time-varying single tone signal.

Chapter 2

Synchronization In Communications Systems

2.1 Synchronization in Digital Communications

In digital communications, the optimum detection of transmitted data requires that both the carrier and clock signals are available at the receiver [24]. The carrier and timing recovery circuits are used to retrieve signal from the noisy incoming waveform. The two fundamental synchronization problems are: timing recovery, which is an essential part of digital communications, and carrier recovery, which is necessary only for coherent detection.

1. Carrier Recovery in Coherent Detection: In general, coherent reception requires knowledge of the basis functions at the receiver; synchronization must be used to recover the basis function. In the special case of sinusoidal carrier signal, the

knowledge of both the frequency and phase of a carrier is required. The basis functions are usually recovered from the received noisy incoming signal by means of a suppressed carrier phase-locked loop.

2. Timing Recovery: Another synchronization process in digital communications is symbol synchronization or timing recovery. In practical systems, not only an isolated single symbol, but also a sequence of symbols, has to be transmitted. To perform demodulation, the receiver has to know exactly the time instants, at which the start and stop times of the individual symbols are, in order to assign the decision time instants and to determine the time instants when the initial conditions of the correlators have to be reset to zero in the receiver.

Compared with carrier recovery, which is required by coherent receivers, timing recovery is a necessary process in digital communications. The decision instants at the receiver must be synchronized with the corresponding ends of symbol intervals T at the transmitter. Symbol synchronization must be obtained as soon as possible after transmission begins, and must be maintained throughout the transmission. Though timing recovery is mandatory in digital communications, it belongs to the decision portion of the data recovery process. In this dissertation we will only focus on carrier estimation and carrier tracking.

2.2 TDMA vs CDMA

We note that in a digital communications system, the output of demodulator must be sampled periodically, such as once per symbol interval, in order to recover the transmitted information. In virtually any form of digital communications, synchronization in time (symbol clock recovery) is a prerequisite before communication begins. Code Division Multiple Access (CDMA) system is also not exempt from this requirement. However, the synchronization in a CDMA system is somewhat different from its TDMA counterpart. In TDMA systems, one requires synchronization in frequency (and, in some cases, phase) before a data clock can be recovered. Often, a dotting sequence $101010\cdots$ is included in the preamble of a TDMA frame to provide the clock synchronization subsystem the necessary signal to lock onto. In a CDMA scenario, since the desired signal is spread in frequency over the entire allotted CDMA band, the acquisition of Pseudo-Noise (PN) code clock, which for most practical systems also implies data clock acquisition, must be achieved in the absence of phase and frequency synchronization. The PN code clock and data symbol clock are derived from a common source. Hence, an acquisition of the PN code clock leads to data symbol clock recovery. This is due to the fact that if one chooses to achieve phase and frequency estimation in the absence of PN code acquisition, the phase and frequency synchronizers must extract synchronization information from a wide-band signal. This, in general, is a formidable task due to the large bandwidth of typical CDMA signals. Hence, in a CDMA system, PN code timing acquisition precedes any other form of synchronization. Upon the recovery of the PN code phase the CDMA signal is de-spread and then an accurate estimate of frequency or

phase (time delay estimate) may be obtained.

2.3 Group Delay

Unlike wired channels that are stationary and predicable, and although electromagnetic wave propagation is fundamentally governed by Maxwell's field equations, a radio channel is extremely random to analyze accurately.

For simplicity, let us consider the plane waves. If we recall that the magnitude of the propagation vector $\mathbf{k}$ of a plane wave is given by

$$||\mathbf{k}|| = \frac{n\omega}{c}, \tag{2.1}$$

then the phase velocity of a plane wave is expressed by

$$v_p = \frac{\omega}{k} = \frac{c}{n} \tag{2.2}$$

where n is medium refractive index, ω is carrier angular frequency, c is light speed in free space [25].

We now consider transmitting a signal that contains information of carrier modulation. Assume a z-directed, y-polarized modulated plane wave packet $E_y(0,\, t)$ at the source location propagating from some initial plane $z = 0$ into a linear but possibly dispersive medium. We therefore represent the modulated signal $E_y(0,\, t)$ at the source

location by

$$E_y(0,\, t) = f(0,\, t)e^{-j\omega_0 t} \tag{2.3}$$

The signal, shown in Figure 2.1, consists of a carrier at frequency ω_0 modulated by a slowly varying envelope $f(0,\, t)$. Let us assume that each frequency component of

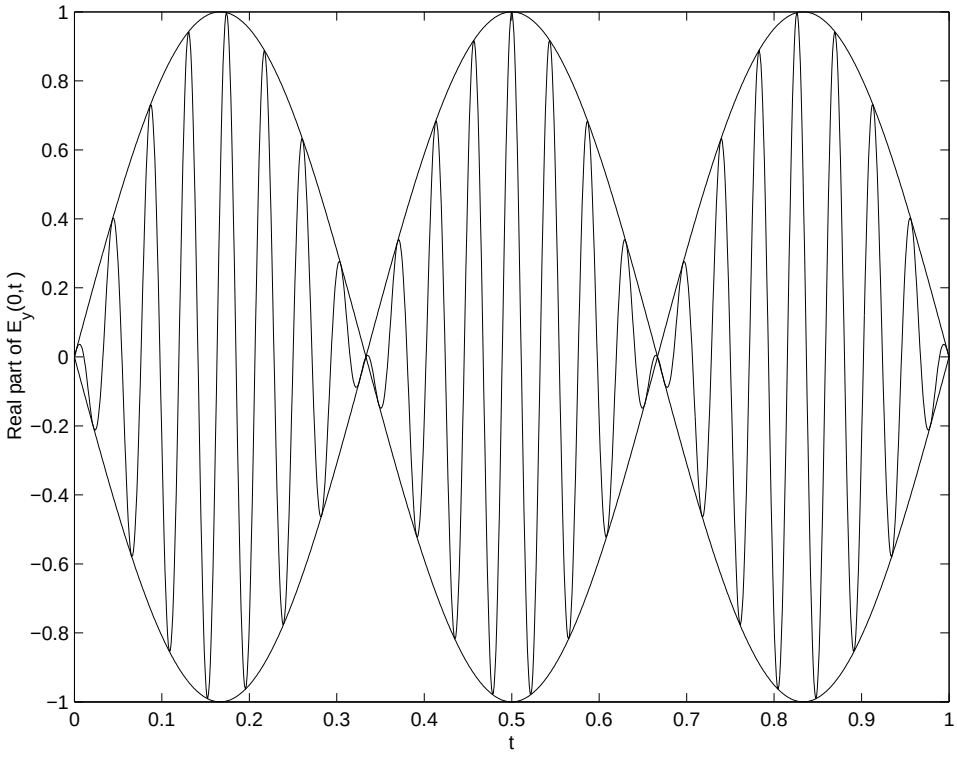

Figure 2.1: A time-domain version of the modulated wave packet of $E_y(0,\, t)$.

$f(0,\, t)$ travels along a propagation direction z with an associated propagation constant $k(\omega)$. By superposition, the received signal $E_y(z,\, t)$ at some arbitrary distance z from the source will be

$$E_y(z,\, t) = f(z,\, t)e^{jk(\omega_0)z}e^{-j\omega_0 t} \tag{2.4}$$

Now, we can relate $f(z,t)$ to $f(0,t)$ by writing

$$E_y(z,t) = \int_{-\infty}^{\infty} E_y(\omega) e^{jk(\omega)z} e^{-j\omega t} d\omega \tag{2.5}$$

where $E_y(\omega) = \frac{1}{2\pi}\int_0^{\infty} E_y(0,t')e^{j\omega t'}dt'$. Substituting (2.3), (2.4) into (2.5) and rearranging terms , we obtain

$$f(z,t) = \int_{-\infty}^{\infty} E_y(\omega) e^{-j(\omega-\omega_0)\left[t-\frac{k(\omega)-k(\omega_0)}{\omega-\omega_0}z\right]} d\omega \tag{2.6}$$

In order to analyze (2.6) further, we now express it in a Taylor series expansion as follows

$$k(\omega) = k(\omega_0) + (\omega-\omega_0)\frac{dk}{d\omega}\Big|_{\omega_0} + (\omega-\omega_0)^2\frac{d^2k}{d\omega^2}\Big|_{\omega_0} + \cdots \tag{2.7}$$

If we limit the accuracy to the first order, then (2.6) takes the particularly simple form

$$f(z,t) = f(0, t - \frac{dk}{d\omega}z) \tag{2.8}$$

It is obvious that from (2.8) we can define an envelope velocity, which is known as the group velocity, v_g, and is given by

$$v_g = \frac{1}{dk/d\omega} \tag{2.9}$$

and the corresponding group delay

$$\tau_g = \frac{z}{v_g}. \tag{2.10}$$

Clearly in the case where higher than first-order derivatives of $\mathbf{k}$ are negligible, the propagation is not dispersive, as we can see from (2.8) that the functional form of the wave remains invariant under propagation.

The point here is that v_p defined in (2.2) is the velocity of the carrier oscillation underneath the wave envelope. The group velocity represents the speed at which the information is transferred from transmitter to receiver. The propagation delay of information is associated with group delay τ_g. Throughout this dissertation, when we refer to time delay, we shall mean the group delay.

2.4 Signal Parameter Estimation

In Section 2.1we mentioned the need for synchronization in order to achieve coherent demodulation for WCDMA system. Synchronization is a process of system identification through which the parameters of a modulated waveform, such as carrier frequency, carrier phase, or timing of symbol can be detected. Let us assume the signal of interest is $s(0,\, t)$ at initial place. The received signal $r(z,\, t)$ at place z is the delayed version of original signal, which is corrupted by Gaussian noise $n(t)$. As discussed in previous

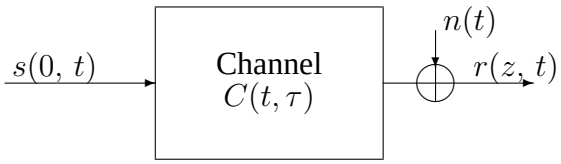

Figure 2.2: Channel model

section, $s(0,\, t)$ can be expressed as

$$s(0,\, t) = s_c(0,\, t)e^{j2\pi f_c t} \tag{2.11}$$

where the $s_c(0,\, t)$ is the complex envelope of signal $s(t)$.

The received signal as illustrated as in Figure 2.2 may be expressed as

$$r(z,\, t) = s(0,\, t) \otimes C(t; \tau) + n(t) \tag{2.12}$$

where $C(t; \tau)$ is the complex impulse response of mobile channel, $\otimes$ is convolution operator.

If we only consider plane wave $s(t)$ traveling through isotropic non-dispersive medium, the received signal may be written as follows:

$$r(z,\, t) = \alpha(t)s_c(0,\, t - \tau)e^{j2\pi f_c(t-\tau)} + n(t) \tag{2.13}$$

where α is the complex attenuation, τ is the propagation delay $\frac{dk}{d\omega}z = \frac{z}{v_g} = \tau_g$ in (2.8) (2.9) (2.10). It seems that only the propagation delay τ needs to be estimated. However, it is not the case in practice. First of all, the oscillator that generates the carrier signal for demodulation at the receiver is generally not synchronous in phase with that

at the transmitter. Furthermore, the two oscillators may be drifting slowly with time, perhaps in different directions [26, page 334]. In addition, the precision, to which one must synchronize in time for the sake of demodulation of received signal, depends on the symbol interval T. The phase $\phi = 2\pi f_c \tau$, which is determined by the product of f_c and τ, will be severely degraded by the inaccuracy of estimation of propagation delay τ because f_c is generally large. In summary, we must consider estimating both the phase and propagation delay τ in order to coherently detect the received signal. Therefore, we rewrite the received signal expression as follows

$$r(t) = \alpha(t)s(t;\phi,\tau) + n(t) \tag{2.14}$$

where ϕ and τ represent the signal parameters to be estimated.

2.5 The Modeling of Fractional Time Delay

Consider the existence of a time difference of arrival or time delay between two real signals, which originate from the same source but travel via different paths. The common approach to time delay estimation as will be explained in the next section, is to find the peak of the correlation of these two signals. Let $s(t)$ and $s_d(t) :\equiv s(t+D)$ be the signal and its delayed version. For discrete signal processing, the two signal sequences $\{s(k)\}$ and $\{s_d(k)\}$ in discrete time domain can be related by sampling theorem. Assume, without loss of generality, that the signal spectrum is band-limited between $-\pi$ and π the sampling time interval T is unity. Therefore, based on sampling theory $s(t) =$

$\sum_{n=-\infty}^{\infty} s(n)\mathrm{sinc}(t-n)$ [27], when $t = k + D$, k is an integer while D needs not be integer, we have

$$s_d(t) = s(k+D) = \sum_{n=-\infty}^{\infty} s(n)\mathrm{sinc}(k+D-n) \tag{2.15}$$

where

$$\mathrm{sinc(k + D - n)} = \frac{\sin \pi(k+D-n)}{\pi(k+D-n)}$$

We now let $m = k - n,$ then $n = k - m$ and (2.15) becomes

$$s_d(k) = \sum_{k-m=-\infty}^{\infty} s(k-m)\mathrm{sinc}(D+m) \tag{2.16}$$

Since k is a finite integer we can rewrite (2.15) as

$$s_d(k) = s(k+D) = \sum_{n=-\infty}^{\infty} \mathrm{sinc}(D+n)s(k-n) \tag{2.17}$$

Thus (2.17) represents the generation of the delayed sequence $\{s_d(k)\}$ from $\{s(k)\}$ through an infinite-order filter whose coefficients are $\{\mathrm{sinc}(D+n)\}$. This result also can be obtained by performing inverse Fourier transform on the quantity $e^{j\omega D}$ [28]. Here we briefly describe the derivation as follows.

Let $F\{\cdot\}$, $F^{-1}\{\cdot\}$ be the Fourier transform and its inverse operation, respectively.

Then

$$s(t+D) = F^{-1}\{e^{j\omega D}\} \otimes s(t) \tag{2.18}$$

In discrete time domain, we assume that the signal spectrum is band-limited within $(-\pi\ \pi]$, hence

$$F^{-1}\{e^{j\omega D}\} = \frac{1}{2\pi}\int_{-\pi}^{\pi} e^{j\omega D}e^{j\omega t}d\omega = \mathrm{sinc}(D+t) \tag{2.19}$$

Substitution of (2.19) into (2.18) gives

$$s(t+D) = \int_{-\infty}^{\infty} \mathrm{sinc}(D+\tau)s(t-\tau)\ d\tau \tag{2.20}$$

The discrete version of (2.20) is given by (2.17).

We have obtained (2.17) using two techniques. It is obvious that an infinitely long filter is unrealizable, and in practice, it is very reasonable to limit $|n|$ to a reasonable number p so that an approximation to (2.17) is

$$\tilde{s}_d(k) = \sum_{n=-p}^{p} \mathrm{sinc}(D+n)\, s(k-n) \tag{2.21}$$

and the continuous time version of $\tilde{s}_d(k)$, $\tilde{s}_d(t)$, is obtained by the sampling theory

$$\tilde{s}_d(t) = \sum_{k=-\infty}^{\infty}\sum_{n=-p}^{p} \mathrm{sinc}(D+n)s(k-n)\mathrm{sinc}(t-k) \tag{2.22}$$

We have now modeled, through (2.21), the time delay as a FIR filter with coefficients $\mathrm{sinc}(D+n)$. The modeling accuracy will increase with increasing p because the truncated error of (2.21) decreases.

2.6 Cross-correlation Between $\tilde{s}_d(k)$ And $s(k)$

It is clear from (2.21) that $\tilde{s}_d(k)$ and $s(k)$ are linearly correlated. Hence their coherence[1] is always 1. Calculating the cross correlation between $s(t)$ and $\tilde{s}_d(t)$ of (2.22), we have

$$\begin{aligned} R_{s\tilde{s}_d}(D+\tau) &= E[s(t+D+\tau)\tilde{s}_d(t)] \\ &= E\Big[s(t+D+\tau)\sum_{k=-\infty}^{\infty}\sum_{n=-p}^{p}\mathrm{sinc}(D+n)s(k-n)\mathrm{sinc}(t-k)\Big] \\ &= \sum_{k=-\infty}^{\infty}\sum_{n=-p}^{p}R_{ss}(t+D+\tau-k+n)\mathrm{sinc}(D+n)\mathrm{sinc}(t-k) \end{aligned} \tag{2.23}$$

where $R_{ab}(t_2-t_1)=E[a(t_2+t)b(t_1+t)]$ is the definition of the cross-correlation of two stationary random processes $a(t)$ and $b(t)$, and τ denotes the correlation shift. Therefore, we can easily obtain the new formula when substituting (2.17) into (2.23)

$$\begin{aligned} R_{s\tilde{s}_d}(D+\tau) &= \sum_{n=-p}^{p}R_{ss}(D+n+\tau)\mathrm{sinc}(D+n) \\ &= \sum_{-n=-p}^{p}R_{ss}(D-n+\tau)\mathrm{sinc}(D-n) \\ &= \sum_{n=-p}^{p}R_{ss}(D-n+\tau)\mathrm{sinc}(n-D) \end{aligned} \tag{2.24}$$

[1] By definition, coherence of $\tilde{s}_d(k)$ and $s(k)$ is $\frac{|S_{s\tilde{s}_d}(e^{j\omega})|}{\sqrt{S_{\tilde{s}_d\tilde{s}_d}(e^{j\omega})S_{ss}(e^{j\omega})}}$ [29].

In [30], the autocorrelation of $s(t)$ can be expressed as follows

$$R_{ss}(\tau) = \sum_{n=-\infty}^{\infty} R_{ss}(n)\text{sinc}(\tau - n) \tag{2.25}$$

Using the same technique in (2.17) on (2.25) and letting $m = n-D-\tau$ (m is an integer), we can easily obtain a new reconstruction formula for autocorrelation as follows

$$\begin{aligned} R_{ss}(\tau) &= \sum_{n=-\infty}^{\infty} R_{ss}(n)\text{sinc}(\tau - n) \\ &= \sum_{n=m+D+\tau=-\infty}^{\infty} R_{ss}(m + D + \tau)\text{sinc}(\tau - m - D - \tau) \\ &= \sum_{m=-\infty}^{\infty} R_{ss}(m + D + \tau)\text{sinc}(-m - D) \\ &= \sum_{m=-\infty}^{\infty} R_{ss}(m + D + \tau)\text{sinc}(m + D) \end{aligned} \tag{2.26}$$

Substituting m in (2.26) with n, we have

$$\begin{aligned} R_{ss}(\tau) &= \sum_{n=-\infty}^{\infty} R_{ss}(n + D + \tau)\text{sinc}(n + D) \\ &= \sum_{-n=-\infty}^{\infty} R_{ss}(-n + D + \tau)\text{sinc}(-n + D) \\ &= \sum_{n=-\infty}^{\infty} R_{ss}(-n + D + \tau)\text{sinc}(n - D) \end{aligned} \tag{2.27}$$

Comparing (2.24) and (2.27), we can obtain

$$\begin{aligned} R_{s\tilde{s}_d}(D+\tau) &= \sum_{n=-p}^{p} R_{ss}(D-n+\tau)\mathrm{sinc}(n-D) \\ &= R_{ss}(\tau) - \sum_{n=-\infty}^{-p-1} R_{ss}(D+\tau-n)\mathrm{sinc}(n-D) \\ &\quad - \sum_{n=p+1}^{\infty} R_{ss}(D+\tau-n)\mathrm{sinc}(n-D) \\ &\approx R_{ss}(\tau) \end{aligned} \tag{2.28}$$

In other words, $R_{s\tilde{s}_d}(D+\tau)$ is an approximation to $R_{ss}(\tau)$ by truncating the right side of (2.27). When p tends to be relatively large, the last two terms, the truncated error or the remainder, become small compared with $R_{ss}(\tau)$ and can be dropped because (2.27) is a process through an ideal delay system as described in Section 3.2.1. (2.28) indicates that the cross correlation of $s(k)$ and $\tilde{s}_d(k)$ will peak at time difference of the signal and its delayed version.

As can be seen from (2.28), there is a remainder of the truncation error. Therefore, usually, the peak of the cross-correlation of $s(t)$ and $\tilde{s}_d(t)$ does not peak at the D. As noted in [28], $s(t)$, $\tilde{s}_d(t)$ is not shifted exactly by D from a band-limited white noise process $s(t)$ as desired because the approximation in (2.21) causes the $R_{s\tilde{s}_d}(D+\tau) \neq R_{ss}(\tau)$. This uncertain truncated error makes the explicit time delay estimate in [17] biased.

2.7 Frequency Estimation

The auto-correlation function is a second order statistics of a stochastic process in time domain. Its counterpart in frequency domain is power spectral density. That means that we can usually decompose signal into its complex sinusoidal components which are well-defined quantities. A number of algorithms, which can be used to estimate the frequency of a single complex sinusoid, have been introduced over the years, most of them are based on a maximum-likelihood (ML) approach. Consider M samples of a single complex sinusoid in additive white Gaussian noise (AWGN). The observed signal is

$$r(k) = \sqrt{E_s} e^{j\,(2\pi f\, k\, T_s + \theta)} + n(k) \tag{2.29}$$

where $0 \leq k \leq M-1$. E_s is signal power, and T_s is the sampling interval. The noise sequence of $\{n_k\}$ is an independent identically distributed (iiD) random complex process with zero mean and variance σ_n^2. We can rewrite the observed signal as

$$r(k) = (1 + v(k))\sqrt{E_s} e^{j\,(2\pi f\, k\, T_s + \theta)} \tag{2.30}$$

where

$$v(k) = \frac{1}{\sqrt{E_s}} n(k) e^{-j\,(2\pi f\, k\, T_s + \theta)} \tag{2.31}$$

is a complex white noise sequence with

$$\text{var } v(k) = \frac{\sigma_n^2}{E_s} = \frac{1}{\text{SNR}_r} \tag{2.32}$$

Now let $v(k) = v_I(k) + j\, v_Q(k)$, then

$$1 + v(k) = 1 + v_I(k) + j\, v_Q(k) \tag{2.33}$$

For $\text{SNR}_r \gg 1$, we can assume that $|v_I(k)| \ll 1$ and $|v_Q(k)| \ll 1$, therefore (2.33) becomes

$$1 + v(k) \approx 1 + j\, v_Q(k) \approx e^{j\, v_Q(k)} \tag{2.34}$$

As Tretter has done in [31], we can now approximate the additive noise with Gaussian phase noise as follows

$$r(k) = \sqrt{E_s} e^{j\,(2\pi f\, k\, T_s + \theta + v_Q(k))} \tag{2.35}$$

Thus, the additive noise has been converted into an equivalent phase noise $v_Q(k)$ with

$$\text{var } v_Q(k) = 0.5\text{var } v(k) = \frac{1}{2\text{SNR}_\text{r}} \tag{2.36}$$

Furthermore, based on Tretter's work in [31], Kay developed in [32] an ML estimator based on differential phase measurements with a delay of one sampling interval. The

delay can be of other value, say m sampling intervals as in [33]. The new observation vector $\mathbf{U}_m$is now as follows

$$\mathbf{U}_m = (U_m, U_{m+1}, \cdots, U_{M-1})$$

where

$$U_k = \arg(r(k)\, r(k-m)^*) = 2\pi m\, f\, T_s + v_Q(k) - v_Q(k-m) \tag{2.37}$$

in here $m \leq k \leq M-1$ and $1 \leq m \leq (M-1)/3$. We note that (2.37) is valid for higher SNR only. Now $\{U_k\}$ is a sequence of multi-variate Gaussian distribution with mean $2\pi m\, f\, T_s$. It is clear from (2.37) that the problem now is to estimate the mean, f, of a Gaussian noise process. This is a standard estimation problem and the method is indicated in [32]. The ML estimator is obtained by minimizing the following quadric form, which is in the exponent of the multivariate Gaussian density function of $\mathbf{U}_m$:

$$Q(f) = (\mathbf{U}_m - 2\pi f T_s \mathbf{I})\Re^{-1} \times (\mathbf{U}_m - 2\pi f T_s \mathbf{I})^T \tag{2.38}$$

where $\Re = E[\mathbf{U}_m^T\, \mathbf{U}_m]$ is the covariance matrix of the observation vector $\mathbf{U}_m$, the super-script T denotes the transpose operation, and $\mathbf{I}$ is an $(M-m)$-dimensional row vector consisting of only ones. Setting the derived quadric form, with respect to the unknown frequency, to be equal to zero, this results in a matrix equation which is easily solved.

The resulting ML estimator of f is

$$\hat{f} = \frac{1}{2\pi T_s m} \frac{\mathbf{I}\Re^{-1}\Re^{T}}{\mathbf{I}\Re^{-1}\mathbf{I}^{T}} \tag{2.39}$$

This algorithm is based on the estimated autocorrelation which requires a relatively large sample size. The decision formula of (2.39) can be simplified by exploiting the eigen-structure of covariance matrix. This simplification depends on signal characteristic. This kind of algorithm, which requires signal to be a stationary process, of which statistical properties are not time-varying, for accurate estimation of the covariance matrix, is not suitable for non-stationary signal whose spectral characteristics (in particular the frequency of the spectral peaks) are varying with time. In a non-stationary environment, the instantaneous covariance matrix has to be recalculated at each iteration.

However in practice, the non-stationary signal is not suited to decomposition into sinusoidal waves; the notion of frequency loses its effectiveness [34]. This situation gives rise to the idea of instantaneous frequency.

Consider a signal $s(t)$, with its corresponding analytic signal $z(t)$ obtained by Hilbert Transformation. The definition of instantaneous frequency of $s(t)$ is the derivative of the phase of $z(t)$ as follows [34]:

$$f_i = \frac{1}{2\pi}\frac{d}{dt}[\arg z(t)] \tag{2.40}$$

or in another form that will be useful for discrete-time implementation:

$$f_i = \lim_{\delta t \to 0} \frac{1}{4\pi\delta t}(\arg z(t+\delta t) - \arg z(t-\delta t)) \bmod 2\pi \tag{2.41}$$

where $\bmod$ denotes modulo 2π operation. Another very important concept is group delay, which is defined below, indicating the propagation time of the frequency of an impulse traveling through a linear system.

$$\tau_g = -\frac{1}{2\pi}\frac{d}{df}(\theta(f)) \tag{2.42}$$

where θ denotes the phase spectrum of signal.

For a general complex signal, the phase spectrum, $\theta(f)$, and hence the group delay (GD), depends on both the phase and amplitude of the time signal; and the signal phase, $\phi(t)$, and hence instantaneous frequency, also depends on both phase spectrum and magnitude spectrum. Group delay describes the localization of various spectral components of the signal in the time domain [34].

Some methods to estimate instantaneous frequency calculate the partial derivative of phase with respect to time difference like in (2.42). However the time difference of δt cannot tend to be zero due to limited sampling interval. One possible approach is to make use of interpolation technique. In this dissertation we address this issue from other approach to be presented in Chapter 5.

2.8 Summary

In this chapter we have presented the basic concepts of synchronization in communications systems from group delay in wave propagation, fractional time delay in discrete time system, frequency estimation using ML and covariance matrix approach.

For time delay estimation issue, the most obvious method is to calculate the cross-correlation of original signal and its delayed version. The location of peak of cross-correlation reflects the time difference between the original signal and delayed version.

The concept of frequency, which is a well defined quantity for stationary signal, is not suitable for non-stationary signal environment. In practice, the most common definition of frequency is in fact an averaging periodic of signal for a particular time interval. In this dissertation, we refer to frequency as instantaneous frequency. It degenerates into ordinary meaning of frequency for stationary signal. We briefly introduced an ML frequency estimator, such as Generalized Kay frequency estimator. The ML approach usually requires a large sample size and its decision formula can be simplified via exploiting its covariance matrix structure.

The simplest way to estimate instantaneous frequency perhaps is to calculate the derivative of signal phase with respect to time t in accordance with instantaneous frequency definition. However the sampling interval will limit the resolution of estimated frequency and the noise will also affect the results severely.

Chapter 3

Time Delay Estimation

As discussed in previous chapters, coherent demodulation requires carrier synchronization. This means that the carrier phase and the frequency offset should be estimated accurately. We note that there are many methods to track the phase and frequency; however, these techniques are based on analog Phase-locked loop (PLL) [1]. In Section 2.5 and Section 2.7, we note that the common approaches to time delay estimation and frequency estimation, which are based on autocorrelation, require a large computation time, and are not suitable for a non-stationary environment. For two sinusoidal signals with the same frequency , we can calculate the phase difference between them in terms of time difference, however as pointed out in Section 2.4 unless the frequency can be accurately determined, otherwise we need to estimate time difference and phase difference separately because a small estimation error in time difference will cause a large phase error due to a relatively large carrier frequency. In this dissertation, we are concerned with the digital techniques, and in this chapter and Chapter 4, we will first de-

scribe digital existing explicit time delay estimation (ETDE) algorithms, which require only modest amount of computation time. Then in Chapter 4 we will introduce a new improved ETDE algorithm that can give accurate time delay estimate even with a low order interpolation filter.

3.1 Introduction

Time delay estimation (TDE) plays an important role in many applications, including synchronization in communications systems, source location by spatially separated antenna, radar and sonar ranging [13]. Conventional TDE is based on the generalized correlator [35], which requires a priori knowledge of signal and noise spectra. However, resolution is limited by the sampling interval. When high resolution and possibly time-varying TDE is required, especially for coherent demodulation, an on-line interpolation is necessary. Let the signal of interest be

$$x(k) = s(k) + \theta(k) \tag{3.1a}$$

$$y(k) = s(k - D) + \psi(k) \tag{3.1b}$$

where k is the time index ($-\infty < k < \infty$), $s(k) = A(k)e^{j\omega_0 k}$ is original source signal with angular frequency ω_0 assumed known, D is time delay normalized by the sampling interval T, and $A(k)$ is a low-pass signal. The $\theta(k)$ and $\psi(k)$ are the corrupting stationary zero-mean white complex Gaussian noises and they are mutually independent. The main task is to track the delay D as fast as possible. This means the algorithm requires a

moderate amount of computation cycles and should be implemented in real time. As is well-known, the explicit time delay estimator (ETDE) [17], which uses the LMS algorithm, is attractive as the delay estimate $\hat{D}(k)$ is explicitly parameterized in the filter coefficients in the iterative adaptation process. The system block diagram for ETDE, which is similar to that of the adaptive system identification algorithms, is shown in Figure 3.1. The time delay estimate of this algorithm has been shown to be unbiased in

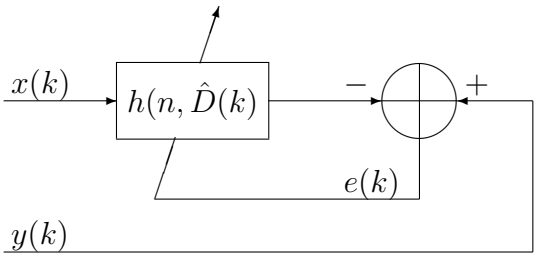

Figure 3.1: System block diagram of the ETDE.

[17] under condition of a broadband white noise-like signal. As mentioned in [13], for a narrow-band signal, the ETDE is actually far from optimal and its performance heavily depends on signal frequency and filter order. This is because the ETDE has been proved to be a poor fractional delay filter (FDF) due to its considerable pass-band ripple [27]. Furthermore, for a wide-band signal, the ETDE has also been proved to be biased in [18]. When $s(k)$ is a narrow-band signal as in our simulation to be described in a later section, we observe that this algorithm is actually biased and its performance depends heavily on signal frequency and filter order because the sinc fractional delay filter has a considerable passband ripple [27]. Though the modulated ETDE (METDE) [13] depends less on signal frequency and filter order, the delay estimate is still biased and

the filter order is high. We observe in our simulation that the mean delay of METDE does not converge to the actual delay.

3.2 Fractional Delay Filter

A fractional delay filter (FDF) is used for band-limited interpolation between samples. The FDF finds applications in numerous fields of signal processing, including communications, array signal processing, speech processing, and music technology. When delaying a signal $x(t)$ by t_D, we get $y(t) = x(t - t_D)$. Converting them into discrete time signal by sampling at time instants $t = k\,T$, T is sampling interval, for simplicity, let T be unity, we can obtain

$$y(k) = x(k - D) \tag{3.2}$$

where D is a positive real number that can be split into an integer and a fractional part as

$$D = Int(D) + d = t_D/T \tag{3.3}$$

When D is a multiple of the adopted sample interval, the delay of the signal works perfectly because the signal samples are simply stored in a buffer memory and we only need to shift the time index to get the delayed signal. For D taking on non-integer values, a band limited interpolation should be used to approximate the delayed value, which lies somewhere between two samples $x(k - Int(D))$ and $x(k - Int(D) - 1)$. The d in

(3.3) is fractional delay of discrete time signal. The $f_s = \frac{1}{T}$ is sampling frequency, and Nyquist angular frequency is $\omega_{Nyquist} = \frac{\pi}{T}$ which is the highest signal frequency that can be completely restored. In this chapter, all the frequencies are normalized by $\omega_{Nyquist}$.

For an ideal discrete-time delay system, the z-domain transfer function is

$$H_{id}(z) = z^{-D} \Leftrightarrow H_{id}(e^{j\omega}) = e^{-j\omega D} \tag{3.4}$$

where $\omega = \frac{\omega_{real}}{\omega_{Nyquist}}$ is the normalized angular frequency, ω_{real} is signal frequency and one solution to this ideal delay system of (3.4) is a so-called ideal fractional delay filter (FDF) whose filter coefficients are [27]

$$h_{id}(n) = \mathrm{sinc}(n - D)\ ,\ -\infty < n < \infty \tag{3.5}$$

This ideal solution is well known but it is an unrealizable filter due to its infinite filter length. It is only of academic value and therefore, one has to find or develop an approximation.

Consider the approximation of the actual overall delay D by an N^{th}-order FIR filter with z-domain transfer function

$$H_D(z) = \sum_{n=0}^{N} h_D(n) z^{-n} \tag{3.6}$$

and the frequency response, phase response, group delay, and phase delay of this filter

are respectively as follows

$$H_D(e^{j\omega}) = \sum_{0}^{N} h_D(n) e^{-j\omega n} \tag{3.7a}$$

$$\arg H_D(e^{j\omega}) = \Theta_D(\omega) \tag{3.7b}$$

$$\tau_g^D = -\frac{\partial \Theta_D(\omega)}{\partial \omega} \tag{3.7c}$$

$$\tau_p^D(\omega) = -\frac{\Theta_D(\omega)}{\omega} \tag{3.7d}$$

The set of filter coefficients $\{h_D(n)\}$ should be chosen such that the chosen norm of the error function in frequency domain given by (3.8) is minimized

$$E(e^{j\omega}) = H_D(e^{j\omega}) - H_{id}(e^{j\omega}). \tag{3.8}$$

The norm of a mathematical object is a quantity that in some sense describes the length, size, or extent of the object. L_2 norm is defined as follows

$$||\phi(x)||_2 = \Big(\int_{-\infty}^{\infty} |\phi(x)|^2 d\,x \Big)^{1/2} \tag{3.9}$$

Now let us consider the approximation to (3.8). When choosing an L_2 norm for the cost function, it is a least square (LS) error design. Via the Parseval relation the frequency-domain error norm can be converted into the time-domain (L_2 norm [27]),

resulting in the following formula

$$\begin{aligned} E_l &= \frac{1}{\pi}\int_0^{\pi} |E(e^{j\omega})|^2 d\,\omega = \frac{1}{\pi}\int_0^{\pi} |H_D(e^{j\omega}) - H_{id}(e^{j\omega})| d\,\omega \\ &= \sum_{n=-\infty}^{\infty} |h_D(n) - h_{id}(n)|^2 \end{aligned} \tag{3.10}$$

There are numerous approaches to approximating the actual delay [27]. In this dissertation we only consider two techniques : the truncated sinc filter and Lagrange interpolation filter. Before discussing particular filters, we first show that if one signal is delayed by D, then the delayed version of the modulated signal can be expressed in terms of the delayed signal as follows. Assume that y is the shifted version of x in (3.2). The corresponding discrete sequences are $\{y(k)\}$ and $\{x(k)\}$, respectively.

Now let $x(k) = x'(k)e^{j\omega_0 k}$, where $x'(k) = x(k)e^{-j\omega_0 k}$. Then

$$x(k-D) = x'(k-D)e^{j\omega_0(k-D)} \tag{3.11}$$

But

$$x'(k-D) = \sum_{n=-\infty}^{\infty} h(n)x'(k-n) \tag{3.12}$$

Substituting (3.12) into (3.11), we obtain

$$\begin{aligned} y(k) = x(k-D) &= \left(\sum_{n=-\infty}^{\infty} h(n)x'(k-n) \right) e^{j\omega_0(k-D)} \\ &= \sum_{n=-\infty}^{\infty} h(n)e^{j\omega_0(n-D)} \left(x'(k-n)e^{j\omega_0(k-n)} \right) \\ &= e^{j\omega_0(k-D)}x'(k-D) = x'(k-D)e^{j\omega_0(k-D)} = x(k-D) \\ \Rightarrow y(k) &= \sum_{n=-\infty}^{\infty} h(n)e^{j\omega_0(n-D)}x(k-n) \end{aligned} \tag{3.13}$$

In the next section we will discuss several existing algorithms: filter definitions and the corresponding delay estimations.

3.2.1 Truncated Sinc FDF and ETDE

The ideal infinitely long FDF defined in (3.3) is unrealizable and hence, one must find an approximation to the ideal solution. We note that the ideal impulse response is a sinc function:

$$h_{id}(n) = \mathrm{sinc}(n-D) \tag{3.14}$$

From (3.10), the L_2-optimal N^{th}-order FIR filter is easily obtained by simply truncating the ideal impulse response to $L = N + 1$ terms. The optimal causal solution can be

expressed as

$$h_D(n) = \begin{cases} \text{sinc}(n - D) & \text{for } M \leq n \leq M + N \\ 0 & \text{otherwise} \end{cases} \tag{3.15}$$

where M is the integer time index of the first nonzero value of the impulse response. The resultant approximation of error (3.10) can be rewritten in the following form by substituting (3.6) into (3.5).

$$E_l = \sum_{n=-\infty}^{M-1} |h_{id,D}(n)|^2 + \sum_{n=M+N+1}^{\infty} |h_{id,D}(n)|^2 \tag{3.16}$$

Here we use $h_{id,D}(n)$ to emphasize explicitly the delay D. We can observe from (3.16) two important characteristics. First, the approximation error decreases as the filter order increases. Second, the smallest error reaches the lowest when the overall delay D is placed at the center of gravity of the ideal impulse response as explained in [27].

Let $n - Round(D) = p$, hence $n = p + Round(D)$. So,

$$\begin{aligned} y(k) &= \sum_{p+Round(D)=-\infty}^{\infty} h_{id}\left(p + Round(D)\right) x(k - p - Round(n)) \\ &= \sum_{p=-\infty}^{\infty} h_{id}(p + Round(D)) x(k' - p) \end{aligned} \tag{3.17}$$

where $k' = k - Round(D)$. It is obvious that the above formula can be simplified as

$$\begin{aligned} y(k' + Round(D)) &= \sum_{p=-\infty}^{\infty} h'_{id}(p)x(k'-p) = x(k-D) \\ &= x(k - Round(D) + Round(D) - D) \\ &= x(k - Round(D) - \tilde{D}) = x(k' - \tilde{D}) \end{aligned} \tag{3.18}$$

where $h'_{id}(p) \equiv h_{id}(p+Round(D))$, $\tilde{D} = D - Round(D)$ lies in the interval $(-0.5, 0.5)$, is so-called subsample or fractional delay; $Round(\bullet)$ denotes rounding to the nearest integer. The corresponding coefficients of an N^{th}-order finite impulse response filter (FIR) which is shown in Figure 3.2, are determined by the formula

$$h_{id,D}(n) = \mathrm{sinc}(n - \tilde{D})\,,\ -M_1 \le n \le M_2 \tag{3.19}$$

where $M_1 = N/2$, $M_2 = M_1$ if N is an even integer and $M_1 = (N-1)/2$, $M_2 = (N+1)/2$ for odd N, and $N \ge 1$.

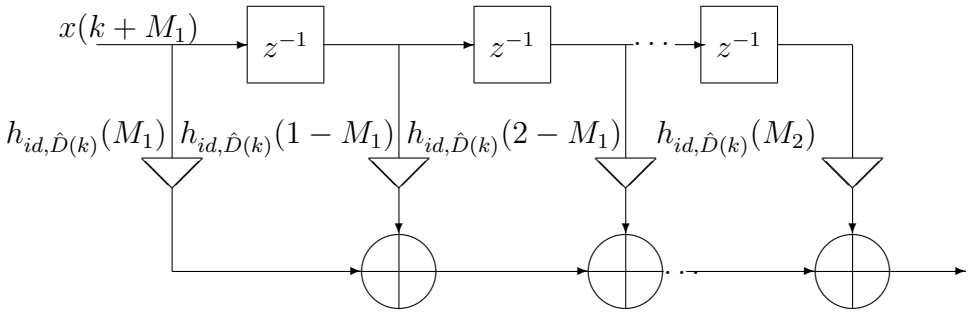

Figure 3.2: Finite impulse response filter.

The ideal impulse response solution to (3.5) is $h_{id}(n) = \mathrm{sinc}(n - D)$, where $-\infty < n < \infty$. When the delay D is an integer, only the sample at $n = D$ contributes to the

output; if the D is a non-integer, there are infinite samples that will contribute to the output. In Figure 3.3, we show that the contribution from the samples, which are far from $n = D$, decays rapidly. In Figure 3.4, we also show the magnitude and phase responses of a truncated sinc filter with the weights $\mathrm{sinc}(n - 5.4),\ 0 \leq n \leq 10$. As can be seen from Figure 3.4, the truncated sinc filter has a well-known feature, the Gibbs phenomenon, which causes ripple in the magnitude response. In Section 3.2, we have given the definitions regarding phase response, group delay and phase delay. All three measures can be used as an indicator of the delay of the system. It is shown in Figure 3.5 that the phase delay and the group delay of the truncated sinc filter are not identical. Which one should be used depends on the particular case.

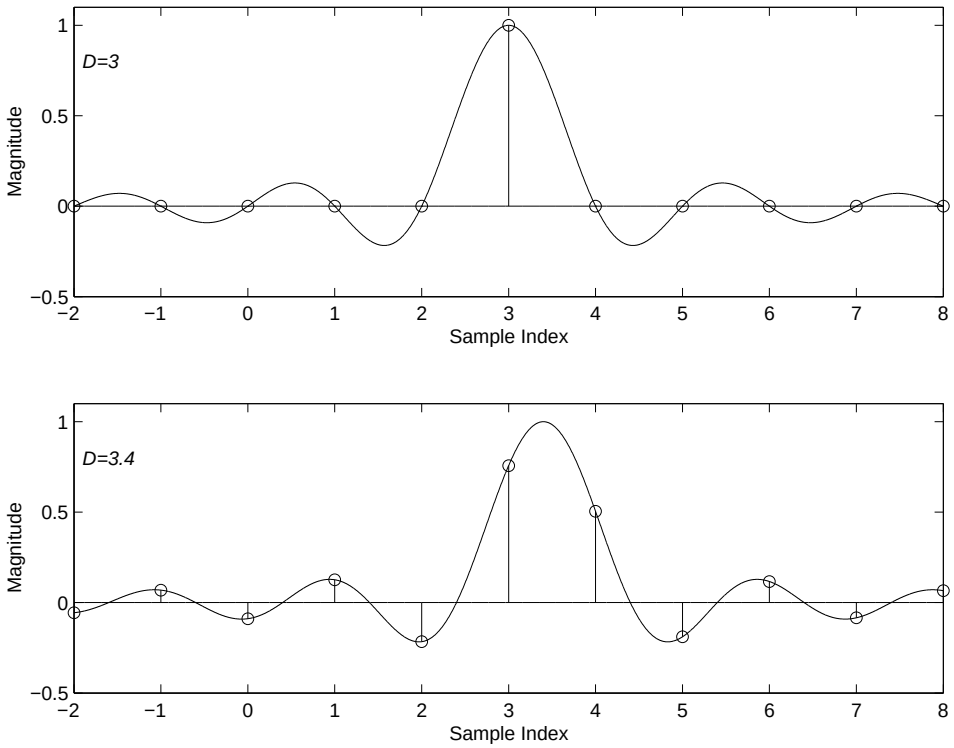

Figure 3.3: Sinc sample function.

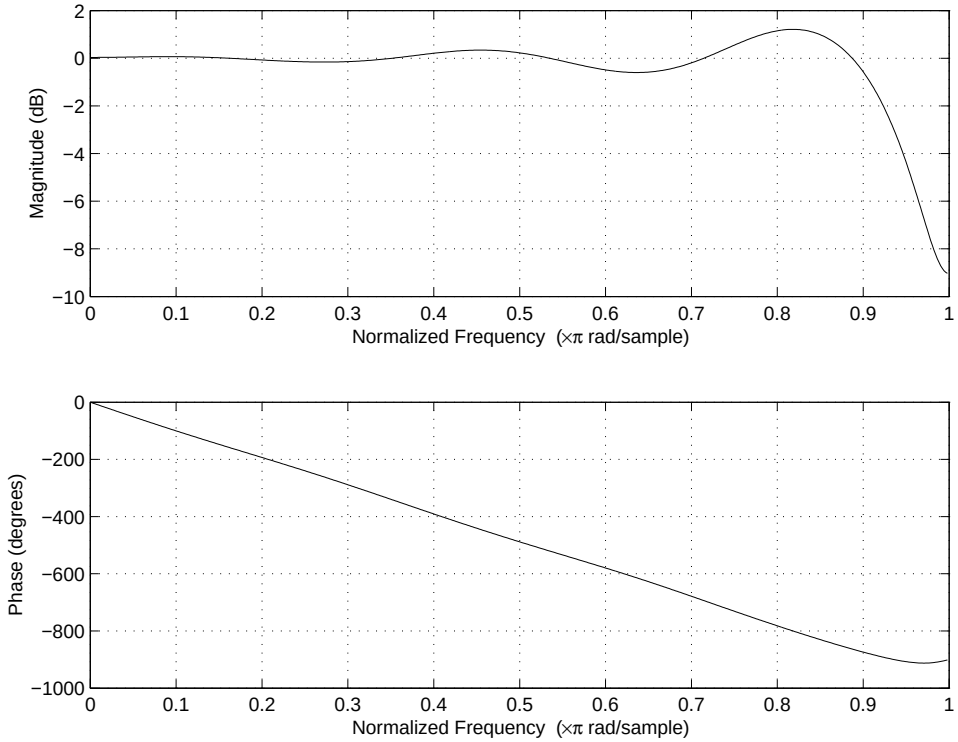

Figure 3.4: Magnitude and phase responses of sinc filter ($\mathrm{sinc}(n-5.4)$, $0 \leq n \leq 10$).

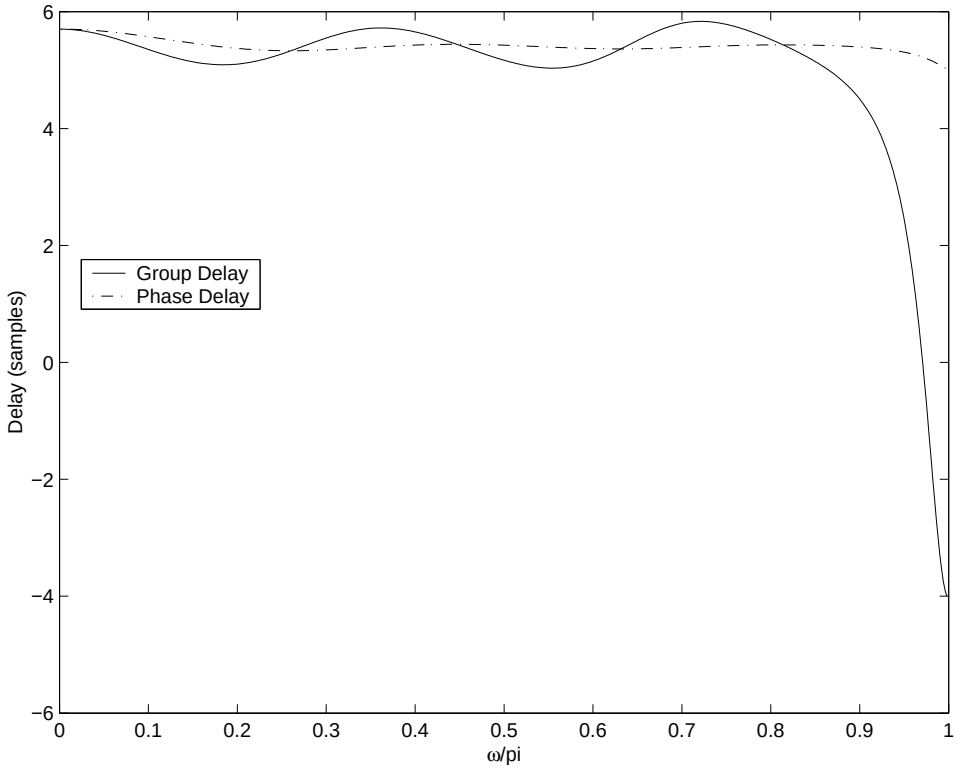

Figure 3.5: Group and phase delay as function of frequency for sinc filter ($\mathrm{sinc}(n-5.4)$, $0 \leq n \leq 10$).

Like the group velocity introduced in Chapter 2, the group delay indicates the delay of the information energy [27]. Based on this knowledge, we choose the group delay as a measure of system delay. The group delay equals the ideal delay D in an ideal discrete-time delay system. The fractional delay here refers to $\tilde{D}$, which can be negative. Hence the total delay can be estimated by assuming

$$\tau_g^D \approx D = M_1 + \tilde{D} \tag{3.20}$$

It should be noted that $\tau_g^D(\omega) = f(\tilde{D},\, \omega)$ is a function of fractional delay filter's parameter $\tilde{D}$ and the normalized angular frequency ω. This unique mapping relationship among $\tau_g^D(\omega)$, $\tilde{D}$, ω means that the group delay caused by the fractional delay filter (FDF) is dependent on the fractional delay $\tilde{D}$.

For ETDE, we replace the $\tilde{D}$ by the $\hat{D}$ estimate and substitute the filter coefficients in (3.19) by $\mathrm{sinc}(n - \hat{D})$. As shown in Figure 3.1, the error is defined as $e(k) = y(k) - \sum_{n=-M_1}^{M_2} h(n,\, \hat{D}(k))x(k-n)$. The ETDE 's delay estimates $\{\hat{D}(k)\}$ are obtained through gradient descent of the instantaneous squared error function $|e(k)|^2$ by differentiating $|e(k)|^2$ in order to locate the global minimum. The ETDE algorithm can be summarized as follows [17]:

$$e(k) = y(k) - \sum_{n=-M_1}^{M_2} \mathrm{sinc}(n - \hat{D}(k))x(k-n) \tag{3.21a}$$

$$\hat{D}(k+1) = \hat{D}(k) - \mu\frac{\partial e^2(k)}{\partial \hat{D}(k)} = \hat{D}(k) - 2\mu e(k) \sum_{n=-M_1}^{M_2} f(\nu)x(k-n) \tag{3.21b}$$

$$f(\nu) = -\frac{\cos(\pi\nu) - \mathrm{sinc}(\nu)}{\nu} \tag{3.21c}$$

The function $f(\nu),\ (\nu = n - \hat{D}(k))$ in (3.21c) is the gradient of the filter coefficient with respect to the time delay estimate $\hat{D}(k)$. For later reference in this dissertation, we refer to $f(\nu)$ as the coefficient adaptation factor (CAF). In the modulated ETDE (METDE) [36], the filter coefficients $\mathrm{sinc}(n - \hat{D}(k))$ in (3.21a) are modified by multiplication of $e^{j\omega(n-\hat{D}(k))}$.

3.2.2 Lagrange Interpolation FIR and ETDE

We have discussed the L_2 norm design of FIR filter in the previous Section 3.2.1. In this sub-section, we will discuss the Lagrange interpolation as a fractional delay filter. The Lagrange interpolation is perhaps the simplest technique to design a FIR filter to approximate the fractional delay $\hat{D}$. In theory, it is equivalent to an FIR filter of which the error function is maximally flat (MF) at a certain frequency, typically at $\omega_0 = 0$. Hence the approximation is at its best close to this frequency and not as good at a more distant frequency. In Figure 3.6, we show the magnitude and phase responses of a Lagrange interpolation filter with $D = 5.4,\ 0 \leq n \leq 10$ (n is filter tap index). In Figure 3.7, we show the phase and group delay of this Lagrange interpolation fractional delay filter. Comparing the magnitude response, phase response, group delay, phase delay with these characteristics of sinc filter in Figure 3.4 and Figure 3.5, we can easily find that the Lagrange interpolation FDF has many advantages over the truncated sinc FDF filter, such as flat magnitude, group delay responses.

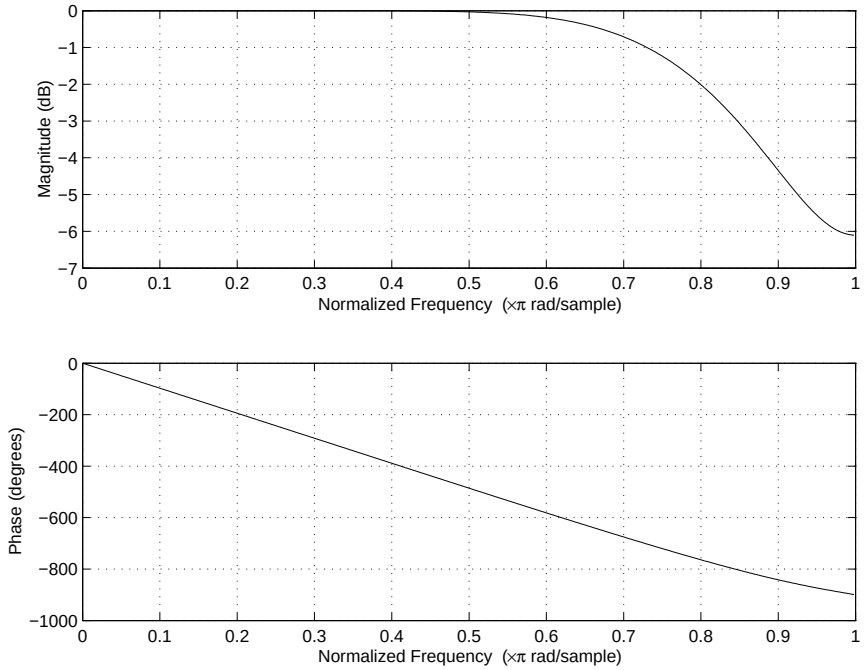

Figure 3.6: Magnitude and phase responses of delay for Lagrange interpolation filter ($D = 5.4$, $0 \leq n \leq 10$).

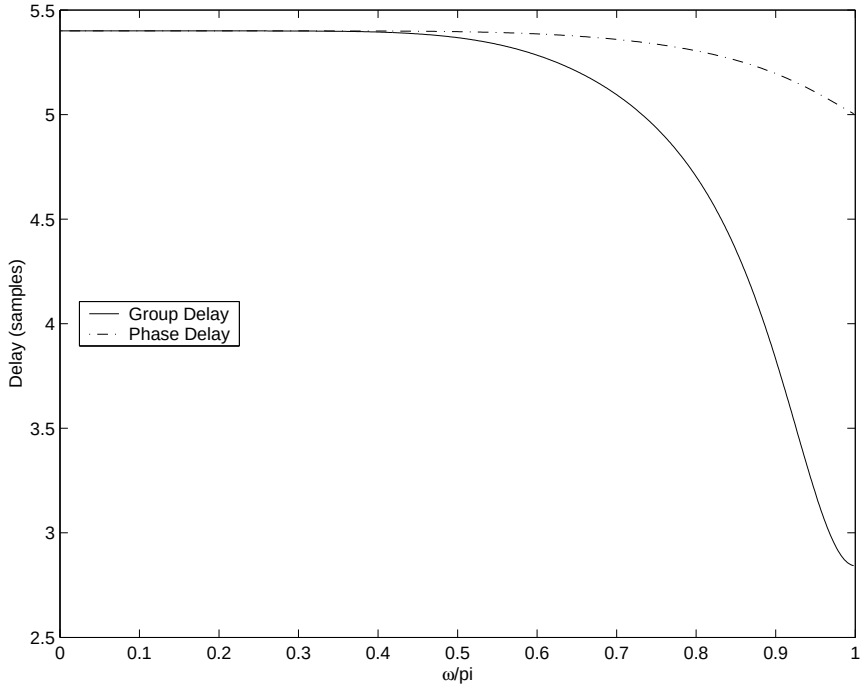

Figure 3.7: Group and phase delay as function of frequency for Lagrange interpolation filter ($D = 5.4$, $0 \leq n \leq 10$).

The Lagrange Interpolation filter (LIF) is equivalent to a maximally flat FDF [27]. MF means that the derivatives up to Nth-order of the frequency-domain error function at a point ω_0 are set to zero, that is,

$$\left.\frac{d^n E(e^{j\omega})}{d\,\omega^n}\right|_{\omega=\omega_0} = 0 \quad \text{for } n = 0, 1, 2, \cdots, N \tag{3.22}$$

where $E(e^{j\omega})$ is the complex error function (3.8) with desired response $H_{id}(e^{j\omega}) = e^{j\omega D}$. The coefficients of this LIF, which is maximally flat at $\omega_0 = 0$, are obtained through the formula below via differentiation and insertion of the value ω_0 in (3.22), and the solution can be written in an explicit form [23].

$$h_D^0(n) = \prod_{\substack{i=0 \\ i\neq n}}^{L-1} \frac{D-i}{n-i} \tag{3.23}$$

The superscript for $h_{\hat{D}}^0(n)$ in (3.23) is used to emphasize that the maximum flatness is at $\omega_0 = 0$.This maximally flat region can be shifted to another frequency ω_0 by applying a complex modulation [23]. Actually it is just a process of frequency shifting [37]. We note that $D = -M_1 + \hat{D}(k)$, hence the filter coefficients can be written in the following form:

$$h_{\hat{D}(k)}^0(n) = \prod_{\substack{i=-M_1 \\ i\neq n}}^{M_2} \frac{\hat{D}(k)-i}{n-i} \tag{3.24}$$

where M_1, M_2 are defined before in (3.19), and $\hat{D}(k)$ lies in the range $(-0.5, 0.5)$. Therefore, the modulated coefficients are

$$h_{\hat{D}(k)}(n) = e^{j\omega_0(n-\hat{D}(k))} h^0_{\hat{D}(k)}(n) \tag{3.25}$$

We can expand (3.24) int a polynomial in $\hat{D}$ in the following form:

$$h^0_{\hat{D}}(n) = \sum_{p=0}^{N} a_p \hat{D}^p(k) \tag{3.26}$$

In this dissertation, this set of expressions is obtained directly by expanding (3.24) and furthermore we can obtain the partial derivatives of $h_{\hat{D}}(n)$ with respect to $\hat{D}(k)$, $n = -M_1, -M_1 + 1, \cdots, M_2$ with respect to $\hat{D}(k)$ as follows

$$f(n, \hat{D}(k)) = \sum_{p=1}^{N} p a_p \hat{D}^{p-1}(k) \tag{3.27}$$

In [13], Dooley and Nandi suggested a minimum mean squared estimation error (MMSE) criterion for selecting an optimum fractional delay filter (FDF) for ETDE but this criterion was amenable only to a trial-and-error simulation approach. So in [13], the authors gave the simulation results without further proofs and derivations, such as convergence to actual delay, standard deviation of time delay estimate, the algorithm's valid signal frequency range, the step-size's range, and convergence rate. Though the signal could be band-pass filtered to obtain high SNR beforehand, the practical system should be usually operated under an SNR range of 20 to 40dB. The performance of the

algorithm should be also tested under this condition.

In summary, the MLETDE algorithm which incorporates the modulated Lagrange interpolation FDF filter into the ETDE [17] is summarized as follows [36]:

$$e(k) = y(k) - \sum_{n=-M_1}^{M_2} h_{\hat{D}(k)}(n)x(k-n) \tag{3.28a}$$

$$\hat{D}(k+1) = \hat{D}(k) - 2\mu Re\left\{e^{\star}(k)\sum_{n=-M_1}^{M_2} f(n,\hat{D}(k))x(k-n)\right\} \tag{3.28b}$$

$$f\left(n,\hat{D}(k)\right) = e^{j\omega_0(n-\hat{D}(k))}\left[f^0(n,\hat{D}(k)) - j\omega_0 h^0_{\hat{D}(k)}(n)\right] \tag{3.28c}$$

$$f^0(n,\hat{D}(k)) = \frac{\partial h^0_{\hat{D}(k)}(n)}{\partial \hat{D}(k)} \tag{3.28d}$$

The $f^0(n,\hat{D}(k))$ in (3.28d) is the CAF in the Lagrange FDF.

3.3 Simulation Results

In the previous sections we have described several existing time delay estimation algorithms such as ETDE, METDE, LETDE, MLETDE. In this section we will present results of simulation tests that have been conducted to verify the performance of these algorithms for single tone signal. The $\theta(k)$, $\phi(k)$ are uncorrelated zero-mean, white Gaussian processes. In the simulations, the signal powers of $x(k)$ and $y(k)$ were set at the same level, also their SNR were set to be the same.

The results of simulations are summarized as follows:

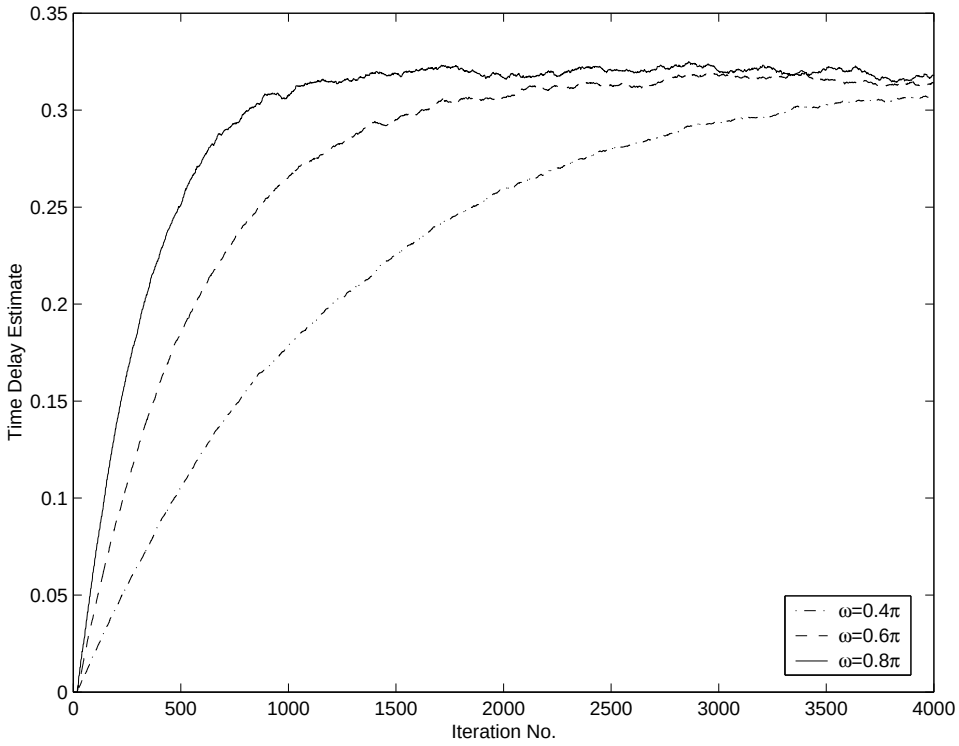

Figure 3.8: Convergence of ETDE for single tone signal, $\sigma_s^2 = 1$, $N = 20$, $\mu = 0.0003$, $\mathrm{SNR} = 20$dB.

3.3.1 SINC FDF ETDE and METDE

The step-size was as $\mu = 0.0003$, the actual delay was set to be 0.3, the filter order was $N = 20$, the noise was set to 0. In Figure 3.8, we show that the convergence performance of ETDE is far from optimal for the single sinusoid signals with the frequencies $\omega = 0.4\pi,\ 0.6\pi,$ and 0.8π. As can be seen from the figure, the delay estimates are biased from the actual delay even using a relative longer filter length. This is because the sinc filter exhibits a considerable passband ripple in its magnitude response [27]. From the simulations we also show that the convergence rate of ETDE depends on signal frequency.

In Figure 3.9, the step-size was set to be $\mu = 0.003$, other conditions were set to be

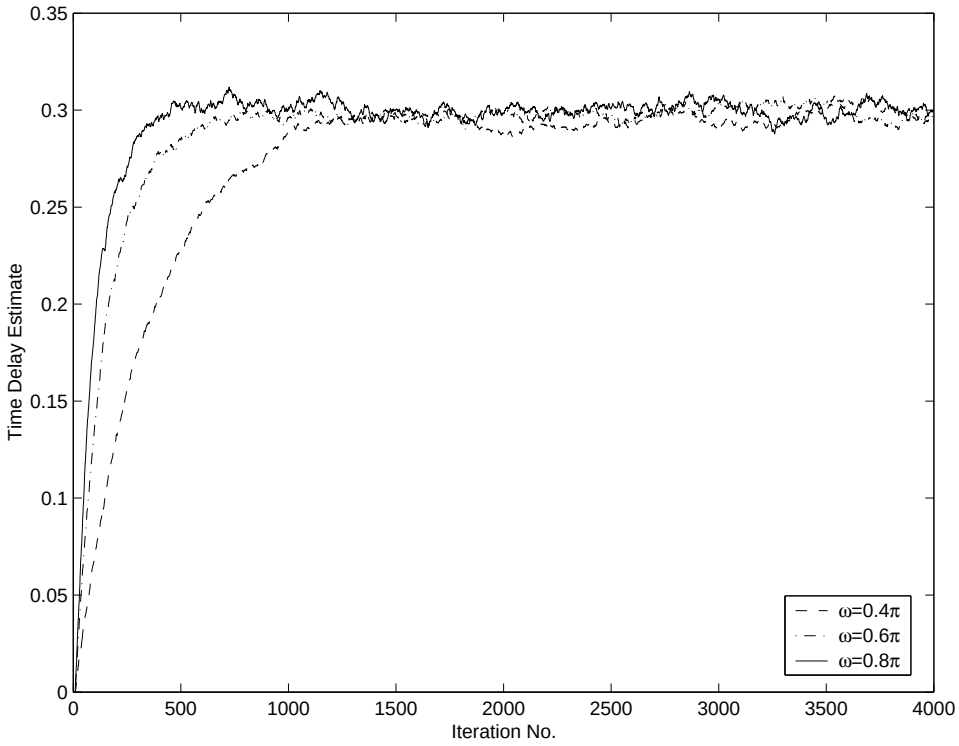

Figure 3.9: Convergence of METDE for single tone signals, $\sigma_s^2 = 1$, $N = 10$, $\mu = 0.003$, $\mathrm{SNR} = 20$dB.

the same as in Figure 3.8. As can be seen from Figure 3.9 , METDE is also biased for sinusoid signal due to sinc-based filter's frequency response characteristic. In Figure 3.9 we show that the convergence rate of METDE depends on signal frequency.

3.3.2 Lagrange Interpolation FDF ETDE and MLETDE

Lagrange interpolation ETDE (LETDE) is reported to be biased in [13]. In Figure 3.10, the time delay estimate, $\hat{D}$, can be seen to be biased from the actual delay of 0.3. The step-size was set as $\mu = 0.003$ and $\mu = 0.0003$, the filter order was set to $N = 2$, the signal power was $\sigma_s^2 = 0.5$, frequency was $\omega = 0.9\pi$, the signal-to-noise ratio (SNR) was set to 50dB. As can be seen from the figure, the time delay estimate fluctuates when

the step-size becomes larger and it is also biased.

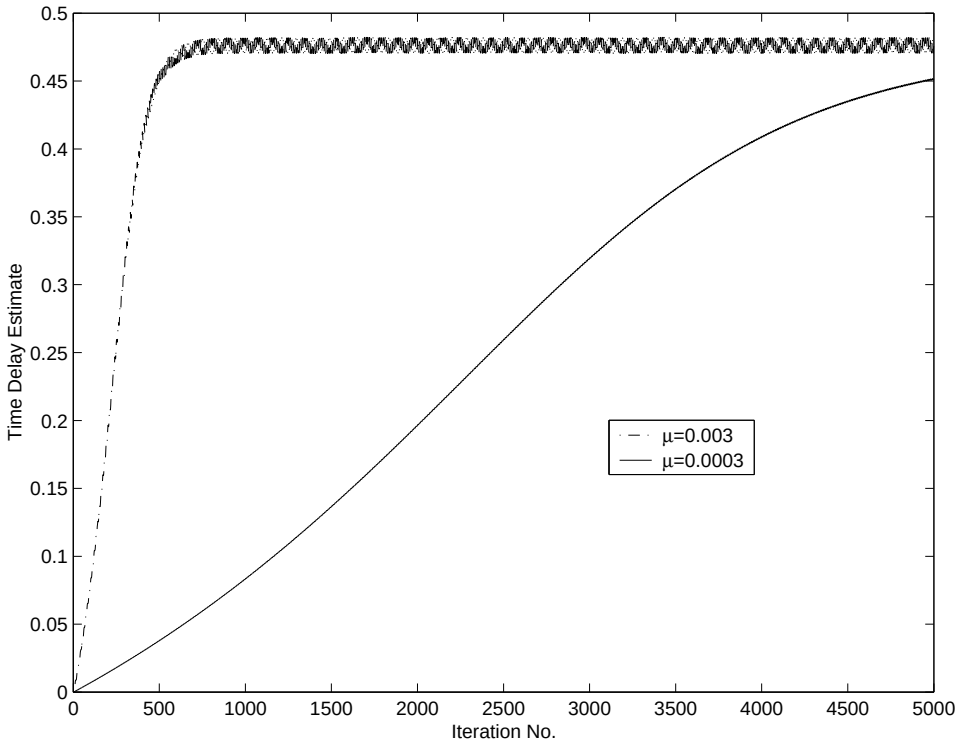

Figure 3.10: The convergence performance of LETDE algorithm for single tone signal.

We tested the LETDE algorithm for the different single tone signals at $\omega = 0.2\pi$, $0.4\pi,\ 0.6\pi$, and 0.8π. The step-size was set to be $\mu = 0.003$, signal power $\sigma_s^2 = 1$, and the filter order $N = 2$. As can be seen from Figure 3.11 the convergence rate is related to the signal frequency. The delay estimate, $\hat{D}$ becomes much more biased from the actual delay $D = 0.3$ when signal frequency increases.

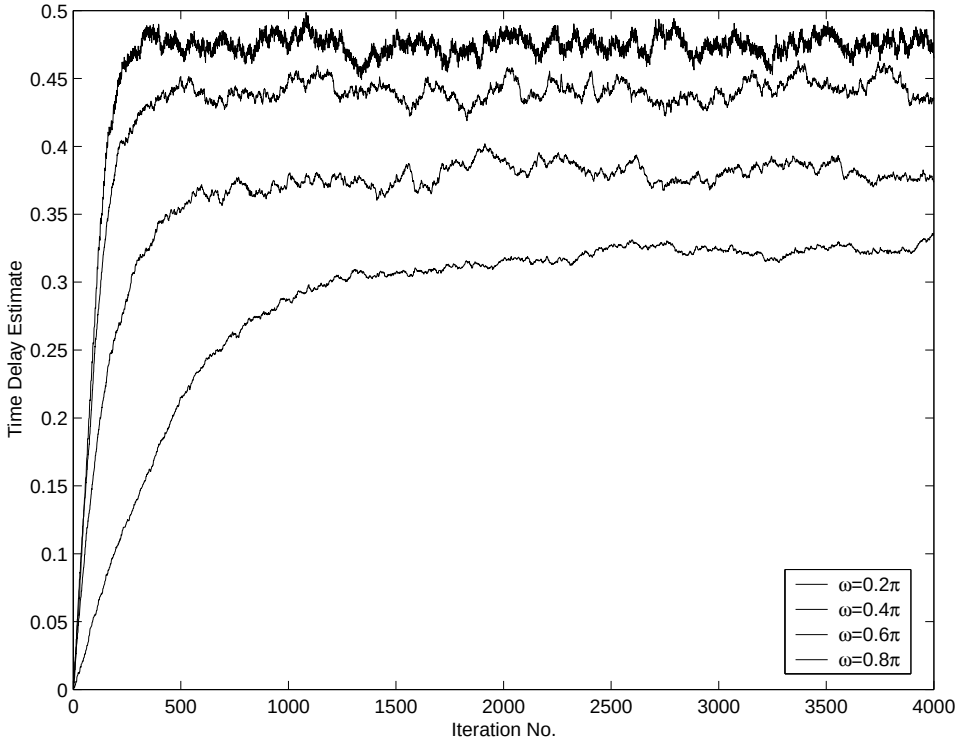

Figure 3.11: The convergence performance of LETDE algorithm for single tone signals, $\sigma_s^2 = 1$, $N = 2$, $\mu = 0.003$, $\mathrm{SNR} = 20$dB.

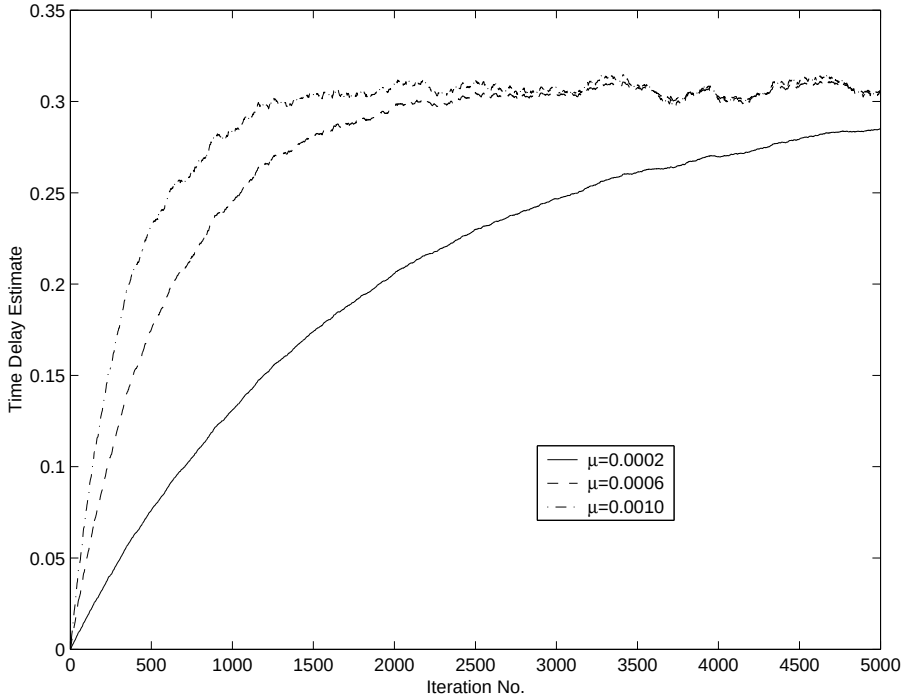

Figure 3.12: Convergence performance of MLETDE algorithm for single tone signal, $\mathrm{SNR} = 20$dB.

The MLETDE was also tested. In Figure 3.12, the signal power was set as $\sigma_s^2 = 1$, the step-size were set to $\mu = 0.0002,\ 0.0006\ , 0.001$, the filter order was set $N = 2$, the SNR was set to 20dB, and the signal frequency was 0.4π. From Figure 3.12 we see that MLETDE is biased.

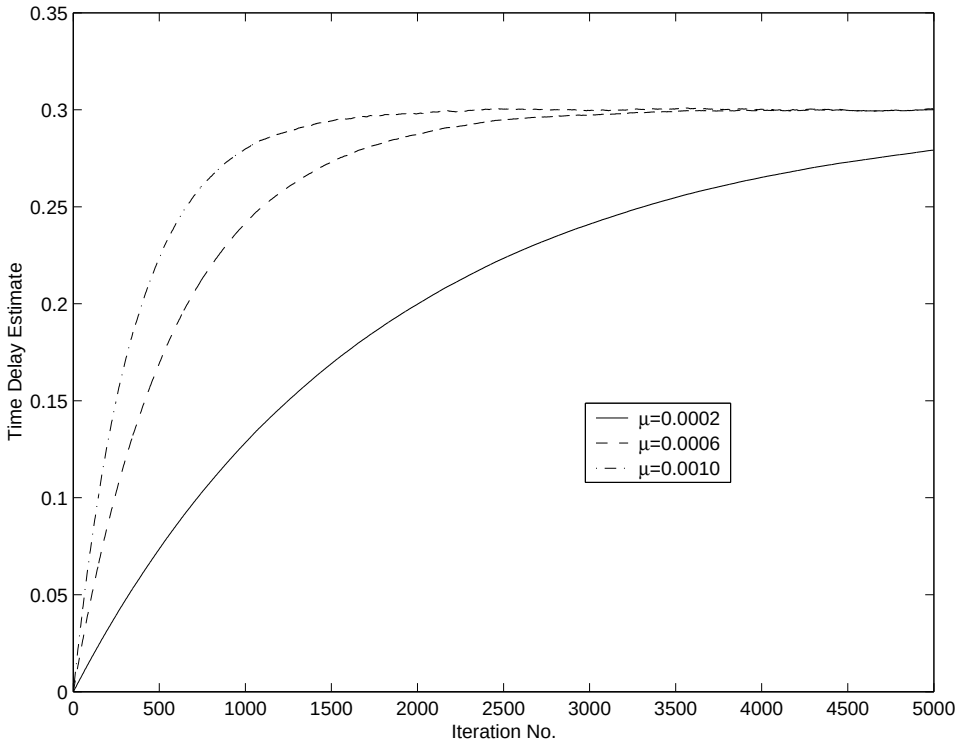

Figure 3.13: Convergence performance of MLETDE algorithm for single tone signal, $\mathrm{SNR} = 40$dB.

We also tested the MLETDE algorithm under a higher SNR of 40dB. Other conditions were set as those in Figure 3.12. In Figure 3.13, we show that the delay estimate is closer to the actual delay when the SNR increases from 20dB to 40dB.

In Figure 3.14, we show the time delay estimate of MLETDE for noise free, single tone signals at various frequencies . The step-sizes were set to be 0.0002, 0.0006, and 0.001. The actual delay was set to 0.3. As can be seen, the MLETDE algorithm has

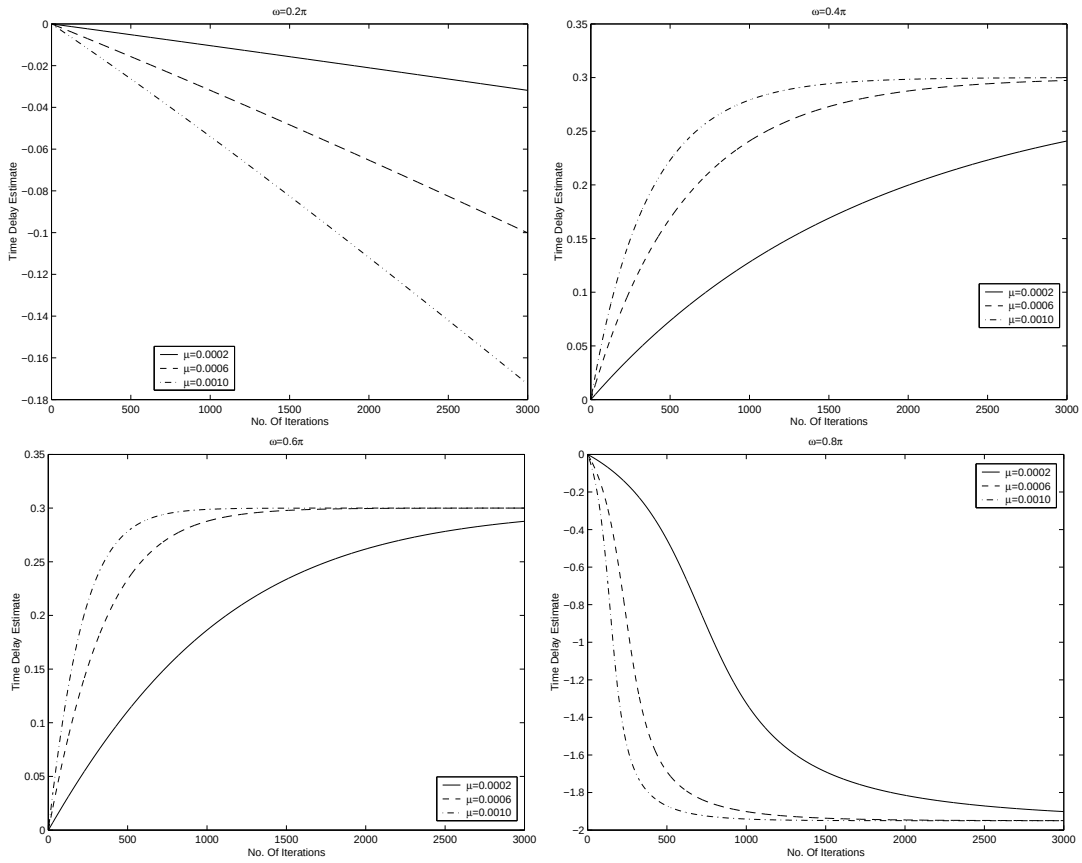

Figure 3.14: Performance of MLETDE algorithm for noise-free, single tone signal, filter order $N = 2$, actual delay $D = 0.3$, $\sigma_s^2 = 1$.

a limited center signal frequency range. At some frequencies such as $0.2\pi,\ 0.8\pi$, the simulation results indicated that the MLETDE failed.

3.4 Conclusion

The goal of this dissertation is to find an unbiased algorithm which can be implemented on real time (lower filter order) to estimate the time delay. From these simulation studies we found that the performance of time delay estimate depended heavily on signal frequency whether it was modulated or unmodulated algorithm for ETDE, METDE,

LETDE, and MLETDE. It was clear that ETDE, METDE, LETDE were biased. In general, modulated algorithms outperformed the corresponding unmodulated ones, and Lagrange interpolation FIR filter has many more advantages over the truncated sinc FIR filter in time delay estimate such as flat frequency response and group delay. From the simulation results also we see that the selection of the step-size μ played an important role which will be discussed in Chapter 4. Finally we should point out that MLETDE does not work when signal frequency was higher than 0.8π. The accuracy of MLETDE also depends on filter order.

After studying the existing explicit time delay estimation algorithm, we can find the limitations of these algorithms. In Chapter 4, we will develop and study the statistic characteristics of a new so-called Mixed Modulated Explicit Time Delay Estimation (MMLETDE) algorithm, which draws from both explicit time delay estimation and modulated Lagrange interpolation.

Chapter 4

Mixed Modulated Lagrange ETDE

We have examined several existing algorithms in Chapter 3. The purpose of this chapter is to find an algorithm for delay estimation that can provide an unbiased estimate with as small a filter order as possible for easy implementation, and we will develop a new algorithm: mixed modulated Lagrange interpolation ETDE (MMLETDE), which can give an unbiased time delay estimation for single tone and a band-limited signal. The convergence and learning characteristic will be discussed in detail in this chapter.

4.1 Mixed Modulated Lagrange ETDE

From our simulation, we have found that the modulated Lagrange explicit time delay estimation (MLETDE) of [36] has a limited range in the signal center frequency variation. In Appendix A, we show that (3.28d) in Section 3.2.2 can be replaced by $f(\nu)$ which is defined in (3.21c). The $f^0(n, \hat{D}(k))$ in (3.28d) is the CAF in the Lagrange FDF. This $f^0(n, \hat{D}(k))$ can be replaced by $f(\nu)$. We further develop it into a new formula,

and now propose a so-called mixed modulated Lagrange explicit time delay estimation (MMLETDE) algorithm, which is formulated as follows and its validity is proved in Appendix B.

$$e(k) = y(k) - \sum_{n=-M_1}^{M_2} h_{\hat{D}(k)}(n)x(k-n) \tag{4.1a}$$

$$\hat{D}(k+1) = \hat{D}(k) - 2\mu\, Re\left\{e^*(k) \sum_{n=-M_1}^{M_2} g(\nu)x(k-n)\right\} \tag{4.1b}$$

$$g(\nu) = e^{j\omega_0\nu}\left[f(\nu) - j\omega_0 \mathrm{sinc}(\nu)\right] \tag{4.1c}$$

$$h_{\hat{D}(k)}(n) = e^{j\omega_0(n-\hat{D}(k))} h^0_{\hat{D}(k)}(n) \tag{4.1d}$$

where

$$\nu = n - \hat{D}(k)$$

This essentially means that in the delay estimate adaptation process, the CAF of the Lagrange FDF is replaced by the CAF of the truncated sinc FDF given in (3.21c). We will show in the simulation to be described in the following section that the new algorithm can give an accurate time delay over a wide frequency range even the filter order is low.

4.2 Convergence Characteristics of MMLETDE

4.2.1 Unbiased Convergence of MMLETDE

In the MMLETDE algorithm,a modulated Lagrange fractional delay filter (FDF), Lagrange interpolation filter is used to approximate the delay of one signal.The delayed signal is compared with the source signal adaptively. The time delay is parameterized into the filter coefficients and the adaptation algorithm for the coefficients is based on the gradient of the truncated sinc filter coefficients with respect to the explicit time delay estimate. The time delay estimate at each iteration is given by

$$\hat{D}(k+1) = \hat{D}(k) - 2\mu\, Re\left\{ e^* \sum_{n=-M_1}^{M_2} g(\nu)x(k-n) \right\} \tag{4.2}$$

where

$$e(k) = y(k) - \sum_{n=M_1}^{M_2} h_{\hat{D}(k)}(n)x(k-n) \tag{4.3}$$

We consider a narrow-band signal with known center frequency of ω_0, $s(k) = A(k)e^{j\omega_0 k}$. Substituting (3.1a), (3.1b) into (4.3), we have

$$\begin{aligned} e(k) &= s(k-D) + \psi(k) \\ &\quad - \sum_{n=-M_1}^{M_2} h_{\hat{D}(k)}(n)s(k-n) - \sum_{n=-M_1}^{M_2} h_{\hat{D}(k)}(n)\theta(k-n) \end{aligned} \tag{4.4}$$

The modulated Lagrange interpolation for a narrow-band signal given by the third term of (4.4) can be written as,

$$\begin{aligned}
&\sum_{n=-M_1}^{M_2} h_{\hat{D}(k)}(n)A(k-n)e^{\omega_0(k-n)} \\
&= \sum_{n=-M_1}^{M_2} h^0_{\hat{D}(k)}(n)e^{j\omega_0(n-\hat{D}(k))}A(k-n)e^{j\omega_0(k-n)} \\
&= e^{j\omega_0(k-\hat{D}(k))} \sum_{n=-M_1}^{M_2} h^0_{\hat{D}(k)}(n)A(k-n) \approx e^{j\omega_0(k-\hat{D}(k))}A(k-\hat{D}(k)) \\
&= s(k-\hat{D}(k))
\end{aligned} \tag{4.5}$$

In arriving at (4.5), we have made the approximation that $\sum_{n=-M_1}^{M_2} h^0_{\hat{D}(k)}(n)A(k-n) \approx A(k-\hat{D}(k))$. This approximation is error-free when $A(k)$ is a constant, because the remainder or truncation error of Lagrange interpolation, which is a function of the $(N+1)^{\text{th}}$ derivative of $A(k)$ is equal to zero [38]. For a slowly varying $A(k)$ in the case of a narrow-band signal, we assume that the approximation is almost error-free.

However we cannot make such an approximation for a wide-band noise $\theta(k)$, therefore we retain the Lagrange interpolation for the delayed version of $\theta(k)$ as in the last term of (4.4). For simplicity, we will use ω to denote ω_0.

In Appendix C, we prove the convergence formula as follows

$$E\big[\hat{D}(k+1)-D\big] = E\big[\hat{D}(k)-D\big]\big(1+2\mu\sigma_s^2\omega^2\big) \tag{4.6}$$

After k iterations it follows from (4.6) that

$$E\big[\hat{D}(k)\big] = D + \big(\hat{D}(0) - D\big)\big(1 + 2\mu\sigma_s^2\omega^2\big)^k \tag{4.7}$$

It can be seen from (4.7) that $E[\hat{D}(k)]$ will converge to the actual delay D when k tends to infinity, provided that $0 < 1 + 2\mu\sigma_s^2\omega^2 < 1$. This implies that the step-size should satisfy the following condition

$$-\frac{1}{2\sigma_s^2\omega^2} < \mu < 0 \tag{4.8}$$

4.2.2 Learning Characteristics of MMLETDE

We consider next the variance of the time delay estimate $\hat{D}(k)$ by calculating the convergence equation of the mean square delay error, $\epsilon(k)$, which is defined as

$$\epsilon(k) = E\Big[\Big(D - \hat{D}(k)\Big)^2\Big] = E\big[\hat{D}^2(k)\big] - 2D\,E\big[\hat{D}(k)\big] + D^2 \tag{4.9}$$

In Appendix D, the learning characteristics of $\epsilon(k)$ is shown to be

$$\epsilon(k) = C^k\big(\hat{D}(0) - D\big)^2 + B\frac{1 - C^k}{1 - C} \tag{4.10}$$

$$C = 1 + 4\mu\sigma_s^2\omega^2 + 2\mu^2\left\{2\sigma_s^4\omega^4 + \sigma_s^2\sigma_n^2\omega^2\pi^2/3\right\} \tag{4.11}$$

$$B = 2\mu^2\left\{-\sigma_n^4\omega^2 + \left\{\sigma_n^4\left(\frac{\pi^2}{3} + \omega^2\right) + \sigma_s^2\sigma_n^2\omega^2\right\}\right\}(1 + E(G)) \tag{4.12}$$

where $G = \left[\sum_p h^0_{\hat{D}(k)}(p)\right]^2$

The sufficient condition for convergence of the algorithm can be obtained by combining (4.8) and $0 < C < 1$ in (4.10). The new condition for convergence becomes

$$\max\left\{-\frac{1}{\sigma_s^2\omega^2+\sigma_n^2\pi^2/6},\ -\frac{1}{2\sigma_s^2\omega^2}\right\} \tag{4.13}$$

Moreover, the mean square error of the delay estimate in the steady state will equal the delay variance, $\mathrm{var}(\hat{D})$, given by

$$\mathrm{var}(\hat{D}) = \epsilon(k) \underset{k\to\infty}{=} \frac{B}{1-C} \tag{4.14}$$

Substituting (4.11) and (4.12) into (4.14), normalizing the signal power $\sigma_s^2 = 1$, and assuming that $SNR = \frac{\sigma_s^2}{\sigma_n^2} >> 1$, thereby allowing the terms containing σ_n^4 in (4.12) to be neglected, (because the signal frequency should not tend to be zero due to (4.7), the middle term in (4.12) can also be dropped), we have

$$\mathrm{var}(\hat{D}) = \frac{\mu\sigma_n^2\sigma_s^2\omega^2\left(1+E[G]\right)}{-2\sigma_s^2\omega^2-\mu\left[2\sigma_s^4\omega^4+\sigma_s^2\sigma_n^2\omega^2\pi^2/3\right]} \tag{4.15}$$

Further, μ is a small value compared to the signal power, we thus obtain

$$\mathrm{var}(\hat{D}) \approx \frac{\mu\left(1+E[G]\right)}{-2/\sigma_n^2} \approx -\mu\frac{1+\bigcirc(1)}{2\,\mathrm{SNR}} \tag{4.16}$$

In (4.16), we have expressed $E[G] = \bigcirc(1)$. This is arrived at because we know that, when $\hat{D}(k) = 1$, since only one coefficient is equal to 1 while the rest are equal to zeros

[39]. For $\hat{D}(k)$ other than an integer, we do not know the exact value of G, but we conjecture that G is of the order of one.

4.3 Simulation Results

Simulations have been conducted to verify the proposed MMLETDE algorithm. We tested the single sinusoidal signal and also a band-limited signal with flat spectrum. The $\theta(k)$, $\phi(k)$ are uncorrelated zero-mean Gaussian variables. The SNR of both inputs $x(k)$ and $y(k)$ were set to be the same. The band-pass signal was generated by filtering a discrete time white noise and down sampling the filtered signal at different time offsets. Thus we obtained the source signal and its delayed version. The bandwidth of the band-pass signal is variable within the range of $(0 \rightarrow \pi)$.

In Figure 4.1, we show that the replacement of (3.28d) for MLETDE in Section 3.2.2 works. The signals were two band-limited white signals with center frequency at $\omega = 0.85\pi$, and the bandwidth was 0.3π. The step-size was set to be $\mu = 0.0003$, and $\mathrm{SNR} = 20$dB. The actual delay was set to 0.3. As can be seen, MLETDE with a replacement of (3.28d) can converge to the actual delay under $\mathrm{SNR} = 20$dB.

In Figure 4.2, the solid line curve is for one observation of time delay estimate and the dash line is ensemble average over 300 trials versus the number of iterations. The signal frequency was set to 0.99π, the step-size was equal to 0.0003, the filter order was also set to 2, the SNR was set to 0dB. As can be seen the ensemble average at each iteration is closer to the actual delay 0.3.

In Figure 4.3, we used a bandpass white noise signal to simulate a narrow band

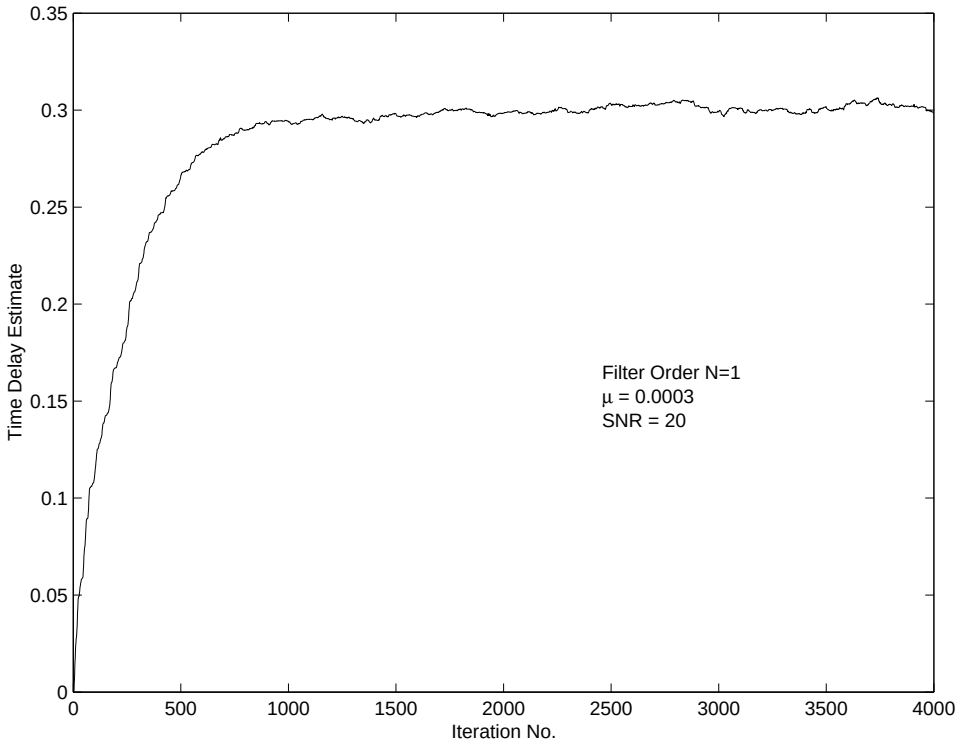

Figure 4.1: Performance of (3.28d) replacement.

signal. The conditions were set as in Figure 4.2, the ensemble average of time delay estimate over 300 trials versus the number of iterations is very close to the actual delay 0.3.

In Figure 4.4(a) we show the convergence characteristics of the MMLETDE with $N = 2$, computed from (4.6), together with the corresponding simulation results. The test signal was a single tone at frequencies of $\omega = 0.3\pi,\ \omega = 0.5\pi,\ \omega = 0.7\pi$ and $\omega = 0.9\pi$. The SNR was set to 20dB, the step-size was $\mu = 0.0003$. As can be seen from the figure, the simulation results match the theory very closely, thus verifying our convergence analysis. Recall from (4.6) that the signal frequency, ω, appears together with the step size, μ, in the same term. Therefore, the convergence speed of the MMLETDE is influenced by the signal frequency. The larger is the frequency, the faster is the conver-

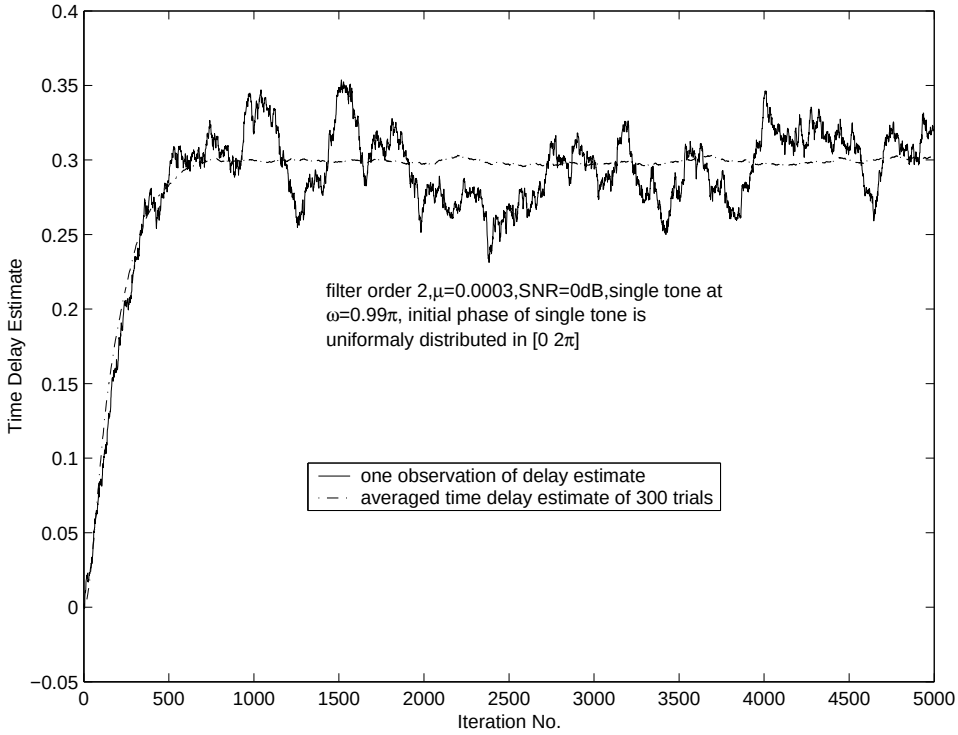

Figure 4.2: Convergence characteristics of MMLETDE for single sinusoid, $\mu = 0.0003$, $\mathrm{SNR} = 0\mathrm{dB}$, $\sigma_s^2 = 1$.

gence. This is now verified by the simulation results shown in Figure 4.4(a).

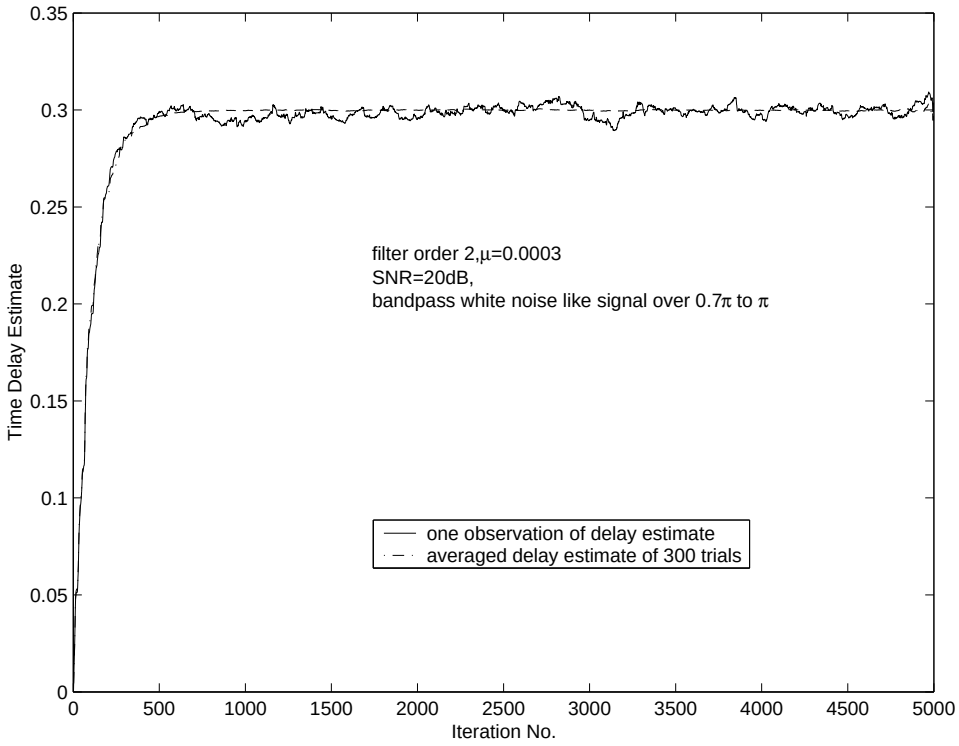

Figure 4.3: Performance of MMLETDE algorithm, bandpass white-noise signal.

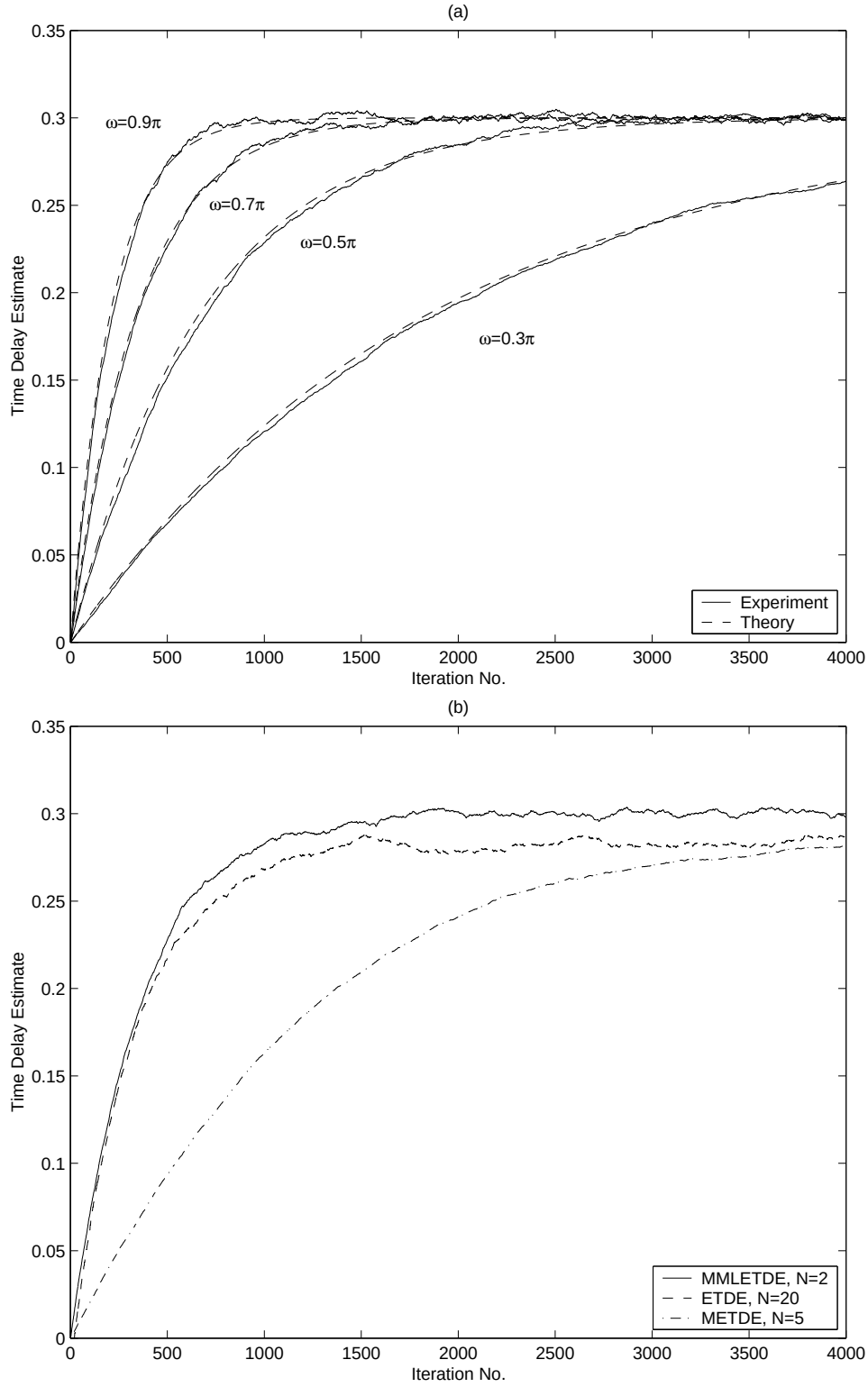

Figure 4.4: (a) Convergence rate of MMLETDE, $N = 2$, $\mathrm{SNR} = 20\mathrm{dB}$, $\mu = 0.0003$. (b) Comparison of convergence rates of MMLETDE, ETDE and METDE, $\omega = 0.7\pi$, $\mathrm{SNR} = 20\mathrm{dB}$, $\mu = 0.0003$.

In Figure 4.4(b), we compare the convergence characteristics of MMLETDE, ETDE and METDE algorithms for sinusoidal signal at $\omega = 0.7\pi$, SNR = 20dB and $\mu = 0.0003$. The actual delay was set to 0.3. As can be seen from the figure, the METDE has a much slower convergence rate than MMLETDE and ETDE. The ETDE has about the same rate of convergence as MMLETDE, but the algorithm converges to a biased delay value.

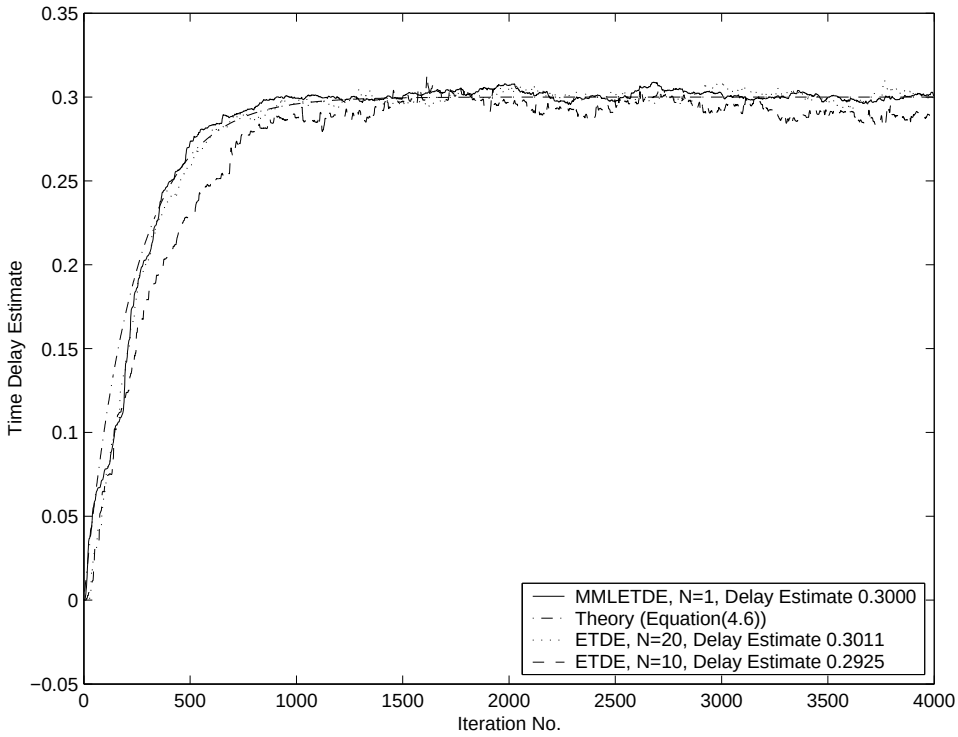

Figure 4.5: Comparison of convergence performance of MMLETDE, ETDE for a band-limited signal at center frequency $\omega_0 = 0.85\pi$, bandwidth of 0.3π, $\mu = 0.0003$, $\sigma_s^2 = 1$.

In Figure 4.5, we compare the convergence characteristics of MMLETDE and ETDE for a bandpass signal with flat spectrum at center frequency $\omega = 0.85$, and a bandwidth of 0.3π. The actual delay was set to 0.3. The convergence curve of MMLETDE matches the theoretical curve obtained from (4.6) closely. And even though a filter order of only $N = 1$ is used, the MMLETDE algorithm converges to the actual delay value. On the

other hand, the ETDE algorithm requires a much longer filter in order to converge to the real delay value. Even with a filter order of as high as 20, there is still a slight bias in the delay estimate.

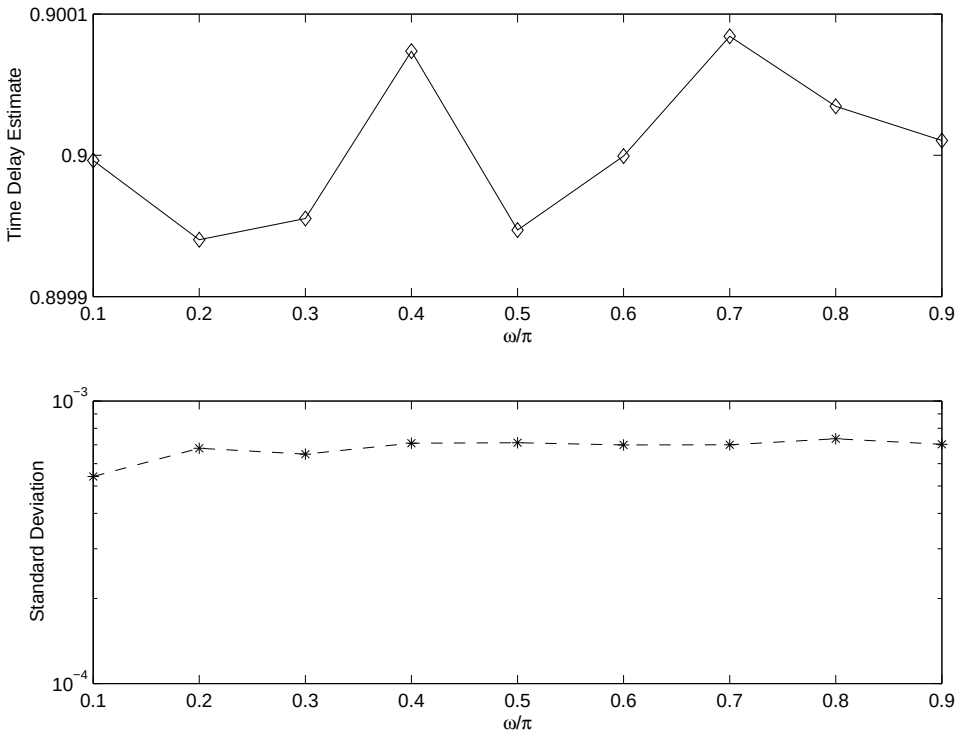

Figure 4.6: Standard deviation and time delay estimate of MMLETDE for single sinusoid signal, $\mu = 0.0025$, $\mathrm{SNR} = 40$dB,filter order $N = 2$, $\sigma_s^2 = 1$.

In Figure 4.6, we show the simulation results on time delay estimate and standard deviation for different single sinusoidal signals with frequency ranging from $\omega = 0.1\pi$ through $\omega = 0.9\pi$. The actual delay was set to 0.9. The step size was set to 0.0025. The time delay estimate was the average of the 4000^{th} to the 6000^{th} iterations. For $\omega = 0.1\pi$, we averaged the delay estimate between the 14000^{th} to the 16000^{th} iterations because with a lower frequency the algorithm converged relatively slower. From these results we can see that the time delay estimate is accurate even under a short filter length

of as low as 2.

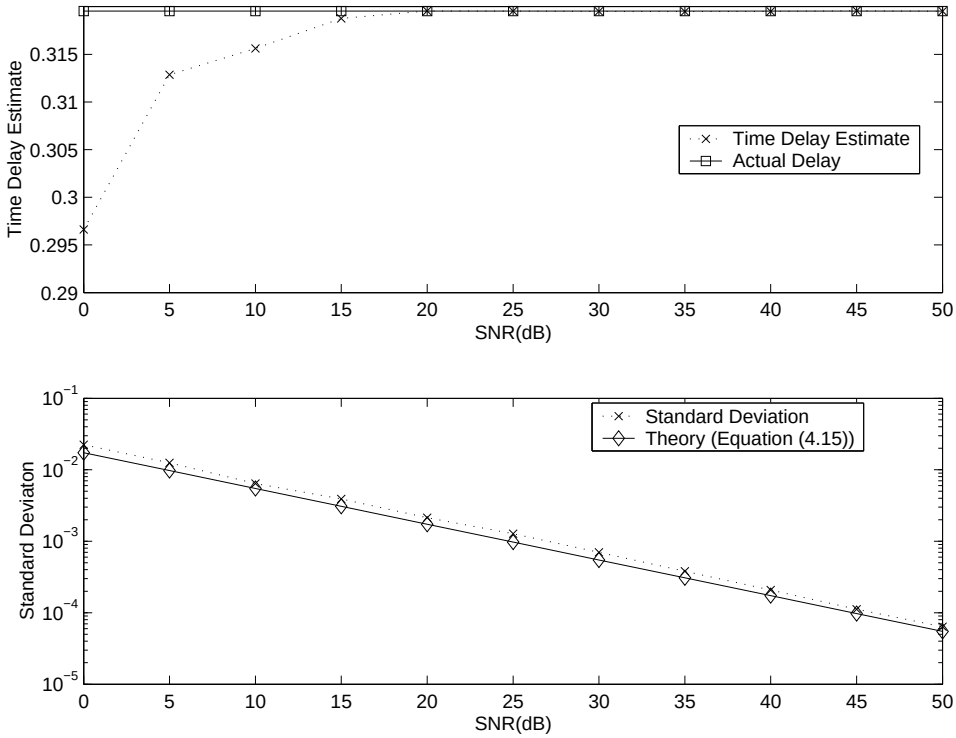

Figure 4.7: Standard deviation and time delay estimate of MMLETDE for single sinusoid signal, $\mu = 0.0003$, filter order $N = 2$, $\sigma_s^2 = 1$.

In Figure 4.7, we show the simulation results for a single sinusoidal test signal with frequency of 0.7π. The actual delay was set to 0.319547. The SNR was set from 0dB through 50dB. The time delay estimates and the standard deviations were obtained by averaging over 20 independent simulation runs. In each run of simulation, the time delay estimate, $\hat{D}$, was obtained by averaging the instantaneous time delay estimates between the 4000^{th} to the 6000^{th} iterations. The theoretical standard deviation was an approximation given by (4.16) and we have let $\bigcirc(1) = 1$. As can be seen in Figure 4.7, the standard deviation obtained from simulation agrees well with the theory.

We note the evidence of a bias in the estimator for the sinusoidal case (Figure 4.7,

top panel) for SNR < 20dB. This is because in our convergence analysis, for low SNR and low filter order, our approximation for $E[T_4]$ as can be seen in (C.4), which makes use of interpolation $\sum_{n=M_1}^{M_2} h^0_{\hat{D}(k)}(n) f(n - \hat{D}(k)) \approx f(0) = 0$, is not so accurate.

In Figure 4.8(a), we compare the root mean square error (RMSE) of the time delay estimates of MMLETDE, LETDE, ETDE and METDE algorithms as function of frequency. The step-size was $\mu = 0.005$. The actual delay was set to 0.3. The SNR was 40dB. The RMSE of each independent simulation run was obtained from 3000^{th} to 5000^{th} iteration. The final RMSE was obtained by averaging 20 independent simulation runs. As can be seen from the figure, the MMLETDE achieves the highest accuracy and is also almost frequency independent. The other three algorithms have poorer accuracy and are frequency dependent.

In Figure 4.8(b), we compare the RMSE of the time delay estimates of MMLETDE, METDE, LETDE and ETDE algorithms as function of SNR. The frequency was0.5π. As can be seen from the figure, the MMLETDE achieves the highest accuracy and the RMSE decreases as SNR increases implying expected improved accuracy with a stronger signal power. On the other hand, the other three algorithms have higher RMSE and the accuracy of the estimate cannot be improved by using a higher SNR. This implies that the estimates of these three algorithms are biased.

In Figure 4.8 we have compared the RMSE performance of our MMLETDE with other algorithms using simulation results. It would be interesting if the comparison can be realized using optimal performance bounds such as Cramer Rao bounds. We intend to carry this out in our future works.

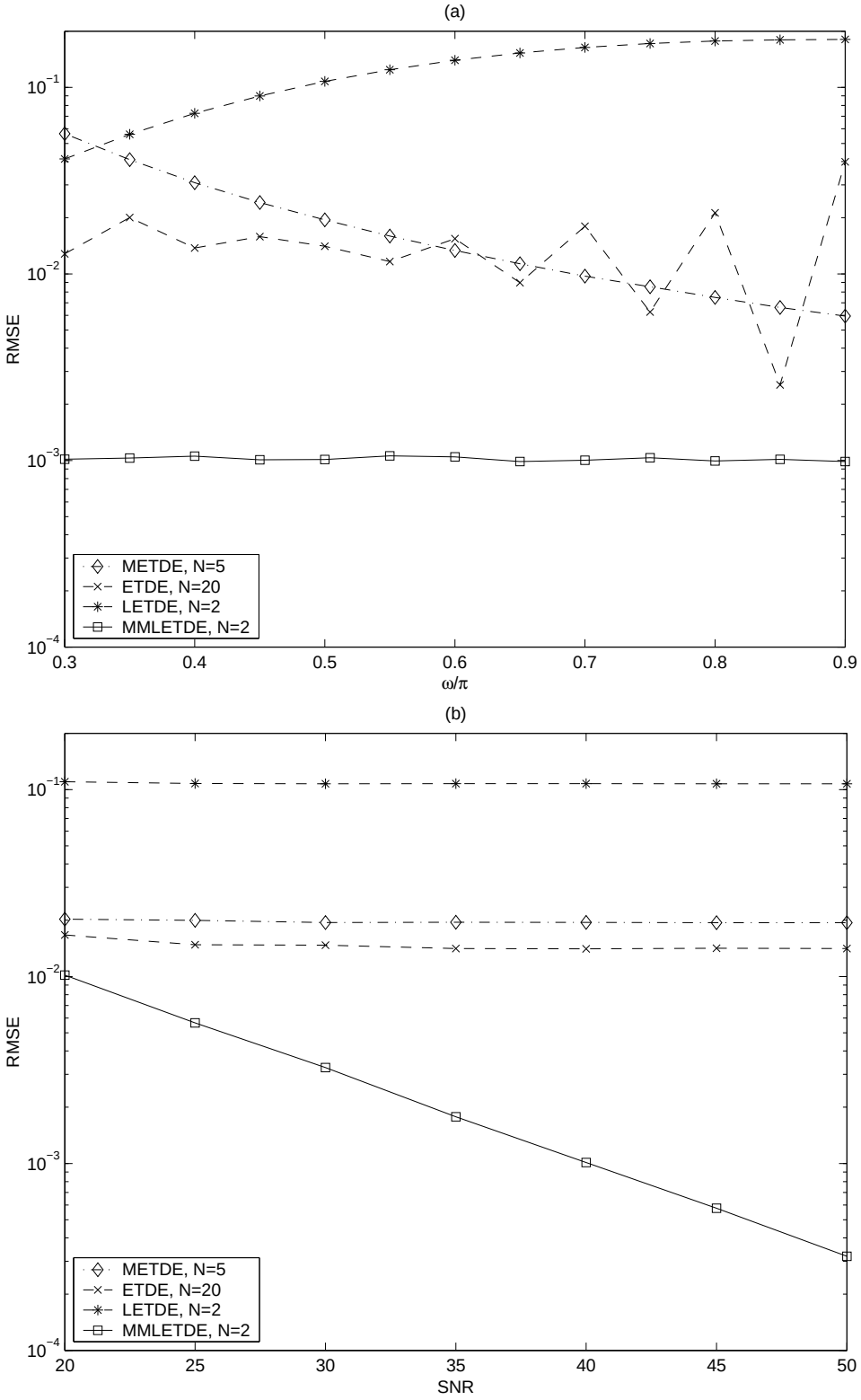

Figure 4.8: RMSE of the time delay estimate of MMLETDE, METDE, LETDE, ETDE for $\sigma_s^2 = 1$, $\mu = 0.005$, actual delay $D = 0.3$, (a) RMSE versus signal frequency, $\mathrm{SNR} = 40\mathrm{dB}$, (b) RMSE versus SNR, signal frequency $\omega = 0.5\pi$.

4.4 Conclusion

In this chapter, we have analyzed an algorithm for estimating fractional sample time delay for narrow-band signals, that draws from both explicit time delay estimation and modulated Lagrange interpolation, so-called mixed modulated Lagrange explicit time delay estimation algorithm (MMLETDE). We develop statistical descriptions of its performance and present simulation results. Our proposed MMLETDE algorithm can give accurate time delay estimates for single sinusoidal signal in a wide frequency range. The filter order can be as low as 1, which is beneficial for non-stationary environment where convergence rate is important. The algorithm is unbiased for a single sinusoidal signal under a high SNR (on the order of 20dB) for filter order as low as 1 and 2. When applied to a band-pass signal with a large bandwidth, the MMLETDE algorithm becomes slightly biased. This we believe is due to the approximation used in the development of the algorithm. We have conducted extensive simulation to contrast the benefits of our proposed MMLETDE algorithm with other competing approaches.

The proposed MMLETDE algorithm was verified in the simulation to converge to the actual delay for a band-pass signal even the filter is very short. The delay estimate of this algorithm became slightly biased when the bandwidth of signal becomes larger. This we believe is due to the approximation used in the development of the algorithm. We have conducted extensive simulation to contrast the benefits of our proposed MMLETDE algorithm with other competing approaches.

Chapter 5

Adaptive Frequency Estimation

5.1 Introduction

The estimation of the frequency of a sinusoidal signal plays an important role in signal processing and communications systems. Popular and modern algorithms that are based on the data auto-covariance matrix as mentioned in [22] and Chapter 2, can give accurate frequency estimates but are computationally burdensome. This is true especially when the frequency to be estimated is time-varying and an adaptive realization of the estimator is required. In [21], Etter and Hush suggested a fresh approach to frequency estimation based on a variable delay element as shown in Figure 5.1. Let the received

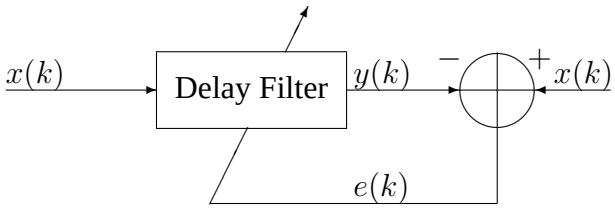

Figure 5.1: Block diagram of adaptive frequency estimation.

signal of interest be $x(k) = s(k) + \theta(k)$, $s(k) = e^{j(\omega(k)k+\phi)}$, where $\omega(k)$ is the instantaneous frequency to be estimated and ϕ is a constant initial phase. The noise $\theta(k)$ is white Gaussian with zero mean and variance of σ^2. Essentially the algorithm is to adaptively seek the delay value that shifts the sinusoid by 180° or 360°, thus maximizing or minimizing the cost function $J = E[e(k)e^*(k)]$, which is the mean squared value of the difference, $e(k)$, between the input $x(k)$ and its delayed version $y(k)$. The delay then provides the information needed to determine the frequency.

Dooley and Nandi [22] later improved upon this technique by introducing a fractional delay filter (FDF), so-called modulated Lagrange interpolation delay filter (MLIDF) to take into account a fractional delay that can be used to fine-tune the frequency estimation. In [21], the cost function is sinusoidal in form in terms of the delay; thereby leading to a simple delay update computation and the determination of the frequency estimate. The MLIDF, on the other hand, being a non-ideal finite impulse response filter (FIR), introduces distortion to the delayed signal and thereby a cost function which is not in a simple analytic form. In this dissertation, the cost function of an MLIDF is derived for a single sinusoidal signal and an explicit frequency estimation algorithm based on this cost function was developed.

5.2 Adaptive Frequency Estimation Using MLIDF

We first consider a Lagrange interpolation delay filter (LIDF) [27]. At each adaptation step, the LIDF coefficients $h^0(n, D(k))$ can be written as

$$h^0(n, D(k)) = \prod_{\substack{i=0 \\ i \neq n}}^{N} \frac{D(k) - i}{n - i} = \sum_{i=0}^{N} a_i D^i(k) \tag{5.1}$$

where N is the filter order, and $D(k)$ is a variable analog delay which is used to approximate the actual delay that lies within $[0,\ N]$. The coefficients a_i in the polynomial representation of $h^0(n, D(k))$ in (5.1) can be readily obtained by Matlab or Mathematica programming. This LIDF is a finite impulse response (FIR) delay system in discrete time domain. In Appendix E, we prove that for an FIR delay system the filter coefficients can be modulated so that it becomes a modulated FIR delay system. In this dissertation, since we adopt the MLIDF as the FIR delay filter, the modulated coefficients are as follows

$$h(n, D(k)) = h^0(n, D(k)) e^{j\omega(n - D(k))} \tag{5.2}$$

The difference between the input $x(k)$ and the filtered output $y(k)$ at kth iteration, is

$$e(k) = x(k) - y(k) = x(k) - \sum_{n=0}^{N} h(n, D(k)) x(k - n) \tag{5.3}$$

In Appendix F, we calculate the cost function of this MLIDF as follows

$$\begin{aligned} J = E\big[e(k)e^*(k)\big] &= (2 - 2\cos(\omega D(k))) \\ &+ \sigma^2\left(1 - 2h^0(0, D(k))\cos(\omega D(k)) + \sum_{n=0}^{N}(h^0(n, D(k)))^2\right) \end{aligned} \tag{5.4}$$

In (5.4), the first term is the autocorrelation function of a single sinusoidal signal, while the last term is introduced by noise. The last term can be dropped under the condition of high SNR, and the cost function reaches the maximum or minimum when the delay $D(k)$ equals $p\pi/\omega$, p is an integer. Correspondingly, the delay itself provides the information regarding the signal frequency.

Consider next the partial derivatives of the cost function with respect to $\omega(k)$ and $D(k)$, and set them to zero as follows

$$\frac{\partial J}{\partial \omega(k)} = 2D(k)\sin[\omega(k)D(k)] = 0 \tag{5.5a}$$

$$\frac{\partial J}{\partial D(k)} = 2\omega(k)\sin[\omega(k)D(k)] = 0 \tag{5.5b}$$

It is clear that for both (5.5a) and (5.5b) to be equal to zero, which is the condition for J to reach extremum points, requires that

$$\omega(k)D(k) = 2\pi \text{ or } \pi \tag{5.6}$$

The algorithm developed in this dissertation is to explicitly track the frequency under the constraint of (5.6), as follows. Following the standard LMS method, we locate the

extremum by taking the gradient of the filter coefficients with respect to the estimated frequency $\hat{\omega}(k)$.

$$\hat{\omega}(k+1) = \hat{\omega}(k) - \mu \nabla J(k) \tag{5.7}$$

where $J(k)$ denotes the instantaneous cost function, μ is step-size.

The MLIDF coefficient in (5.2) is a function of both $\omega(k)$ and $D(k)$. We now adopt a similar idea as in [17], on explicit time delay estimation, in that we introduce explicit frequency estimation by replacing $\omega(k)$ in the MLIDF coefficients in (5.2) by its estimate $\hat{\omega}(k)$. Furthermore, by making use of the constraint in (5.6), we replace $D(k)$ in the MLIDF coefficients in (5.2) by $2\pi/\hat{\omega}(k)$. By proceeding this way we have now proposed a new so-called explicit modulated Lagrange adaptive frequency estimation (EMLAFE) algorithm. We now rewrite the MLIDF coefficient in (5.2) as a function of $\hat{\omega}(k)$ as follows,

$$h(n, D(k)) = h_e(n, \hat{\omega}(k)) = h^0\left(n, \frac{2\pi}{\hat{\omega}(k)}\right) e^{j\hat{\omega}(k)(n - 2\pi/\hat{\omega}(k))} \tag{5.8}$$

The gradient of J with respect to $\hat{\omega}(k)$ is

$$\nabla J(k) = \frac{\partial}{\partial \hat{\omega}(k)} \big(e(k)e^*(k)\big) = 2\, Re\left\{ e^*(k) \frac{\partial e(k)}{\partial \hat{\omega}(k)} \right\} \tag{5.9}$$

Substituting (5.2), (5.3) and (5.9) into (5.7), we have the updating equation for the

explicit frequency estimate as,

$$\hat{\omega}(k+1) = \hat{\omega}(k) - 2\mu Re\Big\{e^*(k)\sum_{n=0}^{N} f(n,\hat{\omega}(k))x(k-n)\Big\} \tag{5.10}$$

where

$$f(n,\hat{\omega}(k)) = \left(\frac{\partial h^0(n,2\pi/\hat{\omega}(k))}{\partial\hat{\omega}(k)} + jnh^0\Big(n,\frac{2\pi}{\hat{\omega}(k)}\Big)\right)e^{j\hat{\omega}(k)n} \tag{5.11}$$

By expressing the filter coefficients $h^0(n,2\pi/\hat{\omega}(k))$ in (5.11) as a polynomial in $\hat{\omega}(k)$ as in (5.1), we can rewrite (5.11) as

$$f(n,\hat{\omega}(k)) = \left(\sum_{i=0}^{N} -i(2\pi)^i\frac{a_i}{\hat{\omega}^{i+1}(k)} + jn\sum_{i=0}^{N}(2\pi)^i\frac{a_i}{\hat{\omega}^i(k)}\right)e^{j\hat{\omega}(k)n} \tag{5.12}$$

5.3 Convergence Analysis

Assuming the noise and signal are uncorrelated, substituting (5.11) into (5.10) and taking expectation on both sides of (5.10), under the condition of high SNR, as proved in Appendix G, we obtain the following formula

$$E[\hat{\omega}(k+1)] - \omega = E[\hat{\omega}(k)] - \omega + 2\mu\frac{4\pi^2}{\omega^2}\big(E[\hat{\omega}(k)] - \omega\big) \tag{5.13}$$

Hence, given the initial guess of $\hat{\omega}(0)$, the recursive expression of (5.13) gives $\hat{\omega}(k)$ as follows

$$E[\hat{\omega}(k)] = \omega + (\hat{\omega}(0) - \omega)\Big(1 + \frac{8\pi^2}{\omega^2}\mu\Big)^k \tag{5.14}$$

Therefore, when $-\mu < \frac{\omega^2}{8\pi^2}$, the mean of $\hat{\omega}(k)$ will converge to the actual signal frequency when k tends to infinity under higher SNR.

5.4 Simulation Results

In this Section, we present simulation results for the EMLAFE algorithm that we have developed for fine and fast frequency estimation and tracking.

5.4.1 Frequency Estimation

In Table 5.1, the test was carried out for single sinusoid with frequency from 0.3π to 0.9π. The step-size μ was set to 0.00225, the signal power was set to $\sigma_s^2 = 1$, and filter order was 8, the signal-to-noise ratio (SNR) was set from 15dB to 50dB. The frequency estimate, $\hat{\omega}$, and its standard deviation, $\mathrm{std}(\hat{\omega})$, were obtained from the frequency estimates from 800^{th} through 1500^{th} iterations. In Table 5.1, the frequency estimate and its standard deviation were obtained by averaging over 20 independent simulation runs. As can be seen from the table, the frequency estimates converge to actual signal frequency while the variances of frequency estimates are almost of the same order for different frequency under the same SNR.

Table 5.1: Frequency estimate versus SNR.

ω/π	SNR (dB)	15	20	25	30	35	40	45	50
0.3	$\frac{\hat{\omega}}{\pi}$	0.2996	0.2999	0.3000	0.3000	0.30000	0.30000	0.30000	0.30000
	std$(\frac{\hat{\omega}}{\pi})$	7.1×10^{-3}	3.8×10^{-3}	2.1×10^{-3}	1.2×10^{-3}	6.7×10^{-4}	3.8×10^{-4}	2.1×10^{-4}	1.2×10^{-4}
0.4	$\frac{\hat{\omega}}{\pi}$	0.4000	0.4000	0.4000	0.4000	0.40000	0.40000	0.40000	0.400000
	std$(\frac{\hat{\omega}}{\pi})$	6.6×10^{-3}	3.6×10^{-3}	2.1×10^{-3}	1.1×10^{-3}	6.5×10^{-4}	3.6×10^{-4}	2.0×10^{-4}	1.1×10^{-4}
0.5	$\frac{\hat{\omega}}{\pi}$	0.4993	0.4998	0.4999	0.49998	0.49999	0.50000	0.50000	0.500000
	std$(\frac{\hat{\omega}}{\pi})$	5.3×10^{-3}	3.0×10^{-3}	1.7×10^{-3}	9.7×10^{-4}	5.4×10^{-4}	3.0×10^{-4}	1.7×10^{-4}	9.4×10^{-5}
0.6	$\frac{\hat{\omega}}{\pi}$	0.6000	0.6000	0.6000	0.60000	0.60000	0.60000	0.600000	0.600000
	std$(\frac{\hat{\omega}}{\pi})$	4.4×10^{-3}	2.4×10^{-3}	1.4×10^{-3}	7.6×10^{-4}	4.4×10^{-4}	2.4×10^{-4}	1.4×10^{-4}	7.7×10^{-5}
0.7	$\frac{\hat{\omega}}{\pi}$	0.7004	0.7002	0.7000	0.70001	0.70000	0.70000	0.700001	0.70000
	std$(\frac{\hat{\omega}}{\pi})$	3.4×10^{-3}	1.9×10^{-3}	1.1×10^{-3}	6.0×10^{-4}	3.4×10^{-4}	1.9×10^{-4}	1.1×10^{-4}	6.0×10^{-5}
0.8	$\frac{\hat{\omega}}{\pi}$	0.8002	0.8000	0.80002	0.80000	0.80000	0.80000	0.800000	0.800000
	std$(\frac{\hat{\omega}}{\pi})$	2.6×10^{-3}	1.5×10^{-3}	8.3×10^{-4}	4.7×10^{-4}	2.6×10^{-4}	1.4×10^{-4}	8.3×10^{-5}	4.6×10^{-5}
0.9	$\frac{\hat{\omega}}{\pi}$	0.8995	0.8999	0.89995	0.89999	0.90000	0.90000	0.900000	0.900000
	std$(\frac{\hat{\omega}}{\pi})$	2.1×10^{-3}	1.1×10^{-3}	6.4×10^{-4}	3.5×10^{-4}	2.0×10^{-4}	1.1×10^{-4}	6.3×10^{-5}	3.5×10^{-5}

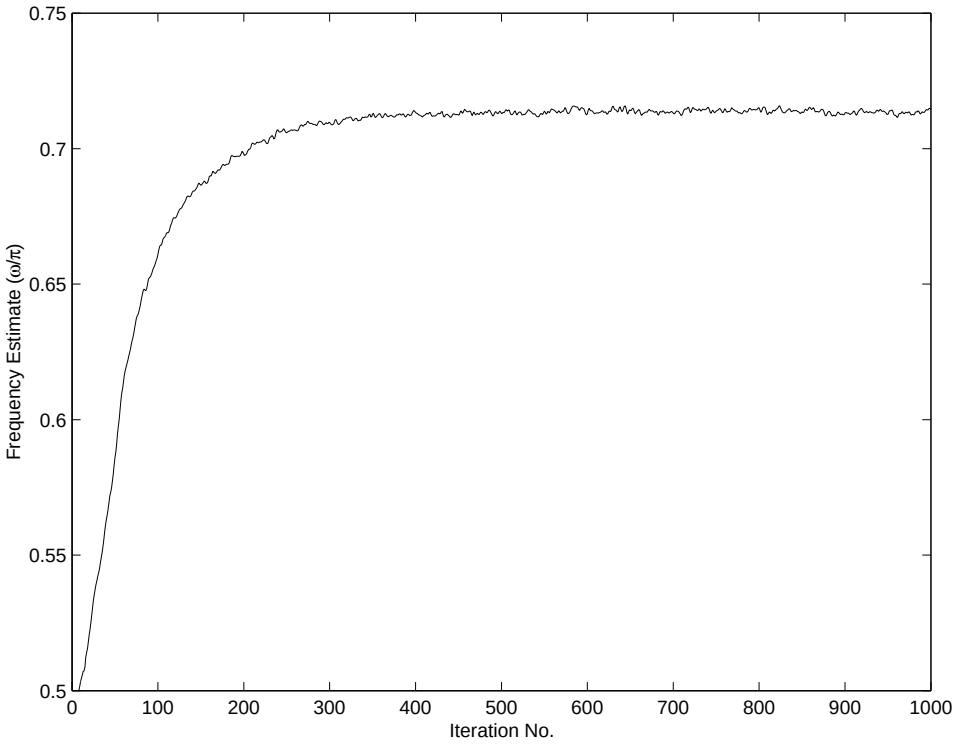

Figure 5.2: Convergence performance of EMLAFE algorithm tracking single tone signal. Filter oder $N = 8$, $\mathrm{SNR} = 10\mathrm{dB}$, $\mu = 0.00025$, $\hat{\omega} = 0.7137\pi$, $\mathrm{std}(\hat{\omega}) = 9.1\times10^{-4}$, actual frequency $\omega = 0.7125\pi$, $\sigma_s^2 = 1$.

In Figure 5.2, we demonstrate the convergence performance of EMLAFE algorithm. The step-size was set to $\mu = 0.00025$, the filter order was set as $N = 8$, the SNR was set to 10dB, and the actual signal frequency was set to 0.7125π. As can be seen, the convergence to the actual frequency occurs from 300^{th} iteration onward.

In Figure 5.3, we show frequency estimates of three different frequency signals, tested to verify the frequency range that can be tracked by the EMLAFE algorithm. From the constraint of (5.6), since $D(k)$ has the range from 0 to N, where N is the filter order, we can decide the range of frequency that can be estimated as $\omega \geq \frac{2\pi}{N}$, and for $N = 8$, $\omega \geq 0.25\pi$. This conclusion is verified in Figure 5.3 as follows. We considered

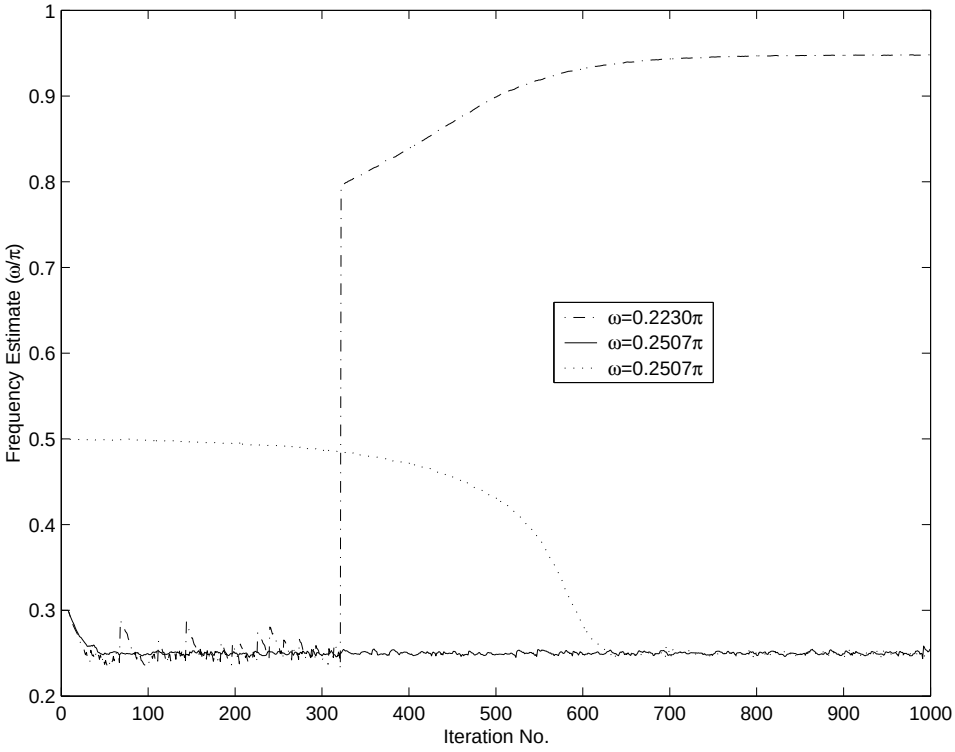

Figure 5.3: Dynamic range of EMLAFE algorithm tracking single tone signal. Filter oder $N = 8$, $\mathrm{SNR} = 17\,\mathrm{dB},\ \mu = 0.00025$, $\sigma_s^2 = 1$.

two sinusoids at angular frequencies $\omega_1 = 0.2230\pi$, $\omega_2 = 0.2507\pi$. In each case, the signal-to-noise ratio was set to 17dB, and the step-size was set 0.00025. As shown in Figure 5.3, the estimation of $\omega = 0.2230\pi < 0.25\pi$ fails, in that the estimate converged to a wrong value. However, for $\omega = 0.2507\pi$, we used two different initial guesses: 0.3π and 0.5π. With the closer initial guess of 0.3π, the frequency estimate converges to the actual value faster than the one initially further away at0.5π. Nevertheless, since the actual frequency $\omega = 0.2507\pi > 0.25\pi$, the estimation was successful.

Given two single tone signals at $\omega_1 = 0.7\pi$ and $\omega = 0.3\pi$, the step-sizes were set to $\mu_1 = 0.0003$ and $\mu_2 = 5.51 \times 10^{-5}$, and the SNR was set to be 20dB. The values of $\mu_1,\ \mu_2$ were determined by $\frac{\mu_1}{\omega_1^2} = \frac{\mu_2}{\omega_2^2}$ according to the convergence formula of (5.14) so

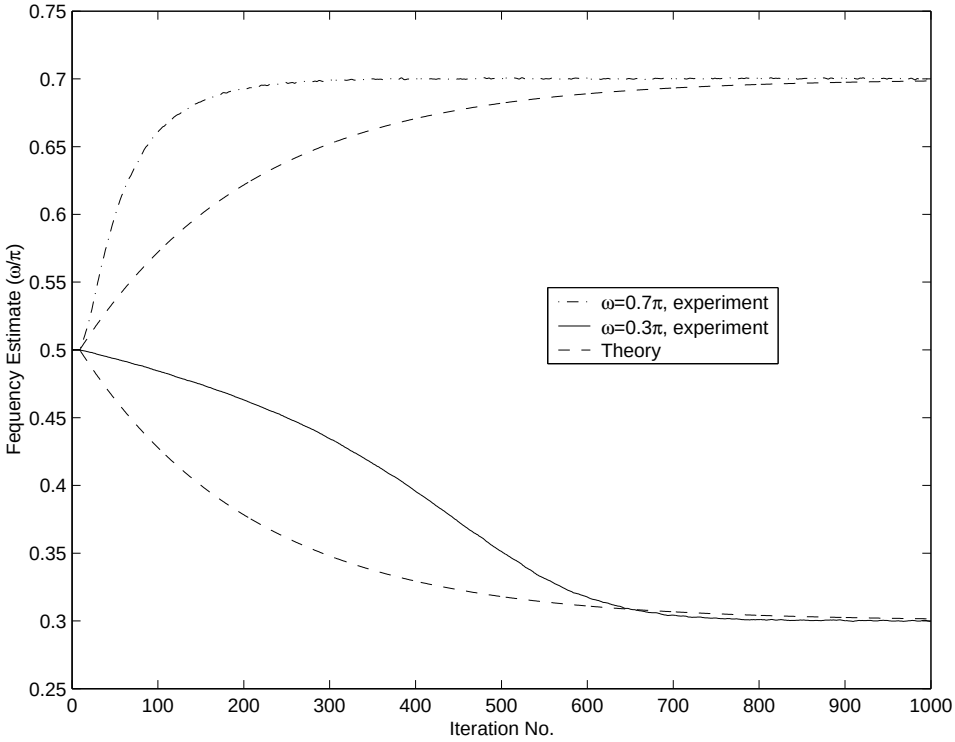

Figure 5.4: Convergence rates of EMLAFE algorithm for different single tone, $\mu_1 = 0.0003$ for signal frequency 0.7π, $\mu_2 = 5.51 \times 10^{-5}$ for signal frequency 0.3π, signal power $\sigma_s^2 = 1$, filter order $N = 8$.

that the convergence rates of the signals at ω_1 and ω_2 should be the same. As can be seen from Figure 5.4, the convergence curves of the frequency estimates for two signals at ω_1 and ω_2, are different. This is because the step-size has absorbed the coefficient $\frac{\omega^2}{\hat{\omega}^2(k)}$ in derivation of (5.13). As can be seen from Appendix G, in deriving the formula (G.4), we exploit the attribute, unchanged sign, of $\frac{\omega^2}{\hat{\omega}^2(k)} = \bigcirc(1)$. It is clear in Figure 5.4, the convergence rate of the signal at $\omega_1 = 0.7\pi$ is accelerated due to $\frac{\omega_1^2}{\hat{\omega}_1^2} > 1$, which means a larger step-size; meanwhile, the convergence speed of the signal at $\omega_2 = 0.3\pi$ is reduced due to $\frac{\omega_2^2}{\hat{\omega}_2^2} < 1$, which means a lower step-size. Therefore, the EMLAFE algorithm exhibits a variable step-size characteristic due to the change of $\hat{\omega}(k)$ with iteration index k.

5.4.2 Frequency Tracking

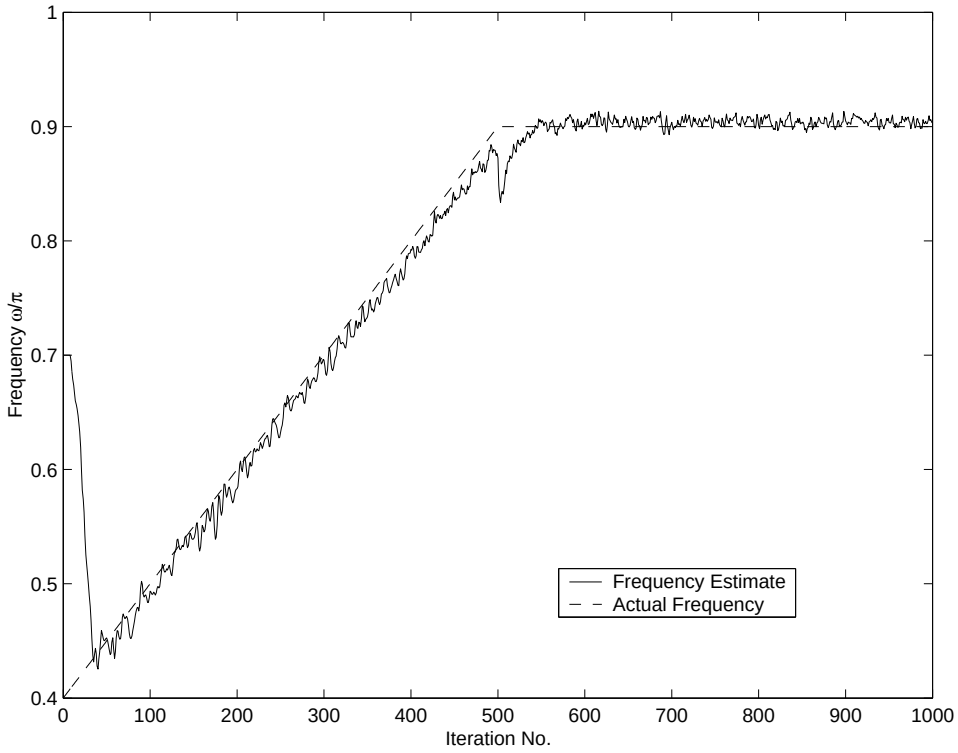

Figure 5.5: Tracking linear chirp frequency signal. Filter oder $N = 8$, $\mathrm{SNR} = 0\mathrm{dB}$, $\mu = 0.00225$, $\sigma_s^2 = 1$.

In Figure 5.5 we show an example in using the EMLAFE algorithm not only to determine frequency, but also to track a slowly changing frequency. The actual time-varying frequency is represented by the dashed line. In this example, the SNR was 0dB, the step-size was 0.00225, and the filter order was 8. As can be seen from Figure 5.5, the EMLAFE algorithm tracks the time varying signal frequency quickly (within about 50 iterations) under a very low SNR. Also when there is a sudden change in frequency, the estimate, after a short departure, returns and follows the actual frequency quickly.

In conclusion, we have developed a new EMLAFE frequency estimation technique and have shown that it is effective even in lower SNR condition. In the simulations we

also showed that the lowest frequency that can be tracked is determined by the filter order N, according to $\omega \geq \frac{2\pi}{N}$. It is around 0.25π for a filter order of 8.

Chapter 6

Joint Explicit Frequency And Time Delay Synchronization

6.1 Introduction

In CDMA and OFDM communication systems, carrier synchronization system is important for coherent detection. As for any multi-carrier transmission scheme, an OFDM signal suffers from nonlinear distortion [40]. Furthermore, it is extremely sensitive to possible uncompensated frequency offsets between the received carrier and local oscillator caused by Doppler shifts or instability of the oscillators at the transmitter and receiver. This calls for a very strict frequency recovery process [8]. One effective way to reduce the inaccuracy of the carrier offset's estimation is to exploit the power of digital signal processing, and using fractional interpolation techniques to improve the resolution of

digital signal processing. Let the received carrier and the carrier of local oscillator be

$$x(k) = e^{j(\omega_x(k)+\phi_x(k))} + \theta_x(k) \tag{6.1a}$$

$$y(k) = e^{j(\omega_y(k)+\phi_y(k))} + \theta_y(k) \tag{6.1b}$$

respectively. The $\omega_x(k)$, $\omega_y(k)$ are frequencies of received signal and local oscillator respectively. Moreover, the $\phi_x(k)$, $\phi_y(k)$ are phases of received signal and local oscillator respectively. Both received signal and local oscillator's signal are corrupted respectively by the zero-mean white Gaussian noises $\theta_x(k)$ and $\theta_y(k)$ with variances assumed to be σ_x^2, and σ_y^2.

The goal of carrier synchronization is to estimate and track the frequency $\omega_x(k)$ and phase $\phi_x(k)$ of the received carrier and to adjust the parameters $\omega_y(k)$ and $\phi_y(k)$ of the local oscillator in the direction of the counterparts of the received signal. After the frequency synchronization is carried out, the phase difference between the received and local oscillator signals can be adjusted via the time delay or time difference of arrival (TDOA) technique in Chapter 3. As mentioned in previous chapters, for a band-limited signal the ETDE is biased for TDOA estimation. MLETDE also exhibits a slight biasedness [13]. This algorithm, in fact, as mentioned in Chapter 3 shows only a limited valid signal frequency range.

In this chapter, the MMLETDE and EMLAFE, which have been presented in Chapter 4 and Chapter 5, are combined to estimate and track the frequency and phase of the received carrier.

6.2 Joint Explicit Time Difference of Arrival And Frequency Estimation

The structure of this JTDFE algorithm is shown in Figure 6.1. The output of the digital oscillator is the duplicate of the received carrier with estimated frequency and phase: $\hat{\omega}'_y(k),\ D(k)$.

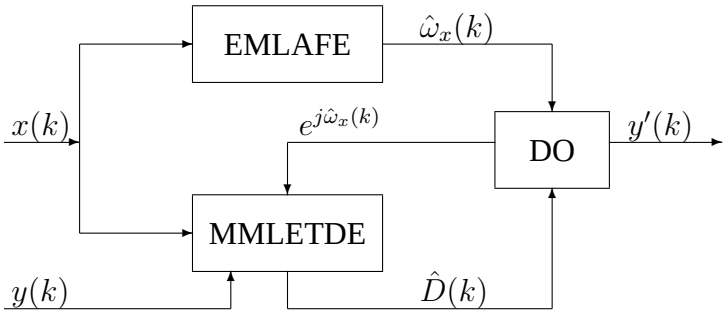

Figure 6.1: Block diagram of joint time delay and frequency estimation.

As shown in Figure 6.1, the whole carrier synchronization process comprises three components: EMLAFE (modulated Lagrange adaptive frequency estimator), MMLETDE (mixed modulated Lagrange explicit time delay estimator) and DO (digital oscillator). The frequency of the received carrier is first estimated and tracked by the EMLAFE algorithm, and it is fed into the MMLETDE component to estimate the time delay between the local carrier and received carrier. The output of DO is the synchronized carrier $y(k)'$ with the estimated frequency and phase.

Before introducing the simulation results of the JTDFE algorithm, we will discuss the validity of MLETDE and MLAFE algorithms.

6.3 Simulation Result

The experiments were under conditions of additive white Gaussian noise. The powers of both signals $x(k)$ and $y(k)$ were set to unity, and SNRs were 25dB. The signals were single tone with frequency $\omega = 0.85\pi$. The actual time delay between $x(k)$ and $y(k)$ was $D = 0.3$. In Figure 6.2, we show the frequency estimation performance of

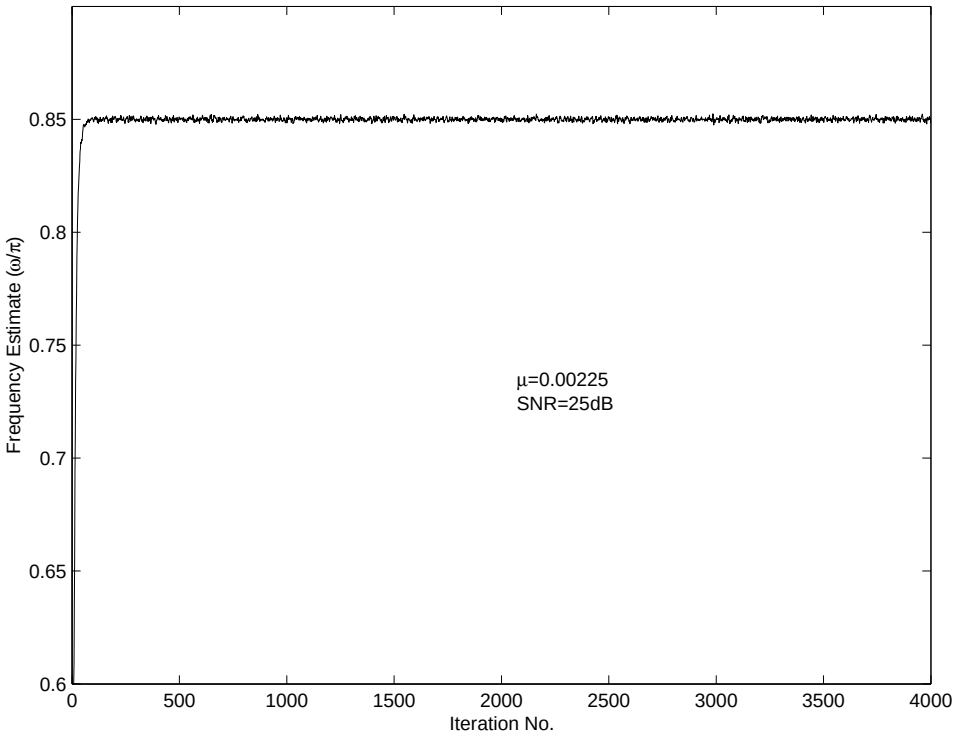

Figure 6.2: JTDFE algorithm: Frequency estimation part.

EMLAFE. The step-size of EMLAFE was set to $\mu = 0.00225$. After reaching the region of convergence, the statistics of one typical simulation are as follows: $\hat{\omega} = 0.8500\pi$, $\mathrm{std}(\hat{\omega}) = 8 \times 10^{-4}$.

At each iteration of JTDFE, the frequency estimate $\hat{\omega}(k)$ was fed into MMLETDE and used as signal frequency and explicitly estimate the time delay D. In Figure 6.3,

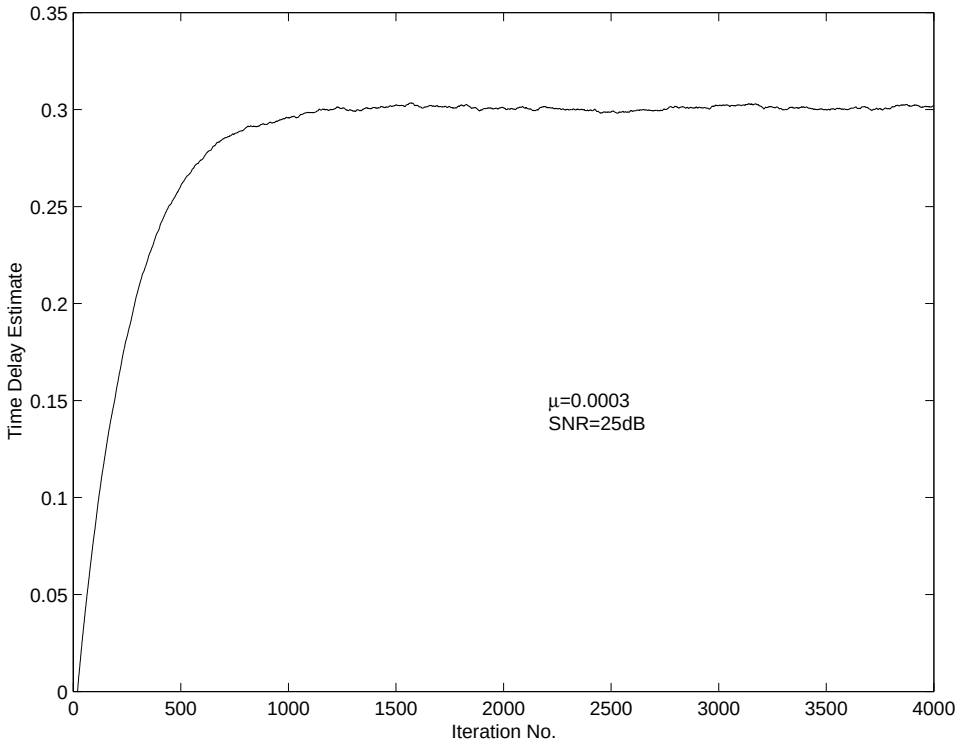

Figure 6.3: JTDFE algorithm: Time delay estimation part.

the result showed that the time delay estimate $\hat{D}$ converged to the actual delay setting. The typical statistics were: the mean of time delay estimates $\hat{D} = 0.3007$, the standard deviation of the time delay estimates $\mathrm{std}(\hat{D}) = 0.001$.

6.4 Discussion

In Figure 6.1, there is a slight difference from the previous chapters. There are three inputs: $x(k),\ y(k),\ e^{j\hat{\omega}(k)}$. If only $x(k)$ exists, then we could treat $e^{j\hat{\omega}(k)}$ as $y(k)$. Otherwise we use $y(k)$- the delayed version of $x(k)$. Then this becomes the time difference of arrival. After the carrier synchronization is achieved, the next issue for communications system is to demodulate the received signal. The remaining offset of carrier synchro-

nization will be incorporated into base band modeling: FIR channel.

Chapter 7

Conclusions And Future Work

In this dissertation, we have examined the existing algorithms on adaptive explicit time delay and adaptive frequency estimation. In Chapter 3, we tested the ETDE, METDE, LETDE, and furthermore in Chapter 4 we developed a new so-called mixed modulated Lagrange explicit time delay estimation and described the statistics of this algorithm. In Chapter 5, we introduce and discuss a new explicit frequency estimation algorithm.

7.1 Finished work

7.1.1 Time Delay Estimation

The ETDE algorithm is developed for full-band white-noise-like signal and because the truncated sinc FDF has a remainder when approximating a delay system, it is biased even under a higher filter order. Also because the truncated sinc FDF is ripple in the magnitude response, this truncated sinc based ETDE is far from optimum when using it

for a narrow-band signal.

By adopting Lagrange interpolation FDF, the LETDE algorithm can use a lower order filter but time delay estimation is still biased.

When using modulation technique, in which the filter coefficients multiply an exponential function, the LETDE becomes a modulated LETDE algorithm. In simulation, we show that the MLETDE algorithm is biased when the signal noise ratio is not very high. The MLETDE is valid only at a limited signal center frequency.

In this dissertation, in order to avoid bias of delay estimation and to use a lower order filter , which is important for non-stationary signal environment and fast convergence, we propose a new explicit time delay estimation algorithm, MMLETDE, which draws from both explicit time delay estimation and modulated Lagrange interpolation. We developed and proved the statistic characteristics of the MMLETDE algorithm and verified via computer simulation. We have also made an extensive comparison among several existing algorithms.

In summary, the truncated sinc based ETDE requires a relatively longer filter and is biased for wide-band white-noise like signal and narrow-band signal while our mixed modulated Lagrange ETDE (MMLETDE) can be used to estimate a narrow-band signal without bias with a lower filter order.

7.1.2 Frequency Estimation

In this dissertation, we derived the cost function of a modulated Lagrange interpolation FIR delay system, and develop a new explicit frequency estimation algorithm under the

constraint of $\omega D = m\pi$ (m is an integer). We also derive the convergence characteristic of this explicit modulated Lagrange adaptive frequency estimation (EMLAFE) algorithm. The EMLAFE algorithm can converge fast and estimate the instantaneous signal frequency in a non-stationary signal environment.

7.1.3 Joint Frequency And Time Delay Estimation

We combine the MMLETDE and EMLAFE algorithms together in Chapter 6. The estimated frequency is fed into MMLETDE component and we can use MMLETDE component to estimate the time delay between received carrier and local oscillator carrier.

7.2 Future Works

As discussed in Chapter 4, the MMLETDE algorithm is unbiased for single tone signal. However time delay estimate will become slightly biased when the signal bandwidth increases. We next should consider the quantitative relationship between signal spectrum and time delay estimate and furthermore find a unbiased explicit time delay estimation algorithm for wide band signal and this algorithm should be able to work under a very low filter order.

The explicit modulated Lagrange adaptive frequency estimation (EMLAFE) algorithm is biased when the signal-noise-ratio is relatively low due to the approximation. In next stage some measures may be considered to compensate the bias. The statistical characteristics of EMLAFE algorithm has not been investigated and may be an area for further research.

Finally, it will be worthwhile to consider how to implement these algorithms practically.

Bibliography

[1] A. J. Viterbi, *Principles of Spread Spectrum Communication*. Addison-Wesley, 1995.

[2] D. H. Youn and N. A. amd G. C. Carter, "On using the LMS algorithm for time delay estimation," *IEEE Trans. Acoust., Speech, Signal Processing*, vol. ASSP-20, pp. 798–801, Oct. 1982.

[3] P. C. Ching and H. C. So, "Two adaptive algorithms for multipath time delay estimation," *IEEE Journal of Oceanic Engineering*, vol. 19, no. 3, pp. 458–463, 1994.

[4] A. Toskala, H. Holma, and P. Muszynshi, "Etsi wcdma for umts," in *Spread Spectrum Techniques and Applications, 1998. Proceedings., 1998 IEEE 5th International Symposium on*, vol. 1, pp. 616–620, Sep. 1998.

[5] M. Raitola and H. Holma, "Wideband cdma packet data with hybrid ARQ," in *Spread Spectrum Techniques and Applications, 1998. Proceedings., 1998 IEEE 5th International Symposium on*, vol. 1, pp. 318–322, Sep. 1998.

[6] "Broadband radio access networks (bran) - inventory of broadband radio technologies and techniques." ETSI Tech. Rep., DTR/BRAN-030001, 1998.

[7] J. E. Kleider and M. Humphrey, "Robust time-frequency synchronization for OFDM mobile applications," in *ISSPA '99. Proceedings of the Fifth International Symposium on Signal Processing and Its Applications*, vol. 1, pp. 423–426, 1999.

[8] M. Luise and R. Reggiannini, "Carrier frequency acquisition and tracking for OFDM systems," *IEEE Transactions on Communications*, vol. 44, pp. 1590–1598, November 1996.

[9] U. Tureli, H. Liu, and M. Zoltowski, "OFDM blind carrier offset estimation: ESPRIT," *IEEE Transactions on Communications*, vol. 48, pp. 1459–1461, September. 2000.

[10] T. Pollet and M. V. B. amd M. Moeneclaey, "BER sensitivity of OFDM systems to carrier frequency offset and Wiener phase noise," *IEEE Transactions on Communications*, vol. 43, no. 2, pp. 191–193, 1995.

[11] J. D. Bard and F. M. Ham, "Time difference of arrival dilution of precision and applications," *IEEE Transactions on Signal Processing*, vol. 47, pp. 521–523, February 1999.

[12] F. A. Reed, P. L. Feintuch, and N. J. Bershad, "Time delay estimation using the LMS adaptive filter-static behavior," *IEEE Trans. on Acoustics, Speech, and Signal Processing*, vol. ASSP-29, pp. 561–571, June 1981.

[13] S. R. Dooley and A. K. Nandi, "Adaptive subsample time delay estimation using Lagrange interpolators," *IEEE Signal Processing Letters*, vol. 6, pp. 65–67, March 1999.

[14] F. A. Reed, P. L. Feintuch, and N. J. Bershad, "Time delay estimation using the LMS adaptive filter-dynamic behavior," *IEEE Trans. on Acoustics,Speech, and Signal Processing*, vol. ASSP-29, pp. 571–576, June 1981.

[15] Y. T. Chan, J. Riley, and J. B. Plant, "A parameter estimation approach to time delay estimation and signal detection," *IEEE Trans. Acoust., Speech, Signal Processing*, vol. ASSP-28, pp. 8–16, February 1980.

[16] P. C. Ching and Y. T. Chan, "Adaptive time delay estimation with constraints," *IEEE Trans. Acoust., Speech, Signal Processing*, vol. 36, pp. 599–602, April 1988.

[17] H. C. So, P. C. Ching, and Y. T. Chan, "A new algorithm for explicit adaptation of time delay," *IEEE Trans. Signal Processing*, vol. 42, pp. 1816–1820, July 1994.

[18] H. C. So, P. C. Ching, and Y. T. Chan, "An improvement to the explicit time delay estimator," in *Acoustics, Speech, and Signal Processing,ICASSP-95., 1995 International Conference on*, vol. 5, pp. 3151–3154, 1995.

[19] S. Haykin and J. Litya, *Radar Array Processing*. Springer-Verlag, 1993.

[20] S. Kadambe and R. S. Orr, "Instantaneous frequency estimation using the crossterm deleted Wigner representation (CDWR)," in *Time-Frequency and Time-Scale Analysis, 1996., Proceedings of the IEEE-SP International Symposium on*, pp. 289–292, 1996.

[21] D. M. Etter and D. R. Hush, "A new technique for adaptive frequency estimation and tracking," *IEEE Trans. ASSP*, vol. 35, pp. 561–564, 1987.

[22] S. R. Dooley and A. K. Nandi, "Fast frequency estimation and tracking using Lagrange interpolation," *Electronics Letters*, vol. 34, pp. 1908–1909, October 1998.

[23] E. Hermanowicz, "Explicit formulas for weighting coefficients of maximally flat tunable FIR delayers," *Elecron. Lett.*, vol. 28, pp. 1936–1937, 1992.

[24] S. Haykin, *Communication Systems*. New York: Wiley, 1994.

[25] A. R. Mickelson, *Physical Optics*. Von Norstrand Reinhold, 1992.

[26] J. G. Proakis, *Digital Communications*. McGraw-Hill, 3rd ed., 1995.

[27] T. I. Laakso, V. Välimäki, M. Karjalainen, and U. Laine, "Splitting the unit delay," *IEEE Signal Processing Magazine*, pp. 30–60, January 1996.

[28] Y. T. Chan, J. M. Riley, and J. B. Plant, "Modeling of time delay and its application to estimation of nonstationary delays," *IEEE Trans. Acoustics, and Signal Processing*, vol. ASSP-29, pp. 577–581, June 1981.

[29] C. H. Knapp and G. C. Carter, "The generalized correlation method for estimation of time delay," *IEEE Transactions on Acoustics, Speech, and Signal Processing*, vol. ASSP-24, pp. 320–327, August 1976.

[30] A. A. Gerlach, *Theory And Applications of Statistical Wave-period Processing*, vol. I, pp. 131–137. Gordon And Breach, Science Publishers, N. Y. 10011, 1970.

[31] S. A. Tretter, "Estimating the frequency of a noisy sinsoid by linear regress," *IEEE Transactions on Information Theory*, vol. IT-20, pp. 832–835, Sept. 1985.

[32] S. Kay, "A fast and and accurate single frequency estimator," *IEEE Trans. Acousti., Speech. Signal Processing*, vol. 37, pp. 1987–1990, Dec. 1989.

[33] E. Rosnes and A. Vahlin, "Generalized Kay estimator for the frequency of a single complex sinusoid," in *ICC 2001*, vol. 10, pp. 2958–1962, 2001.

[34] B. Baoshah, "Estimating and interpreting the instantaneous frequency of a signal - part1: Fundamentals," *Proceedings of the IEEE*, vol. 80, pp. 520–538, April 1992.

[35] Y. T. Chan, J. M. Riley, and J. B. Plant, "Modeling of time delay and its application to estimation of nonstationary delays," *IEEE Transactions on Acoustics, Speech, and Signal Processing*, vol. ASSP-29, pp. 577–581, June 1981.

[36] S. R. Dooley and A. K. Nandi, "Adaptive time delay and frequency estimation for digital signal synchronization in cdma system," in *1998 Conference Record of the Thirty-Second Asilomar Conference on Signals, Systems & Computers*, vol. 2, pp. 1838–1842, 1998.

[37] S. K. Mitra, *Digital Signal Processing Laboratory Using Matlab*, p. 34. Mc Graw Hill, 1999.

[38] S. Yakowitz, *An Introduction To Numerical Computations*, p. 135. Macmillan Publishing Company, New York, second ed., 1989.

[39] G. Dahlquist, *Numerical Methods*, pp. 284–285. Prentice-Hall, N. J., 1974.

[40] H. Sari, G. Karam, and I. Jeanclaude, "Channel equalization and carrier synchronization in OFDM systems," in *Audio and Video Digital Radio Broadcasting Sys-*

tems and Techniques (R. D. Gaudenzi and M. Luise, eds.), Amesterdam: Elsevier, 1994.

[41] A. Jeffrey, *Table of Integrals, Series, and Products*, p. 10. New York: Academic, 1980.

[42] K. Sahanmugan and A. Breipohl, *Random Signals: Detection, Estimation and Data Analysis*, p. 55. New York: Wiley, 1988.

[43] G. Oetken, "A new approach for the design of digital interpolating filters," *IEEE Trans. Acoustic, Speech, Signal Processing*, vol. 27, pp. 637–643, December 1979.

Appendix A

Proof of (3.28d)'s Replacement

We note that in an ideal discrete delay system,

$$y(k) = x(k - D) = \sum_{n=-\infty}^{\infty} h_{id}(n)x(k - n) \tag{A.1}$$

Now let $x(k) = x'(k)e^{j\omega_0 k}$, or $x'(k) = x(k)e^{-j\omega_0}$. Then

$$x(k - D) = x'(k - D)e^{j\omega_0(k-D)} \tag{A.2}$$

But

$$x'(k - D) = \sum_{h_{id}}(n)x'(k - n) \tag{A.3}$$

Substituting (A.3) into (A.2), we have

$$\begin{aligned} x(k-D) = y(k) &= \Big(\sum_{n=-\infty}^{\infty} h_{id}(n) x'(k-n) \Big) e^{j\omega_0(k-D)} \\ &= \sum_{n=-\infty}^{\infty} h_{id}(n) x'(k-n) e^{j\omega_0(n-D)} \end{aligned} \tag{A.4}$$

Therefore,

$$y(k) = \sum_{n=-\infty}^{\infty} h_{id}(n) e^{j\omega_0(n-D)} x(k-n) \tag{A.5}$$

Following the same reasoning as in Chapter 3 of the main text, we place the overall delay D at the center of gravity of h_{id}. Therefore we can write

$$y(t) = \sum_{-\infty}^{\infty} h'_{id}(n) e^{j\omega_0(n-D)} x(k-n) \tag{A.6}$$

Now the error $e(k)$ in the Lagrange FDF is

$$e(k) = y(k) - \sum_{n=-M_1}^{M_2} h^0_{\hat{D}(K)}(n) e^{j\omega_0(n-\hat{D}(k))} x(k-n) \tag{A.7}$$

Substituting (A.6) into (A.7), we have

$$\begin{aligned} e(k) = &\sum_{n=-M_1}^{M_2} \big[h'_{id}(n) - h^0_{\hat{D}(k)}\big(n, \hat{D}(k)\big) \big] e^{j\omega_0(n-\hat{D}(k))} x(k-n) \\ &+ \sum_{n=-\infty}^{-M_1-1} h'_{id}(n) e^{j\omega_0(n-\hat{D}(k))} x(k-n) + \sum_{n=M_2}^{\infty} h'_{id}(n) e^{j\omega_0(n-\hat{D}(k))} x(k-n) \end{aligned} \tag{A.8}$$

The last two terms in (A.8) can be dropped because $h'_{id}(n)$ takes on small values in the range of n outside of $-M_1 \leq n \leq M_2$. Next, with ETDE, we substitute $\mathrm{sinc}(n - \tilde{D})$ by $\mathrm{sinc}(n - \hat{D}(k))$. Hence, we obtain

$$e(k) \approx \sum_{n=-M_1}^{M_2} \big(\mathrm{sinc}(n - \hat{D}(k)) - h^0_{\hat{D}(k)}(n)\big) e^{j\omega_0(n-\hat{D}(k))} x(k-n) \tag{A.9}$$

Let $\nu = n - \hat{D}(k)$ and we express $\mathrm{sinc}(\nu)$ and $h^0_{\hat{D}(k)}(n)$ in the polynomial of $\hat{D}(k)$. Taking Taylor expansion on $\mathrm{sinc}(\nu)$, we obtain

$$\begin{aligned} \mathrm{sinc}(\nu) &= \frac{\sin(\pi\nu)}{\pi\nu} \\ &= 1 - \frac{(\pi\nu)^2}{3!} + \cdots + (-1)^{m-1}\frac{(\pi\nu)^{2m-2}}{(2m-1)!} \\ &\quad + \frac{(\pi\nu)^{2m}}{(2m+1)!}\sin\Big(\delta\pi(\nu) + \frac{2m+1}{2}\pi\Big) \end{aligned} \tag{A.10}$$

where $0 < \delta < 1$, $-\infty < \nu < \infty$. For $\forall\, \epsilon > 0$, there is an integer m, satisfying

$$\left|\frac{(\pi\nu)^{2m}}{(2m+1)!}\sin\Big(\delta\pi\nu + \frac{2m+1}{2}\pi\Big)\right| < \epsilon \tag{A.11}$$

Hence, we retain $m-1$ terms in (A.6), $\mathrm{sinc}(\nu)$ can be expressed as a polynomial in $\hat{D}(k)$ as follow

$$\mathrm{sinc}(\nu) = \sum_{i=0}^{2m-2} a_i \hat{D}(k)^i \tag{A.12}$$

Of course the coefficients $\{a_i\}$ in (A.12) can be evaluated . But in our development of the proof here, we have no need for the exact expression of a_i. It can be shown in the

main text that the Lagrange coefficient $h^0_{\hat{D}(k)}(n)$ defined in (3.24) of the main text can be written as a polynomial in $\hat{D}(k)$ of order $N = M_1 + M_2$

$$\hat{D}(k)^0(n) = \sum_{i=0}^{N} b_i \hat{D}(k)^i \tag{A.13}$$

Again, as will be obvious in our development of the proof here, we do not need the exact expression for b_i in (A.13). We assume that $N < 2m - 2$ and use Landau symbols $\bigcirc$ and $\circ$ to express $\hat{D}(k)^0(n)$ as of the order of $sin(\nu)$

$$\begin{aligned} \mathrm{sinc}(\nu) &= \sum_{i=0}^{N} \frac{a_i}{b_i} b_i \hat{D}(k)^i + \sum_{i=N+1}^{m} a_i \hat{D}(k)^i \\ &= \sum_{i=0}^{N} \bigcirc\big(b_i \hat{D}(k)^i\big) + \circ\big(\hat{D}(k)^N\big) = \bigcirc\left(\sum_{i=0}^{N} b_i \hat{D}(k)^i\right) \end{aligned} \tag{A.14}$$

Next, we have

$$\mathrm{sinc}(\nu) - h^0_{\hat{D}(k)}(n) = \bigcirc\big(h^0_{\hat{D}(k)}(n)\big) - \bigcirc\big(h^0_{\hat{D}(k)}(n)\big) = \bigcirc\big(h^0_{\hat{D}(k)}(n)\big) \tag{A.15}$$

Consider $\frac{\partial \mathrm{sinc}(\nu)}{\partial \hat{D}(k)}$ and $\frac{\partial h_{\hat{D}(k)}}{\partial \hat{D}(k)}$,

$$\begin{aligned} \frac{\mathrm{sinc}(\nu)}{\partial \hat{D}(k)} &= \frac{\cos(\pi\nu)}{\nu} - \frac{\sin(\pi\nu)}{\pi\nu^2} \\ &= \frac{1 + \cdots + (-1)^{m-1} \frac{(\pi\nu)^{2m}}{(2m)!}}{\nu} - \frac{\pi\nu + \cdots + (-1)^{m-1} \frac{(\pi\nu)^{2m+1}}{(2m+1)!}}{\pi\nu} \\ &= \frac{\sum_{m=1}^{\infty} (-1)^{m-1} \frac{(\pi\nu)^{2m}}{(2m-1)!}}{\nu} = \sum_{m=1}^{\infty} (-1)^{m-1} \frac{\pi^{2m} \nu^{2m-1}}{(2m-1)!} \end{aligned} \tag{A.16}$$

We can write it as polynomial in $\hat{D}(k)$ as follow

$$\frac{\mathrm{sinc}(\nu)}{\partial \hat{D}(k)} = \sum_{i=0}^{\infty} a_i \hat{D}(k)^i = \sum_{i=0}^{\infty} \bigcirc\big(a_i \hat{D}(k)^i\big) \tag{A.17}$$

while

$$\begin{aligned} \frac{\partial h^0_{\hat{D}(k)}(n)}{\partial \hat{D}(k)} &= \sum_{i=1}^{N} i b_i \hat{D}(k)^{p-1} \\ &= \sum_{i=0}^{N-1} \frac{(i+1)b_{i+1}}{a_i} a_i \hat{D}(k)^i = \sum_{i=0}^{N-1} \bigcirc\big(a_i \hat{D}(k)^i\big) \end{aligned} \tag{A.18}$$

Finally, it is very easy to obtain

$$\begin{aligned} \frac{\partial \mathrm{sinc}(\nu)}{\partial \hat{D}(k)} - \frac{h_{\hat{D}(k)}(n)}{\hat{D}(k)} &= \sum_{i=0}^{\infty} \big(a_i \hat{D}(k)^i\big) - \sum_{i=0}^{N-1} \bigcirc\big(a_i \hat{D}(k)^i\big) \\ &= \bigcirc\left(\sum_{i=0}^{\infty} a_i \hat{D}(k)^i\right) = \bigcirc\left(\frac{\partial \mathrm{sinc}(\nu)}{\partial \hat{D}(k)}\right) \end{aligned} \tag{A.19}$$

Now, the delay estimate updating equation is

$$\hat{D}(k+1) = \hat{D}(k) - 2\mu\, Re\Big\{e^*(k) \frac{\partial e(k)}{\partial \hat{D}(k)}\Big\} \tag{A.20}$$

Substitute (A.9) and (A.18) into (A.20), we obtain

$$\begin{aligned}
\hat{D}(k+1) &= \hat{D}(k) \\
&\quad - 2\mu Re\Big\{e^*(k)\sum_{n=-M_1}^{M_2} e^{j\omega_0\nu}\big(\bigcirc\big(f(\nu)\big) - \bigcirc(-j\omega_0 h^0_{\hat{D}(k)}(n))x(k-n)\Big\} \\
&= \hat{D}(k) \\
&\quad - 2\mu Re\Big\{e^*(k)\sum_{n=-M_1}^{M_2} e^{j\omega_0\nu}\big(\bigcirc(f(\nu)) + \bigcirc(-j\omega_0 h^0_{\hat{D}(k)})\big)x(k-n)\Big\} \\
&= \hat{D}(k) - 2\mu Re\Big\{e^*(k)\sum_{n=-M_1}^{M_2} e^{j\omega_0\nu} \bigcirc (f(\nu) - j\omega_0 h^0_{\hat{D}(k)}(n))x(k-n)\Big\} \\
&= \hat{D}(k) \\
&\quad - 2\mu \bigcirc \left(Re\Big\{e^*(k)\sum_{n=-M_1}^{M_2} e^{j\omega_0\nu}(f(\nu) - j\omega_0 h^0_{\hat{D}(k)}(n))x(k-n)\Big\}\right)
\end{aligned} \tag{A.21}$$

Simplify the above formula, and we can use a new μ to replace $2\mu\bigcirc$ symbol, then we obtain (3.28d).

Appendix B

Proof of MMLETDE algorithm

As proved in Appendix A, we can express

$$\begin{aligned}\operatorname{sinc}(\nu) - h^0_{\hat{D}(k)}(n) &= \sum_{i=0}^{2m-2} a_i \hat{D}(k)^i - \sum_{i=0}^{N} \frac{b_i a_i}{a_i} \hat{D}(k)^i \\ &= \sum_{i=0}^{2m-2} \bigcirc(a_i \hat{D}(k)^i) - \sum_{i=0}^{N} \bigcirc(a_i \hat{D}(k)^i) \\ &= \sum_{i=0}^{2m-2} \bigcirc(a_i \hat{D}(k)^i) = \bigcirc(\operatorname{sinc}(\nu))\end{aligned} \tag{B.1}$$

Hence, we obtain a new formula for $e(k)$ as

$$\begin{aligned}e(k) &= \sum_{n=-M_1}^{M_2} \bigcirc(\operatorname{sinc}(\nu)) e^{j\omega_0 \nu} x(k-n) \\ &= \bigcirc\Big(\sum_{n=-M_1}^{M_2} \operatorname{sinc}(\nu) e^{j\omega_0 \nu} x(k-n) \Big)\end{aligned} \tag{B.2}$$

The delay estimate updating equation is

$$\hat{D}(k+1) = \hat{D}(k) - 2\mu Re\Big\{e^* \frac{\partial e(k)}{\partial \hat{D}}\Big\} \tag{B.3}$$

Substituting (B.2) into (B.3), we have

$$\begin{aligned} \hat{D}(k+1) &= \hat{D}(k) - 2\mu Re\Big\{e^*(k) \bigcirc \Big(\sum_{n=-M_1}^{M_2} g(\nu)x(k-n)\Big)\Big\} \\ &= \hat{D}(k) - 2\mu \bigcirc \Big(Re\Big\{e^*(k)\sum_{n=-M_1}^{M_2} g(\nu)x(k-n)\Big\}\Big) \end{aligned} \tag{B.4}$$

where

$$g(\nu) = e^{\omega_0 \nu}(f(\nu) - j\omega_0 \mathrm{sinc}(\nu)) \tag{B.5}$$

Using a new μ to substitute $+2\mu\bigcirc$ in (B.4)), we have (4.1b) in the Chapter 3.

Appendix C

Convergence Analysis of MMLETDE

Using (4.3) and (4.2) in the main text, we have

$$\hat{D}(k+1) = \hat{D}(k) - 2\mu Re\{T_1 + T_2 + T_3 + T_4\} \tag{C.1}$$

where

$$T_1 = \left[s^*(k-D) - s^*(k-\hat{D}(k))\right] \sum_{n=-M_1}^{M_2} s(k-n)g(n-\hat{D}(k)) \tag{C.2a}$$

$$T_2 = \left[s^*(k-D) - s^*(k-\hat{D}(k))\right] \sum_{n=-M_1}^{M_2} \theta(k-n)g(n-\hat{D}(k)) \tag{C.2b}$$

$$T_3 = \left[\phi^*(k) - \sum_{n=-M_1}^{M_2} h^*_{\hat{D}(k)}(n)\theta^*(k-n)\right] \sum_{n=-M_1}^{M_2} s(k-n)g(n-\hat{D}(k)) \tag{C.2c}$$

$$T_4 = \left[\phi^*(k) - \sum_{n=-M_1}^{M_2} h^*_{\hat{D}(k)}(n)\theta^*(k-n)\right] \sum_{n=-M_1}^{M_2} \theta(k-n)g(n-\hat{D}(k)) \tag{C.2d}$$

Taking the expected value of both sides of (C.1) gives

$$E[\hat{D}(k+1)] = E[\hat{D}(k)] - 2\mu Re\left\{E[T_1 + T_2 + T_3 + T_4]\right\} \tag{C.3}$$

Because $\{s(k)\}$, $\{\theta(k)\}$, and $\{\phi(k)\}$ are mutually uncorrelated, so $Re\{E[T_3]\} = 0$, $Re\{E[T_2]\} = 0$, and consider next $Re\{E[T_4]\}$ as follows

$$E[T_4] \approx \sigma_n^2 E[g(\hat{D}(k) - \hat{D}(k))] = \sigma_n^2 E[g(0)] = \sigma_n^2[f(0) - j\omega_0 \mathrm{sinc}(0)] \tag{C.4}$$

Taking the real part of (C.4), we have $Re\{E[T_4]\} = \sigma_n^2 f(0) = 0$.

To evaluate $Re\{E[T_1]\}$, we rewrite $g(n - \hat{D}(k))$ in (C.2a) as $\frac{\partial \mathrm{sinc}(\nu) e^{j\omega_0 \nu}}{\partial \hat{D}(k)}$, and then exchanging differentiation and summation operation, we have

$$T_1 = \big(s^*(k-D) - s^*(k-\hat{D}(k))\big) \frac{\partial}{\partial \hat{D}(k)} \Bigg[\sum_{n=-M_1}^{M_2} s(k-n)\mathrm{sinc}(\nu) e^{j\omega\nu} \Bigg] \tag{C.5}$$

The summation term in the square bracket in (C.5) can be approximated as

$$\sum_{n=-M_1}^{M_2} \mathrm{sinc}(n - \hat{D}(k)) e^{j\omega(n-\hat{D}(k))} \approx s(k - \hat{D}(k))$$

Taking the expectation of (C.5), we have

$$E[T_1] = E\Big[\Big(s^*(k-D) - s^*(k-\hat{D}(k)) \frac{\partial}{\partial \hat{D}(k)} s(k-\hat{D}(k))\Big)\Big] \tag{C.6}$$

Substitution of $s(k) = A(k)e^{\omega_0 k}$ in (C.6), and then making the assumption that for a

narrow-band signal, the envelope $A(k)$ varies slowly, such that

$$\frac{\partial}{\partial \hat{D}(k)} \approx (-j\omega_0)A(k-\hat{D}(k))e^{j\omega_0(k-\hat{D}(k))} \tag{C.7}$$

Now we have

$$E[T_1] = \sigma_s^2 j\omega_0(1-e^{j\omega_0(D-\hat{D}(k))}) \tag{C.8}$$

where $\sigma_s^2 = E[s(k)s^*(k)] = E[(A(k))^2]$ is the signal power. Therefore, we obtain

$$Re\{E[T_1]\} = \sigma_s^2\omega_0 \sin\big(\omega_0(D-\hat{D}(k)\big) \tag{C.9}$$

For small $D-\hat{D}(k)$, we can use $\sin(\omega_0(D-\hat{D}(k))) \approx \omega_0(D-\hat{D}(k))$ in (C.9). Substituting (C.9), $Re\{E[T_2]\} = 0$, $Re\{E[T_3]\} = 0$, $Re\{E[T_4]\} = 0$ into (C.3), we easily obtain (4.6) in the main text.

Appendix D

Learning Characteristics of Mean Square Delay Error

Squaring and then taking expectation on both sides of (C.1), we can obtain

$$E[\hat{D}^2(k+1)] = E[\hat{D}^2(k)] - 4\mu \mathrm{Re}\{E[\hat{D}(k)T]\} + 2\mu^2 \mathrm{Re}\left\{E[T\,T^* + T^2]\right\} \quad \text{(D.1)}$$

where $T = T_1 + T_2 + T_3 + T_4$. In arriving at (D.1), we have made use of the identity, $\{\mathrm{Re}(T)\}^2 = \frac{1}{2}\mathrm{Re}\{T\,T^* + T^2\}$. First we evaluate $E[\hat{D}(k)T_2]$ for the second term of (D.1).

$$E[\hat{D}(k)] = E[\hat{D}(k)T_1] + E[\hat{D}(k)T_2] + E[\hat{D}(k)T_3] + E[\hat{D}(k)T_4] \quad \text{(D.2)}$$

Since $s(k)$,$\theta(k)$, $\phi(k)$ and $\hat{D}(k)$ are mutually uncorrelated, $E[\hat{D}(k)T_2]$, $E[\hat{D}(k)T_2]$ are both zeros. next, by referring to (C.4), we have

$$\mathrm{Re}\big\{E\big[\hat{D}(k)T_4\big]\big\} = \mathrm{Re}\big\{\sigma_n^2 E\big[\hat{D}(k)g(0)\big]\big\} = 0 \tag{D.3}$$

And by referring to (C.9), we have

$$\mathrm{Re}\big\{E\big[\hat{D}(k\big]\big\} = \sigma_s^2\omega_0^2\big\{D \times E\big[\hat{D}(k)\big] - E\big[\hat{D}^2(k)\big]\big\} \tag{D.4}$$

Now,

$$\begin{aligned}\mathrm{Re}\big\{E[T\,T^*]\big\} = \mathrm{Re}\big\{E\big[T_1T_1^* + T_2T_2^* + T_3T_3^* + T_4T_4^*\big]\big\} \\ + 2\mathrm{Re}\big\{E[T_1T_2^* + T_1T_3^* + T_1T_4^* + T_2T_3^* + T_2T_4^* + T_3T_4^*]\big\}\end{aligned} \tag{D.5}$$

$$\begin{aligned}\mathrm{Re}\big\{E[T^2]\big\} = \mathrm{Re}\big\{E[T_1^2 + T_2^2 + T_3^2 + T_4^2]\big\} \\ + 2\mathrm{Re}\big\{E[T_1T_2 + T_1T_3 + T_1T_4 + T_2T_3 + T_2T_4 + T_3T_4]\big\}\end{aligned} \tag{D.6}$$

It can be shown that $E[T_1\,T_2]$, $E[T_1\,T_2^*]$, $E[T_1\,T_3]$, $E[T_1\,T_3^*]$, $E[T_2\,T_3^*]$, $E[T_3\,T_4^*]$, $E[T_2\,T_4]$, $E[T_2\,T_4^*]$, $E[T_3\,T_4]$, $E[T_2^2]$, $E[T_3^2]$ are all equal to zero. The other terms are evaluated one by one as follows:

$$\begin{aligned}\mathrm{Re}\{E[T_1T_4]\} &= -2\sigma_s^2\sigma_n^2\omega^2\sin^2\frac{\omega\big(D-\hat{D}(k)\big)}{2} =\approx -2\sigma_s^2\sigma_n^2\omega^4\big(D-\hat{D}(k)\big)^2 \\ &= -\mathrm{Re}\big\{T_1T_4^*\big\} = \mathrm{Re}\,\{T_2T_3\}\end{aligned} \tag{D.7}$$

By referring to (C.8), we have

$$\begin{aligned}\mathrm{Re}\{E[T_1^2]\} &= \mathrm{Re}\Big\{E\Big[\sigma_s^2 j\,\omega\big(1 - j\,\omega\, e^{j\,\omega\left(D-\hat{D}(k)\right)}\big)^2\Big]\Big\} \\ &= E\Big[-\omega^2\sigma_s^4\Big(4\sin^2\big(\omega\big(D-\hat{D}(k)\big)/2\big)\Big) - 2\sin^2\omega\big(D-\hat{D}(k)\big)\Big] \\ &= E\Big[\omega^4\sigma_s^4\big(D-\hat{D}(k)\big)^2\Big]\end{aligned} \tag{D.8}$$

$$\begin{aligned}E[T_1T_1^*] &= E\Big[\Big|\sigma_s^2 j\,\omega\big(1 - e^{j\omega\left(D-\hat{D}(k)\right)}\big)\Big|^2\Big] \\ &= E\Big[\omega^4\sigma_s^4\big(D-\hat{D}(k)\big)^2\Big] = E[T_1^2] \\ E[T_2T_2^*] &= E\Big[2\sigma_s^2\Big(1-\cos\big(\omega\big(D-\hat{D}(k)\big)\big)\Big)\sigma_n^2\sum_{n=-M_1}^{M_2} g(\nu)g^*(\nu)\Big] \\ &= 4\sigma_s^2\sigma_n^2 E\Big[\sin^2(\omega(D-\hat{D}(k))/2)\Big(\sum_{n=-M_1}^{M_2}\big[f^2(\nu)+\omega^2\mathrm{sinc}^2(\nu)\big]\Big)\Big]\end{aligned} \tag{D.9}$$

Using $\sum_{n=-M_1}^{M_2}\mathrm{sinc}^2(\nu) \approx \sum_{n=-\infty}^{\infty} = 1$ and $\sum_{n=-M_1}^{M_2} f^2(\nu) \approx \sum_{-\infty}^{\infty} = \frac{\pi^2}{3}$ [41], we have

$$E[T_2T_2^*] = \sigma_s^2\sigma_n^2\big(\frac{\pi^2}{3}+\omega^2\big)E\big[(D-\hat{D}(k))^2\big] \tag{D.10}$$

$$\begin{aligned}E[T_3T_3^*] &= E\Big[\sigma_n^2\Big(1+\sum_{n=-M_1}^{M_2}\big|h_{\hat{D}(k)}(n)\big|^2\Big)\sigma_s^2\omega^2\Big] \\ &= \sigma_n^2\sigma_s^2\omega^2(1+E[G]),\; G = \sum_{n=-M_1}^{M_2}\big(h^0_{\hat{D}(k)}\big)^2\end{aligned} \tag{D.11}$$

We now evaluate $E\big[T_4 T_4^*\big]$.

$$
\begin{aligned}
E\big[T_4 T_4^*\big] = E\big[\phi^*(k)\phi(k)\big] \sum_{n=-M_1}^{M_2} \sum_{m=-M_1}^{M_2} E\big[\theta(k-n)\theta^*(k-m)\big] \\
\times E\big[g(n-\hat{D}(k))g^*(m-\hat{D}(k))\big] \\
+ \sum_{p=-M_1}^{M_2} \sum_{l=-M_1}^{M_2} \sum_{n=-M_1}^{M_2} \sum_{m=-M_1}^{M_2} E\big[\theta^*(k-p)\theta(k-l)\theta(k-n)\theta^*(k-m)\big] \\
\times E\big[h^*_{\hat{D}(k)}(p) g(l-\hat{D}(k)) h_{\hat{D}(k)}(n) g^*(m-\hat{D}(k))\big]
\end{aligned}
\tag{D.12}
$$

The first tern on the right hand side (RHS) of (D.12) can be shown to be equal to

$$
\sigma_n^4 \sum_n \big|g(n-\hat{D}(k))\big|^2 \approx \sigma_n^4 \big(\frac{\pi^2}{3} + \omega^2\big) \tag{D.13}
$$

Now before we evaluate the second term of RHS of (D.12), for convenience we introduce some notations. Let the zero mean complex white noise be expressed in terms of its in-phase and quadrature components: $\theta(k-q) = a(q) + j\, b(q)$. The index q takes on anyone of the indices $p,\ l,\ n,$ and m. The $a(q)'$s are independent from the $b(q)'$s. They

have the same variance of $\sigma_a^2 = \sigma_n^2/2$. We have

$$\begin{aligned}
&\theta^*(k-p)\theta(k-l)\theta(k-n)\theta^*(k-m) \\
&= a(p)a(l)a(n)a(m) - j\,a(p)a(l)a(n)b(m) + j\,a(p)a(l)b(n)a(m) \\
&\quad + a(p)a(l)b(n)b(m) + j\,a(p)b(l)a(n)a(m) + a(p)b(l)b(n)a(m) \\
&\quad - a(p)b(l)b(n)a(m) + j\,a(p)b(l)b(n)b(m) - j\,b(p)a(l)a(n)a(m) \\
&\quad - b(p)a(l)a(n)b(m) + b(p)a(l)b(n)a(m) - j\,b(p)a(l)b(n)b(m) \\
&\quad + b(p)b(l)a(n)a(m) - j\,b(p)b(l)a(n)b(m) + j\,b(p)b(l)b(n)a(m) \\
&\quad + b(p)b(l)b(n)b(m)
\end{aligned} \tag{D.14}$$

The expressions of all the imaginary components in (D.14) are zero. This is because there is always either a signal $a(q)$ or a single $b(q)$ in the four-fold product. Thus we need to consider only the real terms in (D.14).

It has been shown in [42] if $x_1,\ x_2,\ x_3,\ x_4$ are samples of four different stationary Gaussian random processes, we may write

$$E[x_1x_2x_3x_4] = E[x_1x_2]E[x_3x_4] + E[x_1x_3]E[x_2x_4] + E[x_1x_4]E[x_2x_3] \tag{D.15}$$

Consider now the contribution of the term $a(p)a(l)a(n)a(m)$ to $E\left[T_4T_4^*\right]$ in (D.12).

Using (D.15) we have

$$
\begin{aligned}
&\sum_{p}\sum_{l}\sum_{n}\sum_{n} E[a(p)a(l)a(n)a(m)]E\big[h^{*}_{\hat{D}(k)}(n)g(l-\hat{D}(k))h_{\hat{D}(k)}(n)g^{*}(m-\hat{D}(k))\big] \\
&= \sum_{p}\sum_{l}\sum_{n}\sum_{m}\big\{E[a(p)a(l)]E[a(n)a(m)] + E[a(p)a(n)]E[a(l)a(m)] \\
&\quad + E[a(p)a(m)]E[a(l)a(n)]\big\} \times E\big[h^{*}_{\hat{D}(k)}(p)g(l-\hat{D}(k))h_{\hat{D}(k)}(n)g^{*}(m-\hat{d}(k))\big] \\
&= \sum_{p}\sum_{l}\sum_{n}\sum_{m}\big\{E\big[a(p)a(l)\big]E\big[a(n)a(m)\big] + E\big[a(p)a(n)\big]E\big[a(l)a(m)\big] \\
&\quad + E\big[a(p)a(m)\big]E\big[a(l)a(n)\big]\big\} \times E\big[h^{*}_{\hat{D}(k)}(p)g(l-\hat{D}(k))h_{\hat{D}(k)}(n)g^{*}(n-\hat{D}(k))\big] \\
&= 2\sigma_a^4 E\Big[\sum_{p}\sum_{n} h_{\hat{D}(k)}(p)g(p-\hat{D}(k))h_{\hat{D}(k)}(n)g^{*}(n-\hat{D}(k))\Big] \\
&\quad + \sigma_a^4 E\Big[\sum_{p}\sum_{l} h^{*}_{\hat{D}(k)}(p)g(p-\hat{D}(k))h_{\hat{D}(k)}(p)g^{*}(l-\hat{D}(k))\Big] \\
&= 2\sigma_a^4 E\big[g(0)g^{*}(0)\big] + \sigma_a^4 E\Big[\sum_{p}\sum_{l}\big(h^{0}_{\hat{D}(k)}(p)\big)^2\big(f^2(\nu)+\omega^2\mathrm{sinc}^2(\nu)\big)\Big] \\
&= 2\sigma_a^4\omega^2 + \sigma_a^4\big(\frac{\pi^2}{3}+\omega^2\big)G
\end{aligned}
\tag{D.16}
$$

The condition from the term $b(p)b(l)b(n)b(m)$ in (D.14) to $E\big[T_4T_4^{*}\big]$ in (D.12) is the same as that given by (D.15). The contributions to $E\big[T_4T_4^{*}\big]$ in (D.12), from the other real terms in (D.14), namely, $a(p)a(l)b(n)b(m)$, $a(p)b(l)a(n)b(m)$, $-a(p)b(l)b(n)a(m)$, $b(p)a(l)b(n)a(m)$, $-b(p)a(l)a(n)b(m)$, $b(p)b(l)a(n)a(m)$, can be worked out similarly, resulting respectively, in $\sigma_a^4\omega^2$, $\sigma_a^4\big(\frac{\pi^2}{3}+\omega^2\big)G$, $-\sigma_a^4\omega^2$, $-\sigma_a^4\omega^2$, $\sigma_a^4\big(\frac{\pi^2}{3}+\omega^2\big)G$, $\sigma_a^4\omega^2$.

Thus substituting all these contributions to (D.12), we have

$$E\big[T_4 T_4^*\big] = \sigma_n^4\omega^2 + \sigma_n^4\big(\frac{\pi^2}{3} + \omega^2\big)\big\{1 + E[G]\big\} \tag{D.17}$$

Similarly, we obtain

$$\mathrm{Re}\big\{E\big[T_4^2\big]\big\} = -2\sigma_n^4\omega^2 \tag{D.18}$$

Therefore (D.1) can be simplified as

$$\begin{aligned} E\big[\hat{D}^2(k+1)\big] = E\big[\hat{D}^2(k)\big](1 + 4\mu\sigma_s^2\omega^2) - 4\mu\sigma_s^2\omega^2 D\, E\big[\hat{D}(k)\big] \\ + 2\mu^2\{\alpha \times \epsilon(k) + \beta\} \end{aligned} \tag{D.19}$$

where

$$\epsilon(k) = E\big[(D - \hat{D}^2(k))\big] = E\big[\hat{D}^2(k)\big] - 2\,D\,E\big[\hat{D}(k)\big] + D^2 \tag{D.20}$$

$$\alpha = 2\sigma_s^4\omega^4 + \sigma_s^2\sigma_n^2\omega^2\pi^2/3 \tag{D.21}$$

$$\beta = -\sigma_n^4\omega^2 + \big\{\sigma_n^4\big(\pi^2/3 + \omega^2\big) + \sigma_n^2\sigma_s^2\omega^2\big\}\big(1 + E[G]\big) \tag{D.22}$$

From (D.20) we have

$$\begin{aligned}\epsilon(k+1) &= E\big[\hat{D}^2(k+1)\big] - 2D\,E\big[\hat{D}(k+1)\big] + D^2 \\ &= \epsilon(k)\big(1+4\mu\sigma_s^2\omega^2+2\mu^2\alpha\big) + 2\mu^2\beta + \big(1+4\mu\sigma_s^2\omega^2\big)2\,D\,E\big[\hat{D}(k)\big] \\ &\quad - D^2\big(1+4\mu\sigma_s^2\omega^2\big) - 4\mu\sigma_s^2\omega^2 D\,E\big[\hat{D}(k)\big] \\ &\quad - 2D\,E\big[\hat{D}(k+1)\big] + D^2\end{aligned} \tag{D.23}$$

Substituting (4.6) into (D.23), we can show that the last five terms of (D.23) sum to zero, hence we obtain

$$\epsilon(k+1) = \epsilon(k)\,C + B \tag{D.24}$$

where $C = 1+4\mu\sigma_s^2\omega^2+2\mu^2\alpha$, $B = 2\mu^2\beta$.

From (D.24), it is easy for us to get (4.10) in Chapter 4.

Appendix E

Modulated Finite Impulse Response (MFIR) Delay Filter

We consider a practical discrete delay system for delay D in the form of a finite impulse response filter with coefficients $h_D(n)$ expressed as

$$y(k) = x(k - D) = \sum_{n=0}^{N} h_D(n)x(k - n) \tag{E.1}$$

Now let $x(k) = x'(k)e^{j\omega k}$, then

$$x(k - D) = x'(k - D)e^{j\omega(k-D)} \tag{E.2}$$

But

$$x'(k-D) = \sum_{n=0}^{N} h_D(n)x'(k-n) \tag{E.3}$$

Substituting (E.3) into (E.2), we have

$$\begin{aligned} x(k-D) = y(k) &= \left(\sum_{n=0}^{N} h_D(n)x'(k-n)\right)e^{j\omega(k-D)} \\ &= \sum_{n=0}^{N} h_D x'(k-n)e^{j\omega(k-n)}e^{j\omega(n-D)} \end{aligned} \tag{E.4}$$

Therefore,

$$y(k) = \sum_{n=0}^{N} h_D(n)e^{j\omega(n-D)}x(k-n) \tag{E.5}$$

Equation (E.5) represents an MFIR delay filter.

Appendix F

Cost Function of MLIDF

Define the cost function as

$$J = E\left[|e(k)|^2\right] = E[e^*(k)e(k)] \tag{F.1}$$

From (5.3) in the main text, we have

$$e(k) = x(k) - \sum_{n=0}^{N} h^0(n, D(k))e^{j\omega(n-D(k))}x(k-n),\ 0 \le n \le N \tag{F.2}$$

Substituting (F.2) into (F.1) we get

$$\begin{aligned} J = 1 &+ \sum_{n=0}^{N} h^0(n, D(k)) \sum_{n=0}^{N} h^0(n - D(k)) - 2\cos(\omega D(k)) \sum_{n=0}^{N} h^0(n, D(k)) \\ &+ \sigma^2 \left(1 - 2h^0(0, D(k))\cos(\omega D(k)) + \sum_{n=0}^{N} \left(h^0(n, D(k))\right)^2\right) \end{aligned} \tag{F.3}$$

Let us introduce a $(N+1)\times(N+1)$ Vandermonde matrix, $\mathbf{V}$, and a column vector, $\mathbf{v}$, as follows,

$$\mathbf{V} = \begin{bmatrix} 1 & 1 & 1 & \cdots & 1 \\ 0 & 1 & 2 & \cdots & N \\ 0 & 1 & 2^2 & \cdots & N^2 \\ \vdots & \vdots & \vdots & \cdots & \vdots \\ 0 & 1 & 2^2 & \cdots & N^N \end{bmatrix} \tag{F.4}$$

$$\mathbf{v} = \begin{bmatrix} 1 & D & D^2 & \cdots & D^N \end{bmatrix}^T \tag{F.5}$$

Now solve the equation

$$\mathbf{Vh} = \mathbf{v} \tag{F.6}$$

As shown by Oetken [43], the solution of (F.6), $\mathbf{h}$, is equal to the Lagrange interpolation formulator, that is to say,

$$\mathbf{h} = \begin{bmatrix} h^0(0, D(k)) & h^0(1, D(k)) & \cdots h^0(N, D(k)) \end{bmatrix}^T \tag{F.7}$$

Therefore, it is obvious that

$$\sum_{n=0}^{N} h^0(n, D(k)) = 1 \tag{F.8}$$

Substituting (F.8) into (F.3), we obtain (5.4) in the main text.

Appendix G

Convergence of EMLAFE

We approximate the delayed version of signal $s(k)$ as follows

$$s\left(k-\frac{2\pi}{\hat{\omega}(k)}\right) \approx \sum_{n=0}^{N} h_e(n,\hat{\omega}(k))s(k-n)$$

Taking expectation on (5.10) in the main text, we have

$$\begin{aligned} E[\hat{\omega}(k+1)] = E[\hat{\omega}(k)] - 2\mu\, Re\Bigg\{ E\Bigg[\Big(x^*(k) - \sum_{n=0}^{N} h_e^*(n,\hat{\omega}(k))x^*(k-n)\Big) \\ \times \sum_{n=0}^{N} f(n,\hat{\omega}(k))x(k-n)\Bigg]\Bigg\} \\ = E[\hat{\omega}(k)] - 2\mu\, Re\{E[T_1+T_2+T_3+T_4]\} \end{aligned} \tag{G.1}$$

where

$$T_1 = (s^*(k) - s^*(k - 2\pi/\hat{\omega}(k))) \sum_{n=0}^{N} f(n, \hat{\omega}(k)) s(k-n) \tag{G.2a}$$

$$T_2 = \left(\theta^*(k) - \sum_{n=0}^{N} h_e^*(n, \hat{\omega}(k)) \theta^*(k-n)\right) \sum_{n=0}^{N} f(n, \hat{\omega}(k)) s(k-n) \tag{G.2b}$$

$$T_3 = (s^*(k) - s^*(k - 2\pi/\hat{\omega}(k))) \sum_{n=0}^{N} f(n, \hat{\omega}(k)) \theta(k-n) \tag{G.2c}$$

$$T_4 = \left(\theta^*(k) - \sum_{n=0}^{N} h_e^*(n, \hat{\omega}(k)) \theta^*(k-n)\right) \sum_{n=0}^{N} f(n, \hat{\omega}(k)) \theta(k-n) \tag{G.2d}$$

Since the signal and noise are uncorrelated, $E[T_2] = E[T_3] = 0$. We now evaluate the other terms individually. To evaluate $Re\{E[T_1]\}$, we rewrite $f(n, \hat{\omega}(k))$ in (G.2a) as $\frac{\partial h_e(n,\hat{\omega}(k))}{\partial \hat{\omega}(k)}$, and then exchanging differentiation and summation operation, we have

$$\begin{aligned} T_1 &= (s^*(k) - s^*(k - 2\pi/\hat{\omega}(k))) \frac{\partial}{\partial \hat{\omega}(k)} \sum_{n=0}^{N} h_e(n, \hat{\omega}(k)) s(k-n) \\ &= \left(s^*(k) - s^*\Big(k - \frac{2\pi}{\hat{\omega}(k)}\Big)\right) \frac{\partial}{\partial \hat{\omega}(k)} s\Big(k - \frac{2\pi}{\hat{\omega}(k)}\Big) \\ &= \left(1 - \exp\Big(j\frac{2\pi\omega}{\hat{\omega}(k)}\Big)\right) \frac{\partial}{\partial \hat{\omega}(k)} \exp\left(-j\frac{2\pi\omega}{\hat{\omega}(k)}\right) \end{aligned}$$

Therefore,

$$Re\{E[T_1]\} = E\left[\frac{2\pi}{\omega} \frac{1}{(\hat{\omega}(k)/\omega)^2} \sin\Big(\frac{2\pi}{\hat{\omega}(k)/\omega}\Big)\right] \tag{G.3}$$

We note that after a sufficient number of iterations, $\hat{\omega}(k)$ approaches ω, therefore $x = \frac{\hat{\omega}(k)}{\omega} \sim 1$. Now using $\frac{1}{x} = \frac{1}{1-(1-x)} \approx 1 + (1-x)$ and $\sin\alpha \approx \alpha$ for small α, in (G.3),

we have

$$\begin{aligned} Re\{E[T_1]\} &= E\left[\frac{2\pi}{\omega x^2}\sin\Big(\frac{2\pi}{1-(1-x)}\Big)\right] \approx E\left[\frac{2\pi}{\omega x^2}\sin(2\pi(1-x))\right] \\ &= E\left[\frac{4\pi^2}{\omega}\Big(\frac{1}{x^2}-\frac{1}{x}\Big)\right] = E\left[\frac{4\pi^2}{\omega}\Big(\frac{\omega^2}{\hat{\omega}^2(k)}-\frac{\omega}{\hat{\omega}(k)}\Big)\right] \\ &= E\left[\frac{4\pi^2\omega^2}{\hat{\omega}^2(k)\omega^2}(\omega-\hat{\omega}(k))\right] \approx \frac{4\pi^2}{\omega^2}\big(E[\omega-\hat{\omega}(k)]\big) \end{aligned} \tag{G.4}$$

In the above formula, because $\frac{\omega^2}{\hat{\omega}^2(k)} = \bigcirc(1)$ and more important attribute of this term is that the sign remains unchanged. Hence, for simplicity, we substitute it with 1 by treating it as a variable step-size issue. When the convergence is reached, $\frac{\omega^2}{\hat{\omega}^2(k)}$ will be very close to 1.

Now since the noise is white, we have

$$E[T_4] = \sigma^2\Big[f(0,\hat{\omega}(k)) - \sum_{n=0}^{N} h_e^*(n,\hat{\omega}(k))f(n,\hat{\omega}(k))\Big]$$

Therefore, under a higher SNR condition, that is to say, σ^2 is small, $E[T_4] \approx 0$. Finally, substituting (G.4) into (G.1), we get (5.13) in the main text.

Mathematical Symbols

a	Constant or variable
c	Lignt speed
$s(t)$	Function of t
$\bigcirc$	Landau Operator
$\circ$	Landau Operator
$\mathbf{k}$	Matrix or vector
μ	Step-size
σ^2	Variance
$E[x]$	Expectation of x
$\prod$	Series production
τ	Propagation delay
v_g	Group velocity
ω	Angular frequency
f	Frequency
τ_g	Group delay
$\arg z$	Phase of z

$\|\| \bullet \|\|_p$	L_p Norm
τ_p	Phase delay
$\sum$	Summation
$\bigtriangledown$	Gradient
$\otimes$	Convolution

Author's Publications

[1] Zheng Cheng, T. T. Tjhung, "A new time delay estimator based on ETDE", accepted for publication by *IEEE Transactions on Signal Processing*, and will appear in a July 2003 issue.

[2] Zheng Cheng, T. T. Tjhung, "Accurate Explicit Frequency Estimation Using Modulated Lagrange Delay filter", in *the Proceedings of 2nd IEEE International Symposium on Signal Processing and Information Technology*, Morocco, pp.634-639, December 18-21, 2002.

[3] Zheng Cheng, T. T. Tjhung, "A new algorithm for explicit time delay estimation", in *the Proceedings of DSP 2002 14th International Conference on Digital Signal Processing*, Santorini, Greece, pp.1297-1300 July 1-3, 2002.